Assessment of Urban Air pollution in relation to Land use and Land cover changes over Delhi-NCR region

Thesis submitted to the Jawaharlal Nehru University
in partial fulfilment of the requirements for the
award of the degree of

DOCTOR OF PHILOSOPHY

KUMAR ANANDAM

SCHOOL OF ENVIRONMENTAL SCIENCES
JAWAHARLAL NEHRU UNIVERSITY
NEW DELHI-110067
INDIA

2017

जवाहरलाल नेहरू विश्वविद्यालय
Jawaharlal Nehru University
SCHOOL OF ENVIRONMENTAL SCIENCES
New Delhi-110067
Tele. 011-26704303, 4304

Date: 21/07/2017

CERTIFICATE

This is to certify that thesis entitle ***"Assessment of Urban Air pollution in relation to land use and land cover changes over Delhi-NCR region"*** embodies the original work, carried out in the School of Environmental Sciences, Jawaharlal Nehru University, New Delhi, India. This work has not been submitted in full or partial for any other degree or diploma to any other university or institute.

Kumar Anandam

Kumar Anandam

(Candidate)

Krishn 21/07/2017

Prof. Krishan Kumar

(Co-supervisor)

Prof. V. K. Jain

(Supervisor)

21/7/2017

Prof. Saumitra Mukherjee

(Dean)

प्रो.सौमित्र मुखर्जी / Prof. S. Mukherjee
डीन / Dean
पर्यावरण विज्ञान संस्थान
School of Environmental Sciences
जवाहरलाल नेहरू विश्वविद्यालय,
Jawaharlal Nehru University
नई दिल्ली-110067/New Delhi-110067

Acknowledgements

At first it becomes my duty to show my heartfelt gratitude to Prof. V. K. Jain, my supervisor, for his invaluable advices, continuous supervision, considerable concern, helpful insights and the freedom he gave me to explore the horizons of my ideas, and then encouraging me to go a little further. I will like to thank his profusely for his tolerant attitude. Sir, I am really lucky to have you as my guide because without your support and guidance, I am sure I could not have made this thesis in this present format.

I would like to extend my warmest regards to Prof. Krishan Kumar who have shown me patience, encouragement and undaunted support, precious suggestions and valuable recommendations in all my endeavours. I feel honoured to have had him on my thesis co-supervisor.

I am thankful to Prof. Saumitra Mukherjee, Dean, School of Environmental Sciences, for providing necessary facilities.

Thanks must go to Dr. Deepak Singh and Dr. Amit Kumar for the tremendous help and support. He is the best critics for me and I respect for them.

Special thanks go to Manoj, Shivesh and Dr. Alok Pandey for help during Ph.D thesis submission. I would like to thank my labmates, Dinesh sir, Purnima, Vinay, Ritesh Priyanka and Prabhat.

I would like to extend my deep love to my loving friends, Prabhat, Ratan, and Bablu. A special word of thank to all these friends whose friendship is really an achievement in my life. I would like to extend my deep thanks to Dhiraj, Dr. Akshansh, Deepak, Niraj, Bikram and Naveen for understanding me during tough times in JNU and indirectly becoming my supporting structure.

Special thanks to all SES office staff for caring me. Sincere thanks goes to Gajendra sir for their love, blessing and co-operation.

I am spell bound while talking about my parent's role in my life. I can only say that my research would not have been possible without their blessing and love. Therefore I owe my entire existence to them. The Junior Research Fellowship provided by University Grant Commission (UGC), New Delhi is gratefully acknowledged.

Kumar Anandam

List of Contents

List of Figures

List of Tables

Chapter-1 *Introduction and Literature review*

[1] INTRODUCTION

[1.1] General Overview

In the recent era, rapid urbanization occurred due to industrial and service based economic developments along with a corresponding increase in population. Urbanization is a process in which massive alterations take place in natural environment (atmosphere, lithosphere, and hydrosphere) at local and regional scale. During urbanization, the most remarkable transformation has occurred in natural land-use and land covers (LULC) such as vegetation cover land, agricultural land and natural habitat to impervious surfaces according to the human needs (Dewan and Yamaguchi, 2009; Balcik, 2013; Ward et al., 2016). These LULC changes have enormous influences on the net productivity, biodiversity and meteorological parameters (temperature, humidity, etc.) at the local, regional and global level (Liu et al., 2006; Han and Xu 2013; Zhang et al., 2013; Wang et al., 2016).

Less than 3% of total earth's land surface is covered by cities which are home to more than half (54%) of the global human population (Liu et al., 2014; United Nation. 2014). They produce 78% of the total anthropogenic carbon emissions and an enormous amount of airborne toxin and pollutants (O'Meara et al., 1999). These emissions significantly influence the global climate (Grimm et al., 2008) and also adversely affect air quality at local and regional scales. The production and emissions of air pollutants such as ozone, fine particulate matter, NO_x, carbon monoxide and oxides of sulfur affect human health and wellbeing of biotic community. The exposure of outdoor air pollution was responsible for more than two-and-a-half million deaths each year (470,000 people died as a result of ozone, and 2.1 million deaths were linked to fine particulate matter) (Silva et al., 2013). The anthropogenic emissions of CO_2 and other greenhouse gases (GHG) are a major contributor to climate change resulting rise in the rise in global and regional temperatures and sea level (Dasgupta et al., 2007). An increase in atmospheric

temperature might also exacerbate the effects of air pollution, a modest 1ºC rise in global average temperature could result in 21,600 air pollution-related deaths worldwide (Jacobson et al., 2008).

Urban Pollution Island (UPI) and Urban Heat Island (UHI) are recent phenomena created by the human activities interfering with the natural environment. Superstructures and high-rise buildings are parts of a new urban landscape, where their morphology influences the air temperature distribution that induces upwards and downwards thermal convection flow. The convection flow in turn affects the air pollution dispersion in an urban location (Bereitschaft et al., 2013). Location specific concentration of different pollutants in air interferes with the radiation budget on the land surface which governs the land surface temperature. In the recent past several studies inside various cities have been carried out to measure pollutant concentration and its exposure on human population using data from spatially dense monitoring network and land use regression models.(Jerrett et al., 2005; Beelen et al., 2013; Zhan et al., 2013).

[1.2] LULC studies

Urban growth or expansion particularly the expansion of residential and commercial land use to adjacent agricultural, forest and other naturally pristine land has been considered a symbol of economic prosperity. But, it has a darker side, in term of the impact on the local environment such as deterioration of air and water quality, loss of agricultural, forest and coastal land, and creates socioeconomic disparity or social fragmentation (Squires et al., 2002). A goal of LULC studies is to understand the spatio-temporal patterns of land surface characteristics and the processes governing them (Lambin et al., 2003; Turner et al., 2007). Satellite based data is affordable and most suitable for analyzing changes in LULC in certain time duration. Various methods are employed for the studies LULC changes in an urban environment using satellite images (Yuan et al., 1998). LULC change detection is perceived through classification of satellite images with a different classifier use in GIS software with change detection model. Different approaches of classification and categorization techniques (algorithms) are used for satellite obtained data in LULC studies. There is no single most suitable or ideal classification technique

developed, so for which can be applied as a universal mode of classification of LULC. Recently, an attempt has been towards developing a classification system in which provides a certain guideline for the evaluation and a framework to satisfy the majority of the user (Anderson et al., 1976). Figure 1.1 explains the difficulty level at different stages for analyzing or processing satellite data or classification technique in LULC studies.

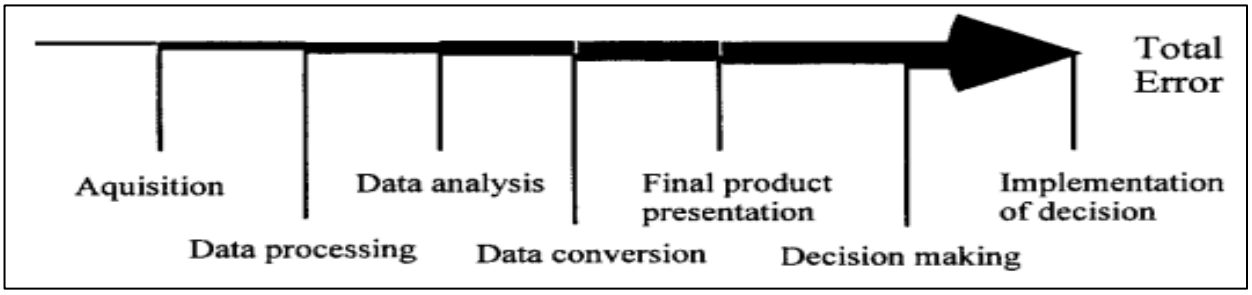

(Source: P. C. Smits et al., 1999).

Figure 1.1 The accumulation of error in remote-sensing data processing method.

For LULC studies by remote sensing technique through GIS platform are needs awareness about accuracy and quality of classification algorithms. Generally, classification algorithms have been lacking two types of accuracy-awareness. First, the inefficiency may arise from choosing the ROI or it may be suited for certain task which creates an unnecessary omission and commission error. Second, no one algorithm is suited for all types of remote sensing image data set e.g. for example Maximum Likelihood Classifier (MLC) is suitable for Landsat dataset, but it may not perform with SAR (Synthetic Aperture Radar) data set (Smits et al., 1999). Table 1.1 describes the common classifier algorithms embedded in GIS software with advantages and disadvantages of their applications.

Mapping of LULC change at global and regional scale based on single algorithm, with medium-resolution satellite data set (Landsat data 30-meter spatial resolution), only provides limited information (particularly in forest dynamics) (Tropek et al., 2014). Landsat data has been useful for analyzing and quantifying effectively the information about LULC changes due to

human interference in the natural environment in the urban area (Kennedy et al., 2014; Wulder et al., 2015).

Table 1.1 Different classifications of algorithms

Classifier	Advantage	Disadvantage
Parellelipiped	Fast and simple; distribution free	Due to corners, pixels may be classified from spectral mean
Minimum Distance	No unclassed pixels; fast	Does not consider class covariance
Mahalanobis	Take the class covariance into account	Over classification of signatures with large value in covariance matrix; parametric; assumes normal distribution
ML/Bayesian	Relatively accurate; variability of classes taking into account	Computationally expensive; assumes normal distribution; over classification of signatures with large value in cov. matrix
Neural network	Distribution free; fast after training	Slow training; no theoretical basis; stochastic convergence

(Source: P. C. Smits et al., 1999)

[1.3] Urban heat island (UHI) studies

LULC change and Urban Heat Island (UHI) have a significant impact on energy consumption and outdoor air quality in the urban area. In recent years, various approaches such as observational and simulation techniques have been applied in studies of UHI formation and finding the mitigation strategy.

[1.3.1] Simulation approaches- Advancement of computational technique in past two decades, has allowed the researchers to use mathematical models for large-scale problems. Among these models, such as energy balance and dynamical numerical approaches are form to be suitable for UHI studies (Parham et al., 2010).

[1.3.2] Observational approaches- This includes empirical studies of different geographical and meteorological parameters with UHI intensity e.g. - wind speed, cloud-cover, city size, population and day and night variation of temperature (Steinecke et al., 1999; Ripley et al., 1996). In observational approach thermal remote sensing based studies are most efficient and more accurate in comparisons to other approaches.

Thermal remote sensing has become an efficient tool for UHI studies. In thermal studies, surface temperature is retrieved from surface reflectivity and thermodynamic properties (such as surface moisture, surface emissivity, surface albedo, the irradiative input at the surface) (Becker et al., 1995). However, the surface temperature in UHI is different from the atmospheric UHI or ambient air temperature (T_{air}). It differs significantly from few degrees in night to 8-10 ºC in a day time (Sobrino et al., 2012). So developing a suitable algorithm employing LST for direct air temperature estimation is a major challenge in remote sensing studies of UHI.

Solar zenith angle model has been used for estimation of air temperature from LST retrieved from satellite data. Cresswell et al., (1999) established a statistical relationship between LST and T_{air}. Whereas, Sun et al., (2005) estimated instantaneous air temperature from land surface temperature derived from remote sensing data based on thermodynamic consideration. Most of the model and algorithms need vast knowledge of meteorological and environmental parameters to estimate T_{air} from LST. Many algorithms for T_{air} estimation use a regression model of the image derived LST against a series of air and surface temperature points collected in the field at the time of imaging for which an R^2 of 0.74 and 0.82 were obtained for day and night time images respectively (Nicole et al., 2013).

[1.4] LULC change influence on LST

Many environmental and meteorological parameters are closely related to temporal changes of LULC. Land surface temperature (LST) is one of them. In past 10- 15 years, too many studies have been done on the relation between the temporal change of LULC with LST (Chen et al.,

2006; Hamdi et al., 2010; Haiyong et al., 2013; Zhang et al., 2013). Some important studies showed the relationship between intra-city LST with an urban area parameters such as LULC, vegetation abundance (NDVI) and soil moisture content (Weng et al., 2004) fraction of impervious surface (Yuan et al., 2007), built-up area, bare Land, water, and semi-bare land (Chen et al., 2006). Jusuf et al.,(2007) studied day night variation of LST with LULC.

LST calculated from Landsat thermal infrared data is serves a valuable input for many climatic and ecological applications such as climate change, hydrological cycle modeling, and urban health, etc. (Han and Xu, 2013; Maimaitiyiming et al., 2014; Weng, 2009). Calculating LST from the thermal band of Landsat is very complicated, and it depends on regional meteorological conditions. At sensor, received radiance is a combination of earth surface and atmospheric emitted radiance. For accurate measurement of LST, emitted radiance by earth surface need to be isolated from atmospheric emitted radiance and corrected for land surface emissivity. In recent years three most appropriate LST retrieval algorithms have been used, namely radiative transfer equation (RTE), the mono-window algorithm (MWA) and generalized single channel algorithm (GSC). Each method required emissivity value as well as with different atmospheric parameters. For example, as RTE needed atmospheric transmittance, upwelling/downwelling radiance whereas MWA and GSC required transmittance with mean atmospheric temperature and precipitable water vapor (PWV) respectively (Windahl and Beurs, 2016). Reported accuracy of these methods depends on the present atmospheric parameters. If PWV present in atmosphere varied 0.5 to 2 g/cm^2, the error lied in LST range between 1 and 2 Kelvin in GSC method (Jimenez Munoz et al., 2009). In RTE and MWA, the expected error 2 and 1-1.5 Kelvin respectively, if the atmospheric transmittance is above 0.8 (Qin et al. 2001; Barsi et al., 2005).

Land surface emissivity (LSE) is an important parameter for LST retrieval from thermal remote sensing and its relation with LULC (Voogt and Oke 2003). Accuracy in LSE estimation has an effect on LST value. A 1% inaccuracy in LSE causes up to 0.78 kelvins error in LST (Van de Griend and Owe, 1993). LSE is an intrinsic property of the surface; it depends on chemical

and physical characteristics of land surface such as water content, chemical composition, roughness, etc. (Snyder et al., 1998). Quantification of LSE is made by the ratio of emittance between the land surface and a blackbody at the same temperature. Exact estimation of LSE is often complicated for natural land surface because the natural surface does not emit radiant energy like a black body at any temperature. Table 2.2 shows depicted a values of emissivity for different land surface materials(Lillesand et al., 2004).

Table 1.2 Emissivity value of some common material used as land surface.

Material	Typical average emissivity (0ver 8-14 μm)
Wet snow	0.98-0.99
Healthy green vegetation	0.96-0.99
Wet soil	0.95-0.98
Brick	0.93-0.94
Wood	0.93-0.94
Dry vegetation	0.88-0.94
Dry snow	0.85-0.90
Glass	0.77-0.81
Aluminum foil	0.03-0.07

Sources: lillesand et al. 2004.

For estimation of LSE, generally, three distinctive method, namely semi-empirical method (SEM), physical based method and multi-channel temperature/emissivity separation (TES) method are applied with varying degree of difficulty level (Dash et al., 2002; Li et al., 2013b). NDVI based emissivity method (NBEM). NBEM is one of the most suitable techniques used for the estimation of LSE for heterogeneous land surface or landscapes (Dash et al., 2005; Li et al., 2013b).The NBEM technique is widely applied to estimate LSE for data of various sensors from visible, NIR and thermal infrared band (TIR) (Sobrino et al., 2008; Momeni and Saradjian, 2007). Some studies tried to establish empirical relationship between NDVI and

surface emissivity for mix pixel (combination of surface type) in satellite data set (Valor and Caselles, 1996; Van de Griend and owe, 1993). Van de Griend and Owe, (1993) reported a high correlation (R^2=0.94) between emissivity and NDVI for advance very high resolution radiometer (AVHRR) data in savannah environment of Botswana. It is expressed by the following equation-

$$\varepsilon = a + bln(NDVI) \quad (1.1)$$

where $a = 10094\ and\ b = 0.047$ derived by regression analysis.

An operational model proposed by Sobrino et al., 2008 to establish a relationship between emissivity and NDVI for Landsat data. They considered the NDVI value less than 0.2 for bare soil and obtained emissivity by reflectance value in red (R) band in dataset.

$$\varepsilon = a + b.\rho red \quad (1.2)$$

Where $a\ and\ b$ are coefficients obtained from laboratory measurements for soil, ρred is reflectance of red region of spectral band.

If NDVI values lie between 0.2 and 0.5, the pixels are considered as to mixture of vegetation and bare soil. The emissivity is calculated as follow-

$$\varepsilon = m.P_V + n \quad (1.3)$$

$$m = \varepsilon_v - \varepsilon_s - (1 - \varepsilon_v)F\varepsilon_v \quad (1.4)$$

$$n = \varepsilon_s + (1 - \varepsilon_s)F\varepsilon_v \quad (1.5)$$

Where $\varepsilon_v\ and\ \varepsilon_s$are vegetation and soil emissivities respectively, F is shape factor its mean value = 0.55 and P_V vegetation proportion computed from NDVI using the following equation Carlson and Ripley, 1997:

$$\mathrm{P_V} = \left[\frac{(\mathrm{NDVI}) - (\mathrm{NDVI})_{\min}}{(\mathrm{NDVI})_{\max} - (\mathrm{NDVI})_{\min}}\right]^2 \quad (1.6)$$

When the NDVI value is larger than 0.5, the pixels are assumed as fully vegetated and emissivity value is considered as 0.99 (Mohamed et al., 2017).

[1.5] Studies of Urban Pollution and relation with LST and LULC changes

In early stages of urban pollution island studies, there was a focus on the comparison of concentrations of air pollutants between the cities(Dockery et al., 1993; Pope et al., 2002; Gotchi et al., 2005) and rural areas, but recently focus has shifted to intra-urban spatial contrast (Beelen et al., 2007). Two most suitable approaches of intra-urban air quality studies are land use regression model (Beleen et al., 2013) and computational fluid dynamic model (based on Renolds average Navier- Stock equation (RANS-CF)) (Santiago et al., 2013). Urban roughness or high-rise buildings decrease wind speed by 0.5-4.0 m/s and increase temperature and turbulent kinetic energy by 1ºC and 1.2 J/m^3 respectively. They increase the nitric oxide concentration by 2-5% in Lujiazui Central Business District (CBD) of Shanghai (Zhan et al., 2013). Urban air pollutant concentrations also depend on configuration of urban setting such as urban street configuration and sky view factor (Eftens et al., 2013). Vegetation setting and form of vegetation (leaf surface area index) along the urban canyon and its seasonal variation (with leaf and leaf shedding season) influence the vertical and horizontal distribution of air pollutant in urban location (Salmond et al., 2013). Air pollution in ambient atmosphere interferes with surface radiation budget, which might influence the LST within an urban location. A study showed a strong correlation between air pollutant concentration (PM_{10}) and LST with intra-city variation (Feizizadeh et al., 2013) at Tabriz city in Iran.

[1.6] $PM_{2.5}$ exposure to human population

Many epidemiology studies have found a statistically significant relationship between concentration of particulate matter (PM) in an ambient environment with acute and chronic diseases in the human population (Dockery and Pope, 1994; Schwartz, 1994; Pope et al., 1995; Samet et al., 1995). In most of above studies typically employed PM concentration data from

stationary air monitoring stations within a region of the interested community as personal exposure of the human population. The population-based studies are expensive in terms of spatial and temporal data of population and air pollutant in an ambient environment. Therefore exposure modeling is one of the most suitable tools for understanding exposures of air pollutant to the human population. In population exposure model a probabilistic approach is applied to randomly sampled data to predict exposure distribution to population (Ott et al., 1988; McCurdy, 1995; MacIntosh et al., 1995; Law et al., 1997; Zartarian et al., 2000). Population exposure model has limitations particularly if sufficient data are not available for identifying variability in exposure factor.

Chronic effect studies focus on the comparison across cities or cohort and between cities and rural area for exposure assessment (Pope et al., 1995). These studies did not assess the intra-city geographic exposure gradient at a micro level. Land use regression model based on stationary air monitoring station data with land use term estimate of air pollutant exposure to population at intra-city locations (Miller et al., 2007; Puett et al., 2009). Recently, a new hybrid method was proposed for assessing exposure to $PM_{2.5}$ to human population based on satellite-retrieved data with LULC term, and meteorological variable interaction (Kloog et al., 2014a; Shi et al., 2016).

[1.7] UHI and urban air pollution in relation to LULC studies over Delhi-NCR

Very few studies have been carried out on the assessment of UHI over Delhi and its relationship with environmental parameters such as particulate matter during winter month (Pandey et al., 2012), retrieval of LST from ETM^+ Landsat imagery (Mallick et al., 2008), relationship between surface temperature, vegetation density and LULC with ASTER image (Kant et al., 2009),retrieved surface emissivity from Landsat TM images and its relation with NDMI (normalized difference moisture index) of different landforms (Mallick. et al., 2012), correlation with UHI and impervious surface in night time using ASTER satellite data (Mallick et al., 2013), and relation between heat flux, LST with Landsat TM images (Chakraborty et al., 2013) and

intra-city UHI variation studies based on in situ measurement and MODIS data derived LST(Mohan et al., 2013). Recently some modelling has attempted intra-city air pollution contrast and exposure to population in Delhi (Saraswat et al., 2013, 2016; Aslam et al., 2017). Till date, to our knowledge, no study has been performed examine direct association between the urban land use/land cover or urban form and emitted concentration of air pollutants. This prompted the reasoned work undertake in the present study with the following objectives:

Objectives: The four major objectives aimed at establishing relation among LULC, LST, air pollutant ($PM_{2.5}$) and pollutant exposure to human are as follows.

(1) To analyze the Population Induced Spatial and Temporal change of Land use/Land cover (LULC) Delhi NCR.

(2) Land Surface Temperature (LST) Retrieval from Satellite data and its relation with LULC change.

(3) Estimation of Urban Pollution Island (UPI) and spatio- temporal change within Delhi NCR area with LULC change.

(4) To analyze the relation between temperature and air pollutants concentration in ambient atmosphere with LULC changes and pollution exposure on human population.

The thesis is organized in the following manner. Chapter 2 contains basic concepts, study area and methodology.

In Chapter 3, an attempt has been made to examine the relation between population growth and spatio-temporal change in LULC during 2003-2014, using satellite data of the NCR in India. In this chapter, the spatio-temporal changes of five LULC types which occurred during 2003 to 2014 are quantified using multispectral band data of Landsat images. For analysis of spatial and temporal distribution of population and its relation to LULC,GIS-based modeling approach has been employed for satellite derived population data.

In Chapter 4, the results of examination of the influence of LULC compositional changes on spatio-temporal LST pattern in National Capital Region (NCR) of India are given. Firstly, spatio-temporal changes in LST retrieved from the thermal infrared band of Landsat L_1 images data during 2003- 2014 period are presented. Secondly, the spatio-temporal dynamics of LST due to LULC pattern changes due to urbanization has been studied.

Chapter 5 deals with the spatial and temporal trend of satellite derived $PM_{2.5}$ concentration and its relation with LULC pattern in the NCR of India. In addition, the results of the exposure of $PM_{2.5}$ to human population residing in intra-urban area in one of the fastest expand NCR area in recent years are presented.

Lastly, Conclusions are discussed in Chapter 6.

Chapter-2 *Basic concepts, study area and Methodology*

[2.1] Basic Concepts

[2.1.1] Land-use and Land-cover (LULC) changes

Land-use is defined as, "land-use is the way in which land and its resources are employed for the purpose of human well-being such as farming, mining, lumbering, etc." Land-cover is the physical form of the land surface as cropland, mountain, forest etc. In a broader sense in recent usages such as impervious surface (including building, pavement or road), natural environmental aspect (soil type and biodiversity) and surface or ground water are distinct Land covers. Human beings are described as a 'keystone predator' species because of their diversity ability through selective predation upon a competitive dominance. Keystone species are defined as "species which alter the natural ecosystem by modifying the ambient area of habitat suited more for their occupant". It changes the community structure without interfering with direct trophic level of other species. At this moment human beings act as keystone species because they alter not only their own environment but also change the structure of ecosystem for all other organisms directly or indirectly. Some researchers have called current geological epoch as "Anthropocene" because of the impact of human beings on regional and global scale ecosystem (Crutzen, 2002; Jarnagin, 2004).

LULC changes impact global processes, such as climate change, resource depletion and bio-geological (nutrient/hydrological) cycle, biodiversity and carrying capacity of the earth (Cohen, 1995; Peskin, 1990; Nobre et al., 1991; Daily, 1997; Houghton et al., 1999; Hurtt et al., 2002; Wilson, 2002). However, the exact quantification of the consequences of LULC changes at the global scale are difficult. LULC changes also impact deforestation, agricultural practices, and carbon cycle at a local and regional scale of an environment (Couzin, 1999; Caspersen et al., 2000; Schimel et al., 2000). Urbanization induced LULC change is deemed to be responsible for an anomaly in local and regional temperature range in recent half century (Kalnay and Cai,

2003). According to World Energy Outlook-2008 estimate, the urban areas contributed a major fraction (67%) of energy consumption, and energy-related CO_2 emission (71%). Many of consequences, such as infectious diseases, invasive species, metal and pesticide in ground and surface water, increased air pollution at local or regional scale and surface temperature anomaly of land and water are attributes to direct and indirect effect of urbanization-induced LULC changes (Daily, 1997; Wilcove et al., 1998; Binder et al., 1999).

Remote Sensing and Geographic Information Systems (GIS) are most suitable and cost-effective tools for assessing the Spatio-temporal dynamics of LULC changes on regional and global scales (Herold et al., 2003; Serrea et al., 2008; Ding et ai., 2013). Satellite-based remote sensing provides valuable multi-temporal data at local, regional and global scale for assessing LULC changes. GIS is a useful tool for analyzing spatial pattern of LULC change from multi-temporal data set (Blodget et al., 1991; Zhang et al., 2002). USGS (United State Geological Survey), NASA (National Aeronautics and Space Administration), NRSC (National Remote Sensing Center) are agencies which provide remotely sensed data through digital archives. This is useful for the study of spatio-temporal pattern changes in the LULC and its relation to other environmental components. Landsat project is a joint initiative between USGS and NASA, which provides calibrated high spatial resolution data to the scientific community, national security agencies and academia. Many earth surface phenomena such as LULC changes and its corresponding Land Surface Temperature (LST) are derived from Landsat level 1 image dataset which is processed according to information provided in the metadata file and Landsat data user Handbook.

The earth observation satellite, Landsat has been providing multispectral data of Earth land surface since 1972. Landsat is the only source which provides calibrated, excellent spatial resolution data of earth's surface through thenational archive at free of cost to the public. The data obtained from Landsat satellite constitutes the longest record of unmatched quality in detail and coverage of the earth surface as seen from space. The Landsat platform is embedded with

multiple remote sensor systems and data relay system along the orbit-adjusted system. It also has a receiver for ground station instruction and the transmitter for sending data to ground station.

First Landsat was launched in 1972 with two earth viewing sensor, a return beam Videocon and an 80m MSS (Multispectral Scanner). Next series Landsat 2 & 3 launched in the year 1975 and 1978 respectively have a similar configuration as Landsat 1. Landsat 4 and 5 (5 as a duplicate of 4) have launched in 1984 with new configuration as MSS and new instruments Thematic Mapper (TM). Due to instrument up-gradation, it improves the ground spatial resolution up to 30 meter and has three new bands. Landsat 5 is still returning useful data even today after 32 years of its launch. Landsat 6 equipped with a 15-meter panchromatic band was lost immediately after a launch in 1993. Landsat 7 with ETM^{+} and scan line corrector (SLC) was launched in 1999, but SLC failed after four years of launch in May 2003. Landsat 8 equipped with two payloads: OLI (Operational Land Imager) and TIRS (Thermal Infrared Sensor) was launched in 2013. OLI and TIRS are designed for taking image simultaneously of every scene but are also capable of independent use in case problem arises with either sensor (Landsat data user handbook 7 and 8).

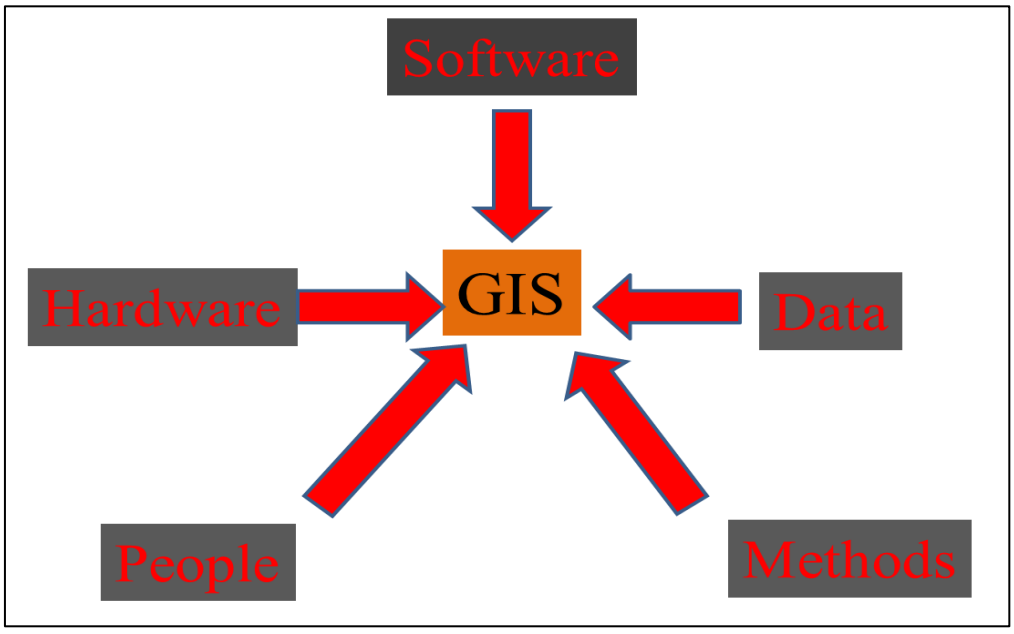

Figure.2.1 GIS working concept (*Source:* http://www.westminster.edu/staff/athrock/GIS/GIS)

GIS sofware as ArcGIS {Environmental Systems Research Institute (ESRI), 380 New York Street, Redlands, CA} and Environment for Visualizing Image Software (ENVI) { Exelis Visual Information Solution Inc, Boulder CO, USA} are efficient tools to visualize, analyze and for data interpretation to establish relationship, pattern and trend of satellite dataset (Dewan and Yamaguchi, 2009). GIS is a computer-based tool for the storage, retrieval, manipulation, analyzing and displaying as a map of the geographical data set. It has capabilities for geographical analysis such as explaining the event, predicting outcomes and future planning. GIS integrates five key components: data, hardware, software, method and people (Figure 2.1).

Many change detection methods have been developed for assessing LULC from satellite data such as digital change detection method (Singh, 1989; Coppin et al ., 2004), Image regression, Vegetation index differencing, Post classification comparison, etc. (Lu et al., 2004). In recent years post-classification method has been extensively used for LULC studies, mainly in supervised spectral signature extraction or supervised classification of satellite retrieved image data (Landsat images) through Classifier algorithm employed in GIS software. Classification technique involves labeling the pixel as belonging to a particular spectral signature (class) using spectral data. For classification of remote sensing image data two procedures are used, namely: unsupervised and supervised classification.

In unsupervised classification procedure pixels in an image are assigned to spectral classes without the user having a name of those classes also called clustering of spectral signature or class. Unsupervised classification is useful for determination of spectral class composition for applying supervised classification methods. In supervised classification methods use is made of suitable algorithms in GIS software for the labelling the pixels having a distinct spectral signature in an image as user defined ground cover type or class. A variety of algorithms are available for supervised classification, which is based on probability distribution model for multispectral space partitioned into defined class. The parametric supervised method is based on the assumption that a statistical probability distribution can model class and parameters of those distributions describing the data. In the other supervised classification, called a non-parametric method,

neither distribution models nor parameters are relevant. A well-known non-parametric method is Maximum Likelihood Classification (MLC) method used for supervised spectral signature extraction from remote sensing image data. In MLC classification method, a pixel at position x in multispectral space is assigned a set of computed probabilities that give the relative likelihood that the pixel belongs to each available class. MLC is based on Bayes classification of spectral classes of image as represented by

$$w_i = 1, \dots \dots M \qquad (2.1)$$

Where, M is total number of classes. To determine the class of particular pixel vector x, the conditional probability is

$$p(w_i \mid \mathrm{x}) \,, \mathrm{i} = 1, \dots . M \qquad (2.2)$$

where measurement of vector x is column brightness value of the pixel. The probability $p(w_i \mid \mathrm{x})$ gives the likelihood of the correct classes,w_i, for a pixel at position x.

Classification is done as

$$x \in w_i, \quad If \quad p(w_i \mid \mathrm{x}) \; > p(w_j \mid \mathrm{x}) \qquad \text{for all} \quad \mathrm{j} \neq \mathrm{i} \qquad (2.3)$$

The pixel at x belongs to class w_i if $p(w_i \mid \mathrm{x})$ is maximum (Richards and Jia, 2005).

[2.1.2] Land Surface Temperature

Land Surface Temperature (LST) is defined as "measurement of hotness and coldness of the surface in a particular location." The surfaces include ice and snow, grass on the lawn, the roof of a building, forest, deserts, etc. whatever the satellite views through the atmosphere to the ground. Thus LST and air temperature which is included in daily weather report, are not the same at a particular location. LST is one of the key parameters which influence the physics of land surface processes such as evaporation, transpiration, hydrological cycle, urban climate and environment,

climate change, etc. at local and global scale (Li et al., 2013). Spatial and temporal changes in LST pattern have been found to occur due to heterogeneity of land surface characteristics such as topography; vegetation cover, urban area, and soil cover or LULC types (Prata et al., 1995; Neteler, 2010). The changes in LULC influence the LST due to the partitioning of sensible and latent heat fluxes of different landforms (Dubreuil et al., 2011). For adequate characterization of spatiotemporal pattern of LST detailed spatial and temporal sampling is required at local, regional and global scale. Ground measurement of LST cannot practically provide values on large scale due to complexity and heterogeneity of land surface. Remote sensing from space or satellite data with high temporal and fine spatial resolution offer a most suitable technique for measuring LST over a regional and global scale. Satellite-based thermal infrared (TIR) band dataare used for retrieving LST through radiative transfer model in GIS software. Remotely sensed images data, such as Landsat TM/ETM^{+} (Thematic Mapper/Enhanced Thematic Mapper) and OLI (Operational Land Imager),with spatial resolution 60 m, MODIS (Moderate Resolution Imaging Spectro-radiometer) having spatial resolution 1 km and ASTER (Advanced Spaceborne. Thermal Emission and Reflection) at spatial resolution of 90 m are employed for retrieving LST (Brabyn et al., 2013; Ding et al., 2013; Jimenej-Munoz et al., 2003; Kloog et al., 2012; Liu et al., 2006; Sobrino et al., 2004; Tomlinson et al., 2012). Landsat data set is one of the best data available to study the association between landform composition and LST because it has fine spatial resolution and delivers multiple spectral range band data simultaneously (Ding et al., 2013; Feng et al., 2014; Sobrino et al., 2004).

The mono-window algorithm has been used to retrieve LST map from the thermal band of Landsat level 1 data. The mono-window algorithm is based on two functions, thermal radiance transfer function, and other Planck's radiance function. There were three critical parameters; emissivity, transmittance and mean atmospheric temperature included in the algorithm (Z. Qin, A. Karnieli and P. Berliner, 2001). Planck's law states that all objects, which have the temperature greater than absolute zero, emit radiation which can be expressed by the following equation:

$$\boldsymbol{B}_{\lambda}(T) = \frac{C_1}{\lambda^5 \left[\exp\left(\frac{C_2}{\lambda T}\right) - 1\right]} \qquad (2.4)$$

$\boldsymbol{B}_{\lambda}(T) = spectral\ radiance\ of\ a\ black\ body\ at\ temperature\ T\ in\ Wm^{-2}\mu m^{-1}sr^{-1}$

$C_1\ and\ C_2\ are\ Pysical\ connstants\ having\ values\ 1.191 \times 10^{8} W\mu m^{4} sr^{-1} m^{-2}\ and\ 1.439 \times 10^{4} \mu m.K, respectivly$

$\lambda = wavelength\ in\ \mu m$

Onboard Infrared sensor of a satellite viewing earth's surface measures radiation emitted by the earth and its atmosphere along the line of sight. According to Figure 2.2 (Li et al., 2013), radiance transfer equation can be written as

$$I_i(\emptyset, \varphi) = R_i(\emptyset, \varphi)\tau_i(\emptyset, \varphi) + R_{at_i}(\emptyset, \varphi) + R_{sl}(\emptyset, \varphi) \qquad (2.5)$$

$I_i(\emptyset, \varphi) = Infrared\ radiation\ recieved\ by\ sensor\ at\ TOA$

$R_i(\emptyset, \varphi)\tau_i(\emptyset, \varphi) = surface\ outgoing\ radiation\ attenuated\ by\ atmosphere$

$R_{at_i}(\emptyset, \varphi) = Atmospheric\ emission$

$R_{sl}(\emptyset, \varphi) = Atmospheric\ scattering$

$$R_i(\emptyset, \varphi) = \varepsilon_i(\emptyset, \varphi)B_i(T_s) + [1 - \varepsilon_i(\emptyset, \varphi)]R_{at_i} + 1 - \varepsilon_i(\emptyset, \varphi)R_{sl_i} + \rho_{b_i}((\emptyset, \varphi, \emptyset s, \varphi s)E_i \cos(\emptyset s)\, \tau_i(\emptyset s, \varphi s) \qquad (2.6)$$

$\varepsilon_i(\emptyset, \varphi)B_i(T_s) = Surface\ emission$

$[1 - \varepsilon_i(\emptyset, \varphi)]R_{at_i} = Surface\ reflected\ downweling\ atmospheric\ emission$

$[1 - \varepsilon_i(\emptyset, \varphi)]R_{sl_i} = Surface\ reflected\ downwelling\ atmospheric\ scattering$

$\rho_{b_i}((\emptyset, \varphi, \emptyset s, \varphi s)E_i \cos(\emptyset s)\, \tau_i(\emptyset s, \varphi s) = Surface\ reflected\ downwelling\ solar\ beam$

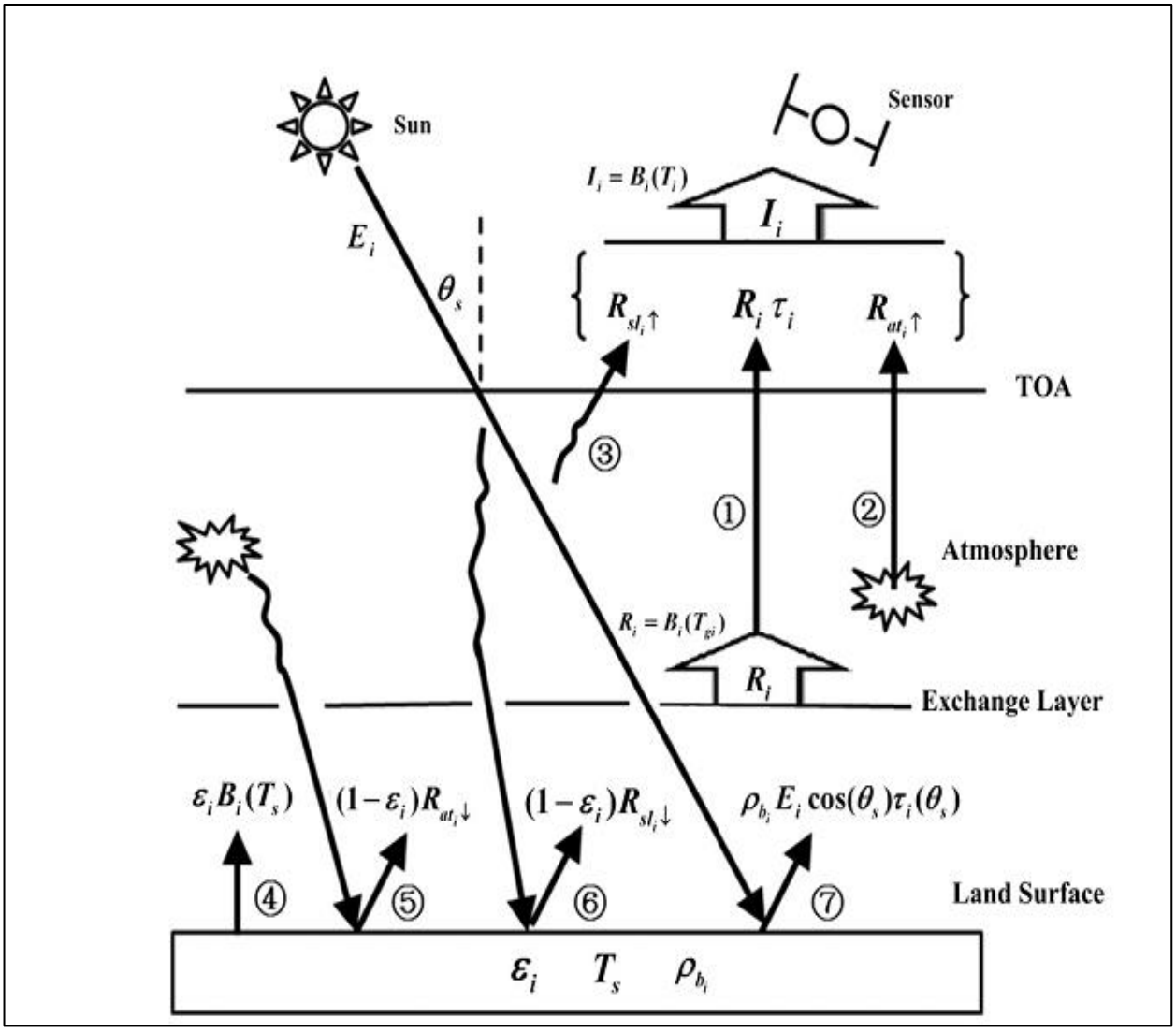

Figure 2.2 Illustration of radiative transfer equation in infrared regions *(Source: Li et al., 2013)*

[2.1.3] Urban Air Pollution with LULC change

Air pollution is defined as contamination in the ambient environment (outdoor and the indoor environment by any physical, chemical and biological agent which altered the natural properties of the atmosphere. Urban pollution includes all forms of pollution which arises due to disproportionate use of natural resources during urbanization process. In recent times urban air quality has come to be recognized as a major public health concern because the majority of the population lives in urban areas of the world. Air pollutants such as particulate matter, ozone,

oxidized form of carbon, sulfur, and nitrogen are identified as of major public health concern and are considered as criteria pollutants determining air quality of an area. LULC effects the ambient air quality by influencing local and regional meteorological parameter such as LST, humidity, wind pattern, etc.

Early studies on air pollution primarily focused at macro level on the comparison of concentration in air pollutants between the urban and rural area situated at far location (Dockery et al., 1993; Pope et al., 2002; Gao et al., 2012). Ambient air pollutants are not evenly distributed in the whole urban area and it is creating intra-city hot spots depending on LULC (Kandlikar, 2007). Nowadays, macro level research has shifted to micro-level studies such as intra-urban spatial contrast of air pollution and its exposure to the human population (Hoek et al., 2002; Beelen et al., 2008; Saraswat et al., 2013; Lee et al., 2016). Long-term exposure to ambient pollutants such as fine particulate matter, NO*x* and ozone has been associated with morbidity and premature mortality in the human population (Dockery et al., 1993; Pope et al., 2009; Brauer et al., 2012). Assessment of the health effects, due to long-term exposure to the pollutants, depends on the accurate representation of the spatial and temporal distribution of pollutant concentration. A long-term trend of pollutants concentration provides information about appropriate mitigationsteps. Mapping of long-term pollution is faced with many problems because of complex geography of emission sources and complex dispersion processes in an urban environment. Thus, the level of air pollution varies in very short distance, often few meters and kilometers (Hewitt, 1991). Sparsely situated ground-based monitoring stations data are not appropriate for comprehensive assessment of long-term exposure to an air pollutant. Satellite-based observatory data of air pollution are most suitable for long-term exposure assessment of pollutant in an urban environment. Satellite based data minimize the effect, that might arise due to regional differences (biased monitoring station) in data obtained by ground level observatory network. The satellite data facilitates studies aimed at long-term pollutant concentration exposure on regional and global scales.

In recent years, $PM_{2.5}$ has been identified as one of the leading factors for premature death. A study shows 3.2 millions premature mortality per year due to ambient $PM_{2.5}$ exposure (Lim et al., 2012). For the derivation of $PM_{2.5}$ concentration, Donkelaar et al. (2015) used GEOS-Chem chemical transport model for converting AOD to near-ground level $PM_{2.5}$ ($\mu g/m^3$). Aerosol Optical Depth (AOD) is defined as "the amount light extinction by atmospheric column due to the aerosol presence in the atmosphere." Different design characteristics of satellite and their retrieval methodology are beneficial for the specific application of data set. MODIS instrument aboard on Tera (EOS AM-1) and Aqua (EOS PM-1) satellite provide accurate daily global AOD data (Levy et al., 2007). MISR (Multi-angle Imaging Spectroradiometer) is new type of instrument on board Tera satellite designed to view the Earth with nine different angles. It provides more accurate AOD data and trend, but it has at emporal resolution of six days (required around six-day for global coverage) (Diner et al., 2005; Martonchik et al., 2009). Sea Star Spacecraft carried SeaWiFS (Sea-viewing Wide Field-of-view Sensor) applicable for more desirable temporal trend (Eplee et al. 2011), but its AOD data is less accurate on land as compared with MODIS and MISR (Petrenko and Ichoku 2013). The global annual $PM_{2.5}$ data in the three-year running grid form is derived from AOD data obtained from the combination of three satellites MODIS, MISR and SeaWiFS(http://sedac.ciesin.columbia.edu/data/set/sdei-global-annual-avg-pm2-5-modis-misr-seawifs-aod-1998-2012/data-download).

Mann-Kendell-Trend-Model (MKTM) is a widely used non-parametric statistical test for assessment of environmental time series data. MKTM statistically assesses a monotonic temporal trend (either upward or downward trend) of the variable. A monotonic upward and downward trend means that the variable increases and decreases respectively over time but the trend might be linear or otherwise. MK test is nonparametric (distribution-free) test, more suitable as compared to parametric linear regression analysis which requires normally distributed residual (Mann, 1945; Helsel, 2002; Yu et al., 2002). The details and mathematical equations of MKTM model are discussed in the methodology section in Chapter 5.

The interpolation method has been used for generating continuous surface (raster floating point format) of pollutant concentration in desired spatial resolution over a region of interest from point data set. Kriging model (Interpolation method) is a geo-statistical method of auto-correlation, which measures the geo-statistical association amongst the points and predicts missing value with high accuracy at high confidence level (Zhou et al., 2007). Kriging is based on the probability model, in which the weights are chosen for the nearby sample on the basis of bias and error variance. Kriging equation is given as follows (Chun and Griffith, 2013):

$$Y_m = X_m.\beta + \sum_{mo}\sum_{oo}^{-1}(Y_0 - X_0\beta) \qquad (2.7)$$

where, $Y_m = Missing\ value\ of\ variable$

$Y_0 = Observed\ value\ of\ variable$

$X = 1\ for\ ordinary\ Kriging\ and\ covariate\ for\ co-Kriging\beta$

$= Deviation\ from\ mean$

[2.1.4] Exposure to air pollutant to the human population

According to WHO estimates (2012), outdoor air pollution is a major environmental hazard irrespective of developed and developing world. Pollution specific diseases are distributed in a disproportionate manner all over the world, as low and middle-income countries experience the 87% premature death (WHO) estimates 3 million premature deaths per year in 2012). It has been observed that 72% of premature death due to pollutants exposure in human beings occurs because of Ischemic heart disease and strokes. Deaths by chronic obstructive pulmonary diseases (COPD)and acute lower respiratory or lung cancer are 14% of the total pollution related death. Particulate matter is a major component of air pollution which has been most closely associated with lung cancer in both urban and rural area. Mortality due exposure to fine particulate matter (diameter << 10μm) which are responsible for severe diseases such as cardiovascular, respiratory disorder and cancer in the population living in the area. As per WHO, Air Quality Guidelines

(AQG), long-term exposure of annual average concentration of $PM_{2.5} \leq 10$ µg/m^3, was chosen safe to the human population. Beside AQG value, three interim target (IT) values are defined by long-term risk assessment relative to the AQG value for $PM_{2.5}$. In IT1, an annual average concentration of $PM_{2.5}$ 35 µg/m^3 is associated with 15% higher long-term risk of mortality as compared with the AQG value. IT2 and IT3 values, 25 µg/m^3 and 15 µg/m^3 annual average concentration of $PM_{2.5}$, respectively, have a lower long-term risk of premature mortality as compared to IT1. The exposures of IT2 value level have the lower risk of premature mortality rate by 6% as compared with IT1 value level. The long-term exposure of $PM_{2.5}$ at equal to IT3 value level reduces the premature mortality rate by approximately 6% relative to IT2 value level. Figure 2.3 explains the mechanism and effect of $PM_{2.5}$ on our body. It is absorbed into target cell altering the cellular physiological and biochemical process by inducing oxidative stress, genotoxicity, inflammation etc.

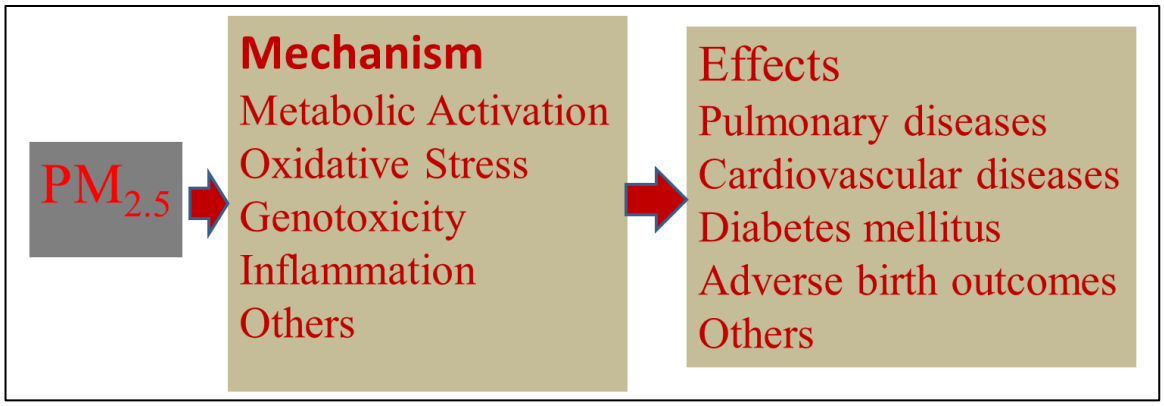

Source: (Feng et al., 2016)

Figure 2.3 The effect and mechanism of $PM_{2.5}$ on human health

Exposure of air pollutant to population is defined as any contact between the surface of a human being either outer (skin) or inner (respiratory tract epithelium) with airborne pollutant in an ambient environment. Exposure is determined by the two simultaneous occurred parameters pollutant concentration in particular region, population residing in that area and duration of contact with the population (Duan 1982; Ott 1985).

The development of a model for exposure assessment in micro-environment (intra-urban area) needed geographic data with pollutant concentration at a particular time. GIS-based model is one of the best suitable models for assessing exposure because it is capable of combining both information (geographic data and monitored data of air pollutant at a particular time simultaneously). Many models have been applied in the past for assessing intra-urban exposure of air contaminants to population such as proximity-based assessment (Venn et al., 2000), statistical interpolation (Jerrett et al., 2001a), land-use regression model (Briggs, 2000; Hoek et al., 2001), line dispersion model (Bellander et al., 2001) integrated emission meteorological models (AMD and NOAA-EPA, 2003) and hybrid model (Hoek et al., 2001; Zmirou et al., 2002). Models by need suitability requirement and implementation cost are arranged in Table 2.1. Proximity models provide crude and quick evaluation of the effect pollution has on population, but it lacks of physicochemical characteristics of pollutants. Statistical interpolation models need well-distributed dense monitoring network data and spatial statistic software. Land-use regression models provide a reliable estimation of pollution if land is used as independent variable and pollution monitoring data is treated as a dependent variable. Dispersion and integrated meteorological emission models need a substantial amount of meteorological data and more sophisticated integrated specialized software with improved expertise. A drawback of above-discussed models is that their results predict exposure of pollutant at a coarse spatial resolution and expensive in terms of data requirement and computing power. Personal monitoring is most accurate and direct way for measuring the exposure of air pollutant, but its implementation is biased (spatial and temporal biased) due to a number of sample observations (Jarrett et al., 2005). Satellite-based observatory pollutant data are more suitable for measuring exposure because an absence of spatio-temporal biasness and fine spatial resolution in data set. So, here a satellite-based observatory data has been employed for assessment of exposure to air pollutant on the human population.

Table 2.1 Details of different air pollutant exposure models

Model	Theory concept match	Limitation to health studies	Data requirement	Need for Updated data	Software expertise	Overall implementation cost	Marginal benefit	Transferability
Proximity based	Low	Crude exposure estimate	Traffic volume Distance from line source Questionnaire	Low	GIS statistics	Experiment: low Software: low Personnel: medium	Base case	Low
Geostatical	Medium	Depends on the density of monitoring network	Monitoring measurements	Low	GIS Spatial Statistics	Experiment: medium Software: medium Personnel: low	Transferability Error structure of estimate	Low
Land use regression	Medium	Depends on density of observations	Traffic volume Monitoring measurements Land use Meteorology	Medium	GIS statistics Monitor experts	Experiment: medium Software: medium Personnel: medium	Transferability Error structure of estimate	Medium
Dispersion	Medium	Extensive inputs Unrealistic assumption about pollutant transport	Traffic volume Meteorology Monitoring measurements Topography Emission of point sources	Medium	GIS statistics Monitor experts, dispersion software	Experiment: high Software: High Personnel: medium	Emphasis on process	High
Integrated meteorological emission	Medium	Course resolution	Traffic volume Meteorology Monitoring measurements Topography Emission of point sources	High	GIS statistics Monitor experts	Experiment: high Software: high Personnel: high	Emphasis on process	Medium
Hybrid (personal monitoring and one of the preceding method.	High	Small and Biased sample Depends on combination	Questionnaire Depends on combination	Depends on consideration	Personal monitor experts Survey Design Depends on combination	Experiment: high Software: depends on combination Personnel: depends on combination	Depends on combination	Low

Source :(Jarrett et al., 2005)

[2.2] Study Area

The study area, National Capital Region (NCR) of India is located between latitude 28^0 $10^{'}$ $00^{"}$N to 29^0 $00^{'}$ $00^{"}$ N and longitude between 76^0 $50^{'}$ $00^{"}$ E to77^0 $35^{'}$ $34^{"}$ E (Figure 2.4) and altitude lies between 213 and 305 m above msl. NCR is surrounded by Indo-Gangetic alluvial plain in east and north, Thar Desert in west and by Aravalli hill range in south.

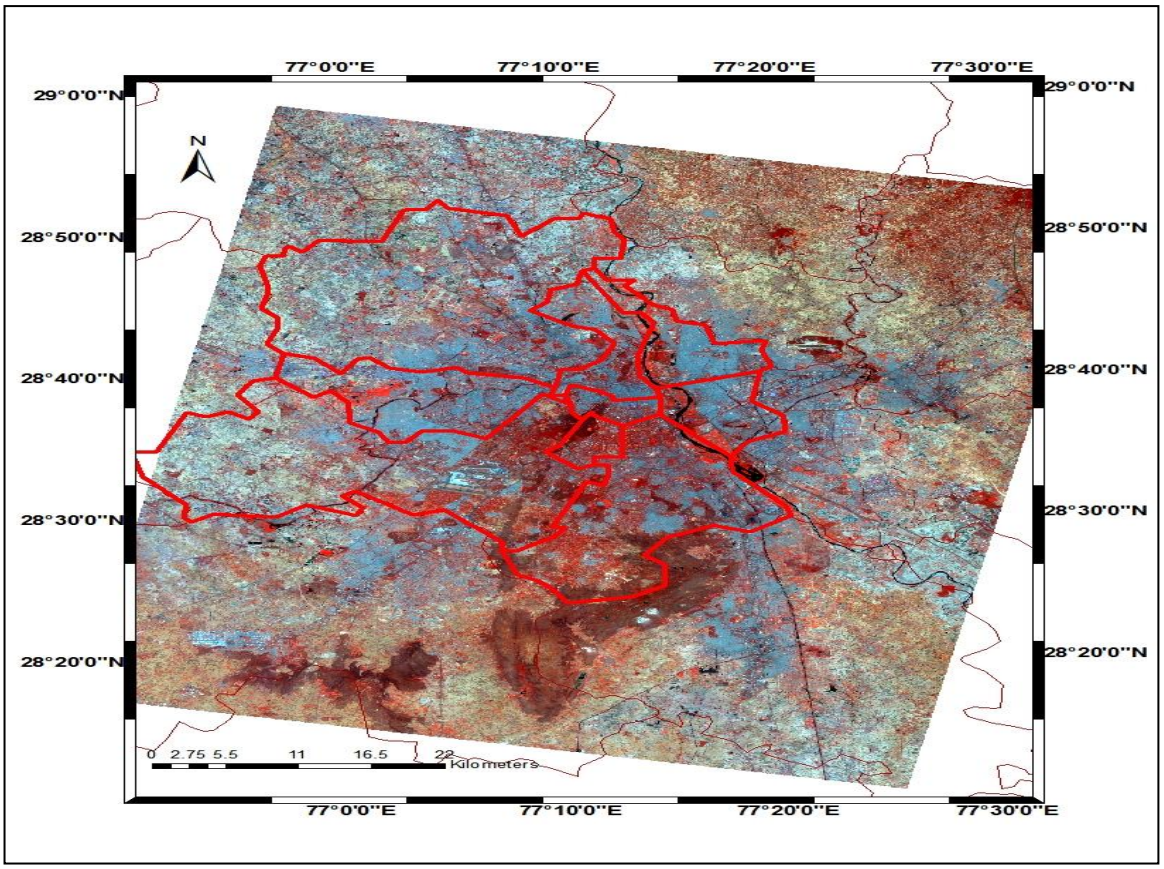

Figure 2.4 FCC image of Delhi-NCR (Landsat 8)

It lies in composite climatic zone with annual rainfall of 714 mm, of which 3/4thrainfall mostly occurs in July to September months. During the summer months, temperature ranges between 40-45 °C whereas winter temperature falling to 4-5 °C in months of December-January. Average Monthly rainfall and temperature are shown in Table 2.2. Prevailing wind direction in the region is northwesterly, except during July – mid-September when it is southeasterly. NCR is a one of the fastest growing region in India in terms of economic and population growth. As per

the 2014-15 economic survey, GDP (Gross Domestic Product) registered a growth up to 78% as compared to the 2009-10. According to census-2011, the decadal growth of population has been 21.2% during 2001 to 2011.

Despite rapid expansion of infrastructure due to ever increasing population and economic growth, the forest cover has increased in substantial amount in last 30 years in this region. In Delhi region the forest cover has increased from 0.76% of total area in 1980 to 20.22% in 2015 (state profile Delhi &Forest Survey of India).Sand and stone is primarily the mineral present in NCR which is useful for construction activities. After 1984 stone quarries have been shut down in ecological sensitive ridge area. A variety of soils are present in NCR region because its geographical location and geomorphological characteristics. These soils have entirely different properties compared to soils present in the alluvial plains.

Table 2.2 Annual (monthly average) temperature and rainfall in Delhi-NCR

Months	Temperature (Max) in ºC	Temperature (Min) in ºC	Rainfall (mm)
January	21	07	25
February	24	10	22
March	30	15	17
April	36	21	07
May	41	27	08
June	40	29	65
July	35	27	211
August	34	26	173
September	34	25	150
October	35	19	31
November	29	12	01
December	23	08	05

Source: *State Profile. http://delhi.gov.in/DoIT/DOIT_DM/state%20profile.pdf*

[2.3] Methodology

For population estimate, gridded 1 km (30 arc-second) spatial resolution population estimate data from SEDAC has been used (Socioeconomic Data and Applications Center, 2016) http://sedac.ciesin.columbia.edu/data/set/gpw-v4-population-count/data-download.Three different Landsat L_1T cloud cover free data of Landsat 5 (TM), 7 (ETM^{+}), and 8 OLI have been taken from USGS online archived GLOVIS (http://glovis.usgs.gov/) for NCR of India. Data pre-processing has been done with ENVI software on the information provided in metadata file of Landsat image. For LULC classification, a well-known parametric MLC algorithm has been employed for supervised spectral signature extraction of all Landsat images in Arc-GIS software. The thermal Infrared band (10.4-12.4 µm) data of Landsat images have been used for retrieval of LST. The extraction of LST has been carried out using mono-window algorithm. For $PM_{2.5}$ concentration, data set contain floating point value of three-year running mean grids from 1998 to 2012 has been obtained from http://sedac.ciesin.columbia.edu/data/set/sdei-global-annual-avg-pm2-5-modis-misr-seawifs-aod-1998-2012/data-download.

Mann-Kendell trend test at 95% confidence level employed for statistical significance and trend analysis of $PM_{2.5}$ concentration at 42 points located in different LULC types. The $PM_{2.5}$ point data has been converted to a raster floating point data format in 30 m spatial resolution by an ordinary Kriging model (Interpolation method) run in Arc-GIS software. Overlaying technique is employed between population and $PM_{2.5}$ concentration raster map for exposure assessment to human population. Data sources and methodologies have been discussed in detail in subsequent chapters 3 to 5.

Chapter-3 *Population Induced LULC changes*

[3.1] Introduction

In the recent decades, industrial and service based economic developments along with corresponding increase of population have rapidly changed the Land-use and Land-cover (LULC) composition in the urban areas. Urbanization process has picked up momentum since last decade (Balcik 2013). This phenomenon is often associated with increased levels of residential, commercial, industrial and transportation activities concentrated within a relatively small geographical areawhich alters the Land-use and Land-cover (LULC) composition of that area. Urbanization leads to the loss of vegetation cover and agricultural area in order to fulfill human needs (Balcik 2013; Dewan and Yamaguchi 2009; Ward et al. 2016).

National Capital Region (NCR), situated in the north-western Indo-Gangetic plains, is one of the fastest growing regions in India in terms of economic and population growth. As per the 2014-15 economic survey, NCR's Gross Domestic Product (GDP) grew up by 78% as compared to the 2009-10. According to census-2011, the NCR recorded a decadal growth of 21.2% in its population from 2001 to 2011.The fast growing economy and population has induced significant alteration in the Land-use and Land cover (LULC) of entire NCR.

In the present study (Chapter 3), an attempt to find out the population induced spatio-temporal changes in LULC of NCR during 2003-2014 has been made using satellite data (Landsat). In this chapter, two objectives were identified and fulfilled: 1) Quantification of spatio-temporal changes in LULC pattern during 2003 to 2014. 2) Applying GIS-based modeling approach for evaluating spatial and temporal changes of satellite derived population in studied area during 2000-2015.

[3.2] Data processing and Methodology

[3.2.1] Data Sources

Three different Landsat L_1T datasets [(Path146/Row040) (Landsat 7 ETM^+ (10 May 2003), 5 TM (18 May 2009) and 8 OLI (16 May 2014)] have been taken from USGS online archived GLOVIS (http://glovis.usgs.gov/) portal for NCR of India. Landsat 5 TM data consists of six bands in the Visible Region (VR) and Near Infrared Region (NIR) with 30 m spatial resolution and one band in the Thermal Infrared Region (TIR) with 120 m (resampled 30 m) spatial resolution. Landsat 7 provides eight bands, i.e. three each in the VR and NIR with 30 m spatial resolution, one in TIR with 60 m (resampled 30 m) spatial resolution and one panchromatic band with 15 m spatial resolution (http://LANDSAT. usgs.gov/band_ designations_ LANDSAT_ satellites.php). The OLI sensor gathers image in eight VR, NIR and short wave infra-red (SWIR) with a 30 m spatial resolution, one 15 m panchromatic and two 100 m (30m resampled) TIR bands (data users' handbook of Landsat 8)**.** Landsat images are one of the most suitable data for LST analysis and LULC changes over time because of the fine spatial resolution in VR, NIR, SWIR and TIR spectral bands.

The toposheets of Delhi-NCR region, having 1:50000 m scale, were taken from Survey of India (SOI) outlet for image to image registration of Landsat images. **G**ridded population estimates having spatial resolution of approx. 1 km x 1 km (30 arc-second) were also obtained from Socioeconomic Data and Applications Center (SEDAC) website http://sedac.ciesin.columbia.edu/data/set/gpw-v4-population-count/data-download. The data product GPWv4 (Gridded Population of the World Version 4) consists of human population count estimate based on national censuses and population registers worldwide. The population count grids contain total number of persons per grid cell allocated by gridding algorithm utilizing 12.5 million sub-national and national administrative units (http://sedac.ciesin.columbia.edu/data/collection/gpw-v4).

[3.2.2] Data preprocessing

For the present study, data free from cloud cover has been procured. Spatial registration has been done in ENVI tool (GCP image to image registration) with digitized toposheet (resampled 30 m spatial resolution) of NCR by choosing 15 control points. The selection of 15 control points has been carried out based on unchanged structures for long time such as road intersection and old buildings.

Landsat images are processed as absolute radiance using 32-bit unit floating point which were further converted to 16-bit integer (Digital Number unit) value in level 1 product (data users' handbook of 8.The conversion of integer value to original 32-bit unit floating point spectral reflectance has been done by scaling factor allocated in metadata file of each band data in ENVI (Band Math tool) software using following equations discussed below:

$$P_P = \frac{M_P . Q_{cal} + A_P}{\sin(\Theta)} \qquad (3.1)$$

M_P is reflectance multiplicative scaling factor for the band; A_P is reflectance additive scaling factor for the band and Θ is solar elevation angle (Landsat 8 Handbook).

[3.2.3] Image classification and accuracy assessment

A well-known parametric Maximum Likelihood Classifier algorithms (MLC) was employed for supervised spectral signature extraction of all images. In each composite bands, image 100 ROI (Region of Interest) were chosen to establish each LULC type having all spectral signature adequately represented in the training statistics. Different band combination (R.G.B) was employed for distinct LULC for ROI selection in Arc-GIS image classification tool (training sample manager) as per detail given in Table 3.1. (https://esri.com/esri/arcgis/2013/07/24/band-combinations-for-landsat-8)

Table 3.1 RGB bands combination for ROI selection

Landform	R.G.B bands combination for TM & ETM^{+} Image	R.G.B bands combination for OLI Image
Built-up Area	7.5.3	7.6.4
Water Bodies	4.5.3	5.6.4
Green Vegetation	4.5.1	5.6.2
Rocky Area	5.4.3	6.5.4
Bare Land	4.5.3	5.6.4

Five distinct LULC types (Built-up area, Water body, Green vegetation, Rocky area and Bare land) were identified in all three images acquired (Table 3.2). The rocky area situated at south to central ridge covered by sparse scrub vegetation showed distinct spectral signature identified in individual landform. The urban areas are composed of asphalt and concrete covered road, buildings and all types of impervious surfaces. The Bare land included dry land, agricultural land without crops, landfill site etc.

Table 3.2 LULC types for classification

LULC Type	Abbreviations	Descriptions
Built-up Area	BA	Road, Building and Residential area
Water Bodies	WB	River, Ponds and Drainage system
Green Vegetation	GV	Forest, Farmland tree, Roadside tree and Vegetation around water bodies.
Rocky Area	RA	Rocky area and Sparse scrub vegetation
Bare Land	BL	Dry desert land, Open un-vegetated land, Bare soil and Sandy area

Assessment of classification accuracy is indispensable for accurate estimation of change detection in each classified images. Accuracy assessment procedure has been carried out with

assigned ancillary data such as digitized toposheet of NCR and Google earth image as reference. Firstly, 200 random points were created from subset image of study area and then assigned each random point a value from digitized toposheet (for TM and ETM^{+}) and Google earth image for OLI data. Extract the value of each LULC type for each 200 assigned random points from classified image. Accuracy assessment was done to create confusion matrix between assigned point and extracted value of each LULC type. It was observed that the overall accuracy with Kappa coefficient for corresponding three classified images ETM^{+}, TM and OLI are 0.89, 0.93 and 0.95, respectively. The detection of LULC changes over the studied time period has been carried out using a post-classification differentiation method by randomly selecting 10000 points in each classified image. Gridded population estimate at 1km spatial resolution is resampled onto 30 m for overlaying with LULC map created in Arc-GIS software. We have adopted overlaying technique between population map and LULC map for analyzing population induced spatio-temporal changes of LULC in NCR region.

[3.3] Results and Discussion

[3.3.1] Spatial and temporal pattern of human population

Gridded population estimate at 1 km spatial resolution is manually classified into five classes on the basis of number of person per grid cell. These five classes are classified as Sparse, Lower, Moderate, Higher and Highest density which comprise of <500, 500-1500, 1500-2500, 2500-3500 and >3500 persons per grid cell respectively. The spatial and temporal patterns of human population in the period 2000-2015 have been shown in Figure 3.1(a-c). It can be observed from Figure 3.1(a) that Highest density class of population dominated a major part of Delhi in the year 2000.Only the northern part of Delhi shows Moderate population density class and the south-western part shows the High population density class. An examination of Figure 3.1(b) reveals that the south-western part of Delhi which was in the High Population density class in the year 2000, predominantly changed to the Highest population density class in the year 2010, while the northern part of Delhi still remained in the Moderate Population density class. In the year 2015

(Figure 3.1(c)), the entire south-western part of Delhi came under the Highest population density class, while the northern part came under the High population density class. It is also seen that by the year 2015, almost entire Delhi except its northern part was under the Highest population density class. Spatial and temporal change in population can be observed from the Figure 3.1 (d-e). It is seen that almost entire Delhi-NCR witnessed increase in the population from 2000 to 2015, but this increase was more pronounced along the west-central-eastern parts of Delhi. Figure 3.1(f) shows the percentage of total area covered by different population density classes in the years 2000, 2010 and 2015. It can be observed that percentage of total area in the Highest population density class has undergone significant increases both in 2010 and 2015 over the previous years. On the contrary, percentage of total area in the Sparse population density class has undergone significant decrease during this period. A decrease in the percentage of total area under the other classes of population density is also noticed from 2000 to 2015. These trends are witnessed because more and more areas under other classes changed to the Highest class of population density during this period.

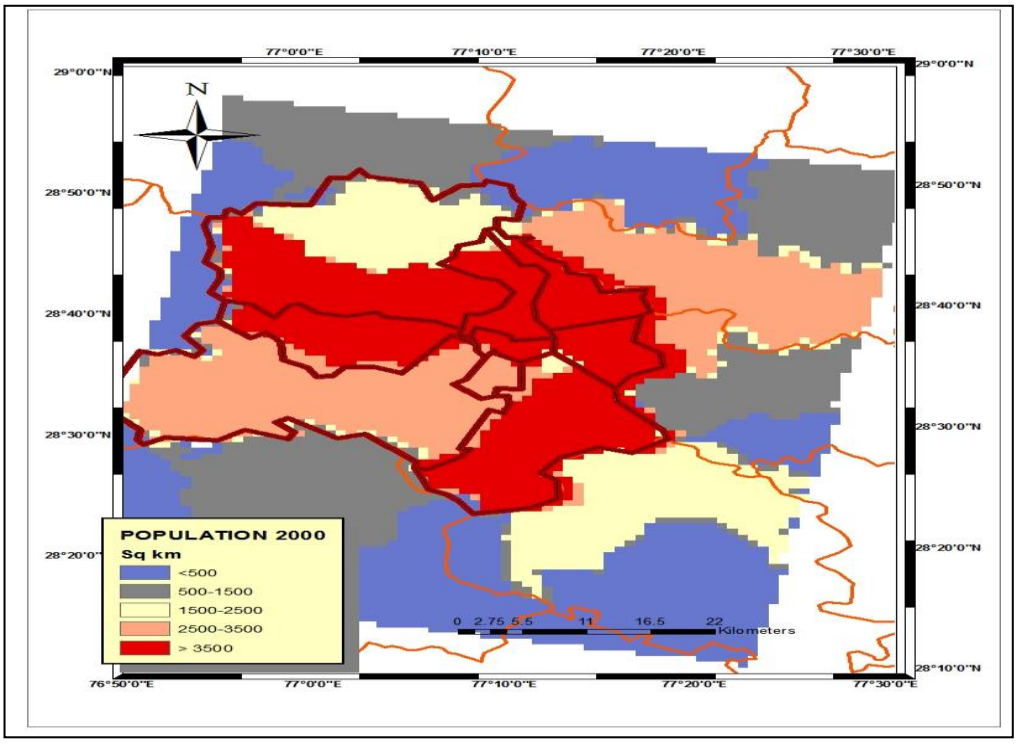

Figure 3.1 (a) Spatial distribution of population in 2000

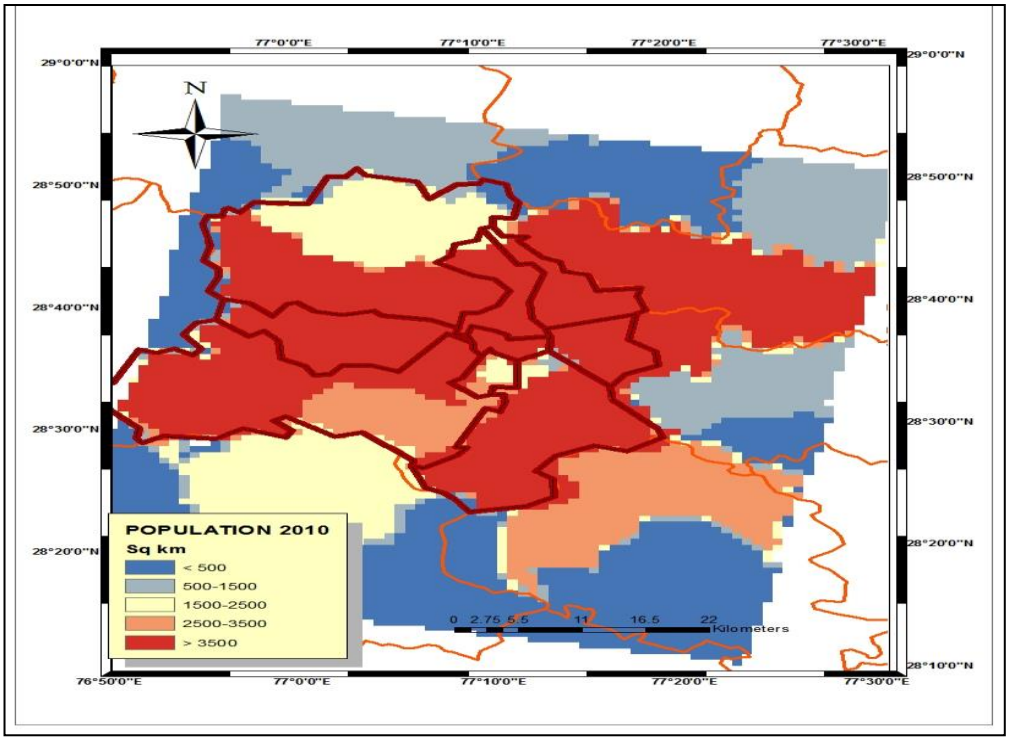

Figure 3.1(b) Spatial distribution of population in 2010

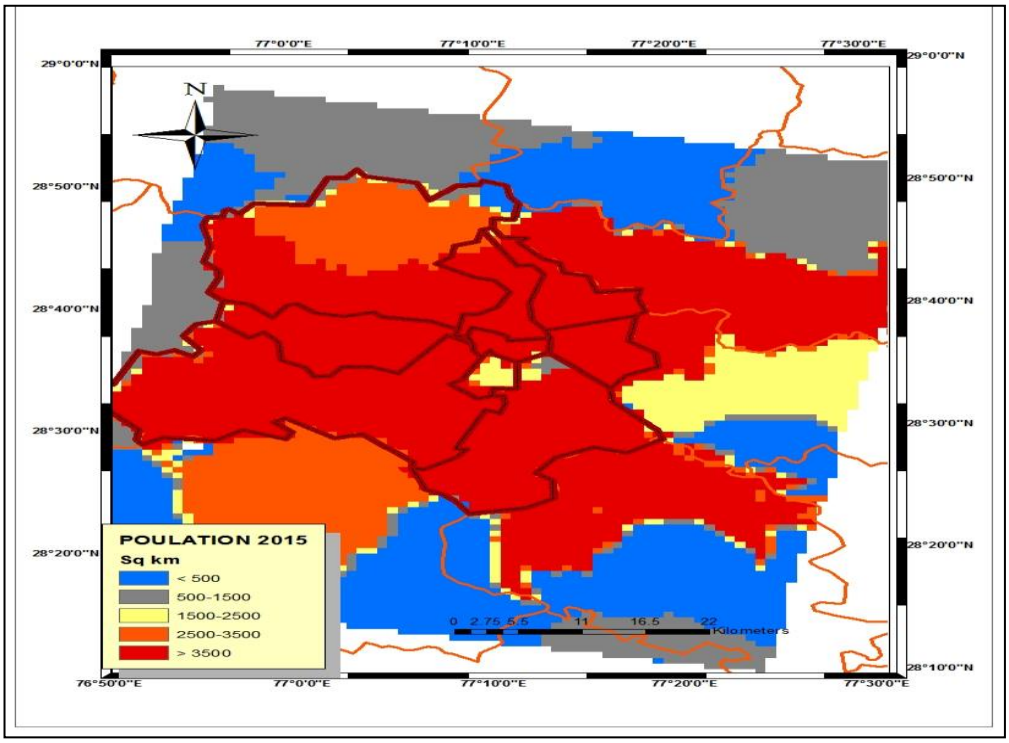

Figure 3.1(c) Spatial distribution of population in 2015

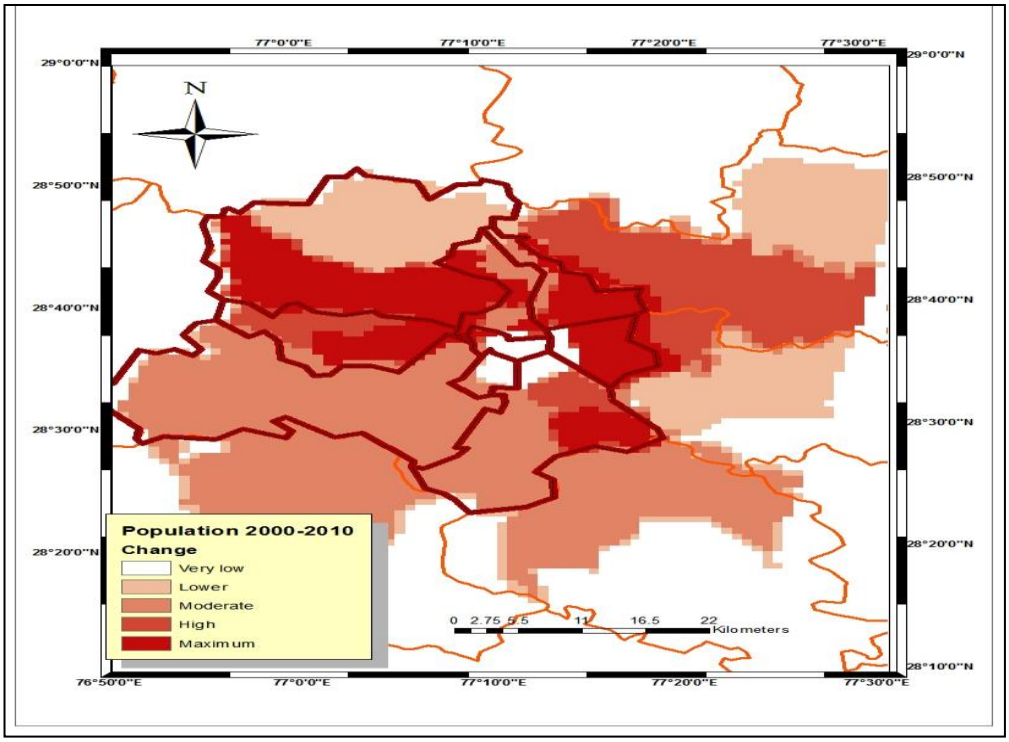

Figure 3.1(d) Spatial and temporal changes of population in 2000-2010

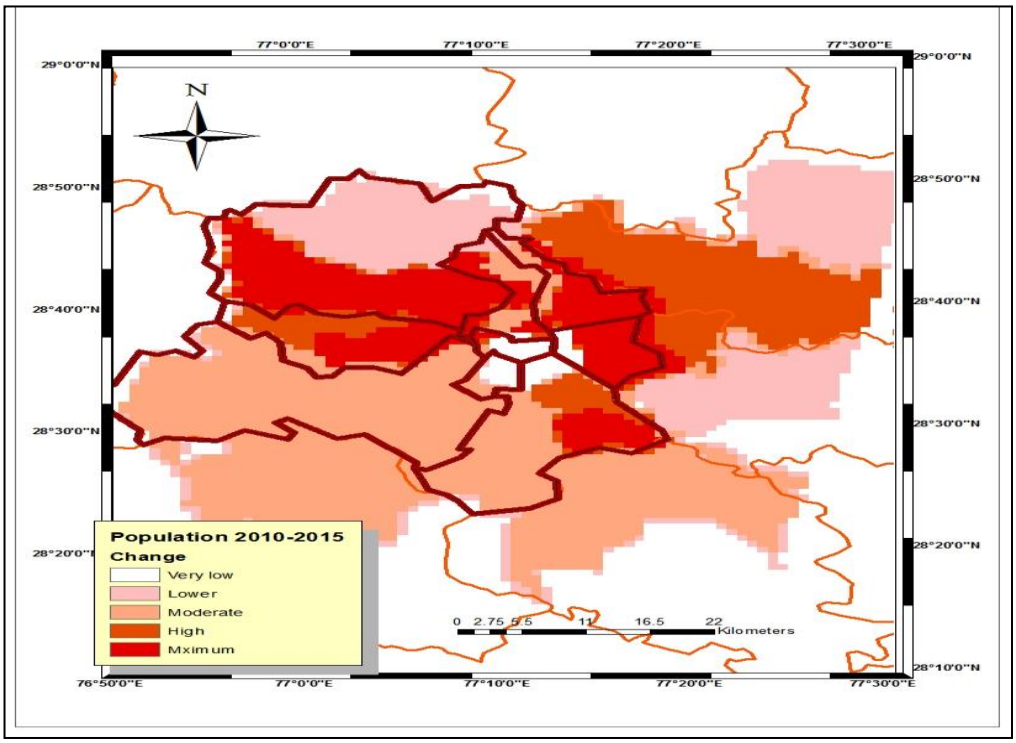

Figure 3.1(e) Spatial and temporal changes of population in 2010-2015

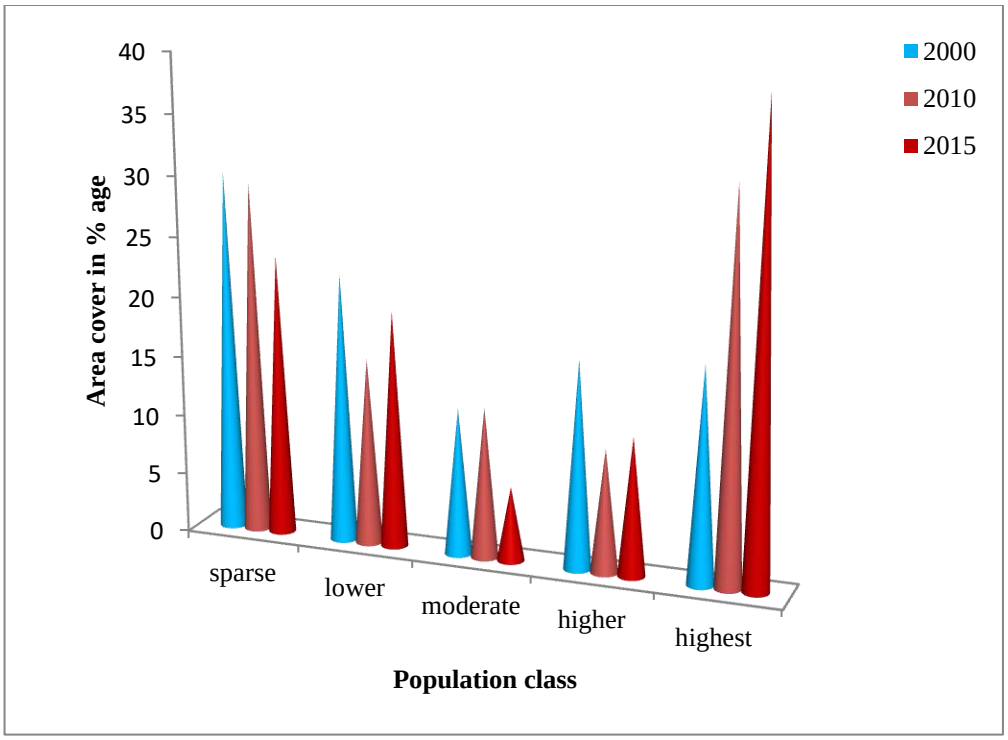

Figure 3.1(f) Area cover by different population density class during 2000-2015

[3.3.2] Spatial and temporal change of different LULC

Spatial pattern of distinct LULC over Delhi- NCR for three different years for the month of May are shown in Figure 3.2 (a-c). Area retrievals from the LULC maps show that during the period 2003 and 2009, built-up area expanded from 5.84% to 10.26% (almost double). Further, it can be seen that the green vegetation area has grown from 8.72 to 11.05 % primarily in central and south ridge area during the period 2003 to 2009. Rocky area has decreased from 12.99 to 8.41 % from year 2003 to 2009 because of rapid expansion of urban built-up area and conversion of sparse scrub vegetation into green vegetation due to artificial plantation and natural processes. Further, it can be observed that Bare land and water body which contributed 72.04 % and 0.39 % respectively during the year 2003 got changed to 69.35 % and 0.91% respectively during 2009. Bare land has been converted into built-up area in Delhi's surroundings mainly in east and north-east direction which is mostly agricultural land and fallow land. In south, south-west and west direction, built-up area has developed at cost of rocky area (ridge area) and dry non-arable land

(desert land). Also, a slight increase in water body area has been observed in year 2009 due to increase in average rainfall from 6 mm in May 2003 to 65.8 mm rainfall occurred in 2009 (Statistical Abstract Delhi 2012). Due to this rainfall most of the pits and dried ponds were full with water in 2009 which is detected as water body area rather than Bareland detected in 2003.

Further, it can be observed in year 2014 that the contribution of built-up area, water body, green vegetation, rocky area andBareland were found to be 11.78%, 0.51%, 14.83%, 4.19% and 68.67 %, respectively. It was found that built-up area expansion rate in period between 2009 and 2014 reduced in comparison to 2003-2009 period. This was due to slow and stagnant economic growth and strict enforcement of government rules and regulations related to construction activities in these ecological sensitive zones such as ridge area in the foothills of Aravalli hill (Statistical Abstract Delhi, 2012 &2014). Green vegetation zone has expanded in rocky area due to conversion of scrub into green vegetation in central and southern ridge area in NCR.Overall, significant increase in built-up area (84.58%), green vegetation (58.60%) and water body (30.76%) has been observed from the year 2003 to 2014. The rocky area and Bareland decreased by 75% and 0.5%, respectively during this period. Summary of the composition of major LULC changes that occurred over past 11 years is depicted in Figure 3.3 and 3.4.

Overlaying technique has used in Arc-GIS software to establishes a relation between population density and LULC types.We observed that similar spatial patterns follow theHighest density class and built-up area changes in between 2003 to 2014.

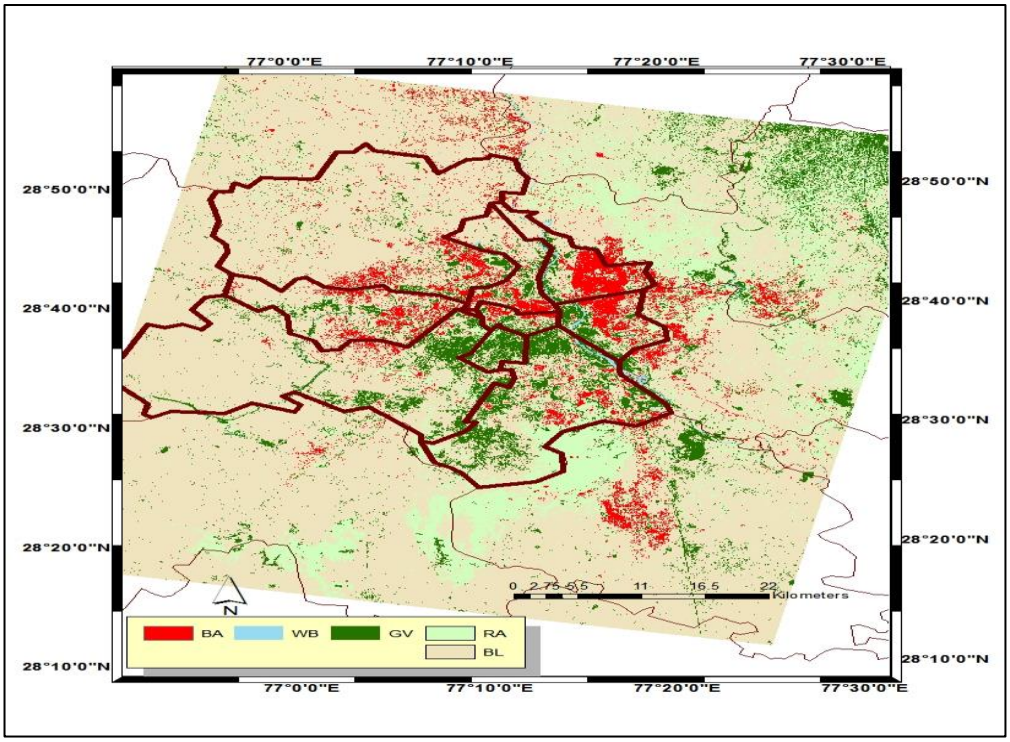

Figure 3.2 (a) Spatial distribution of LULC types in May 2003 in Delhi-NCR

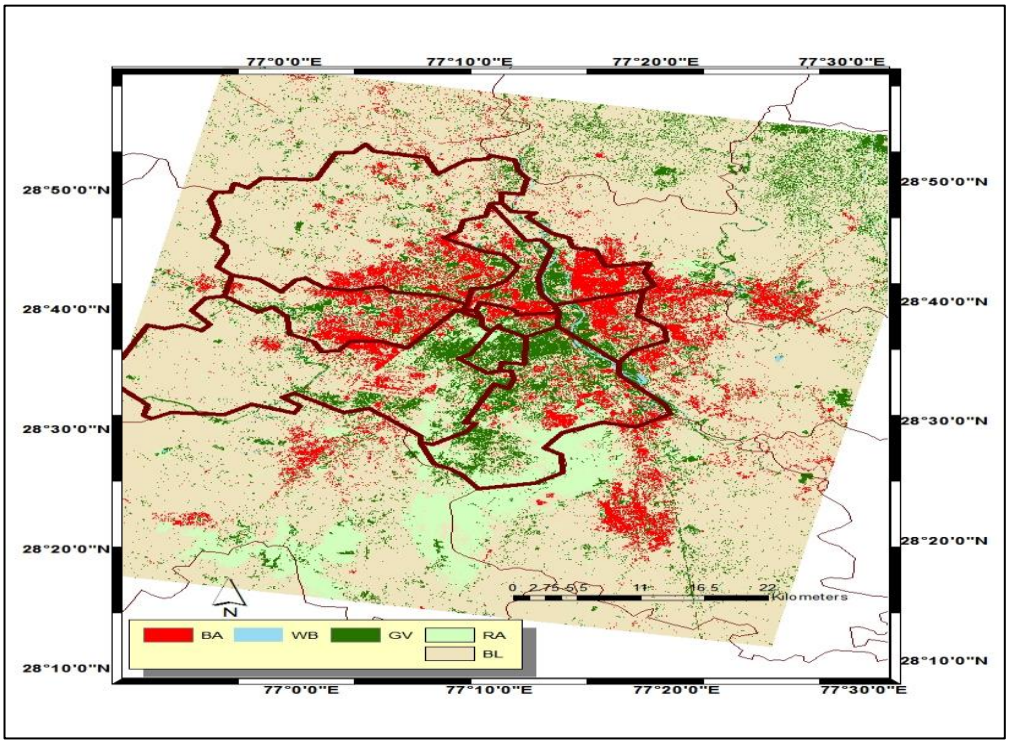

Figure 3.2 (b) Spatial distribution of LULC types in May 2009 in Delhi-NCR

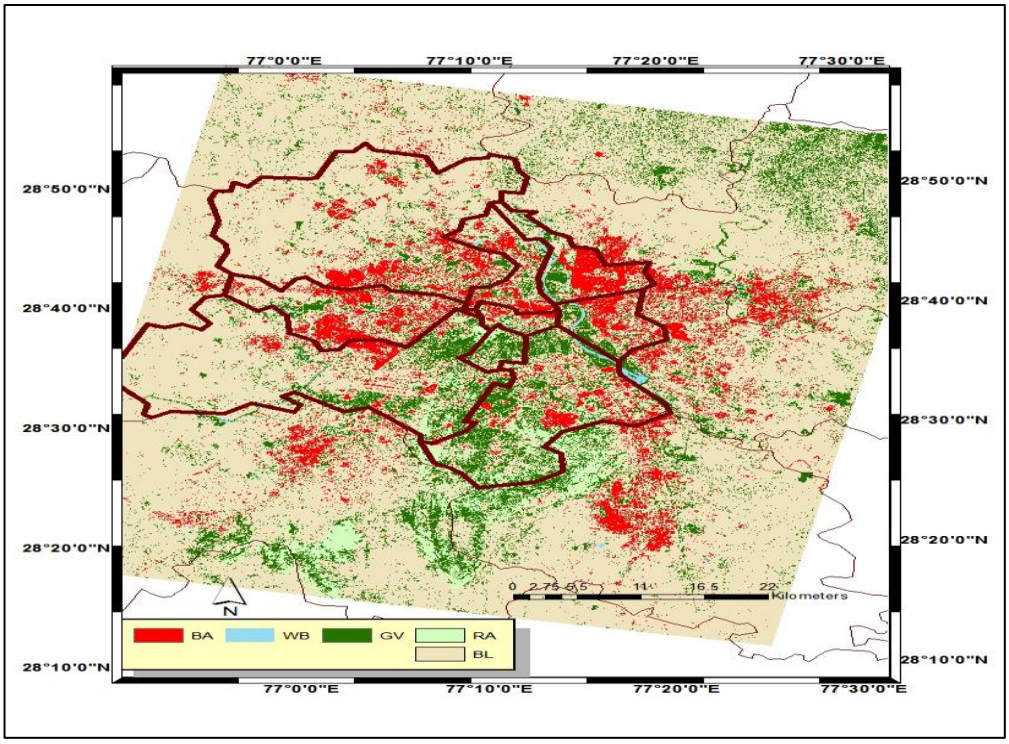

Figure 3.2 (c) Spatial distribution of LULC types in May 2014 in Delhi-NCR

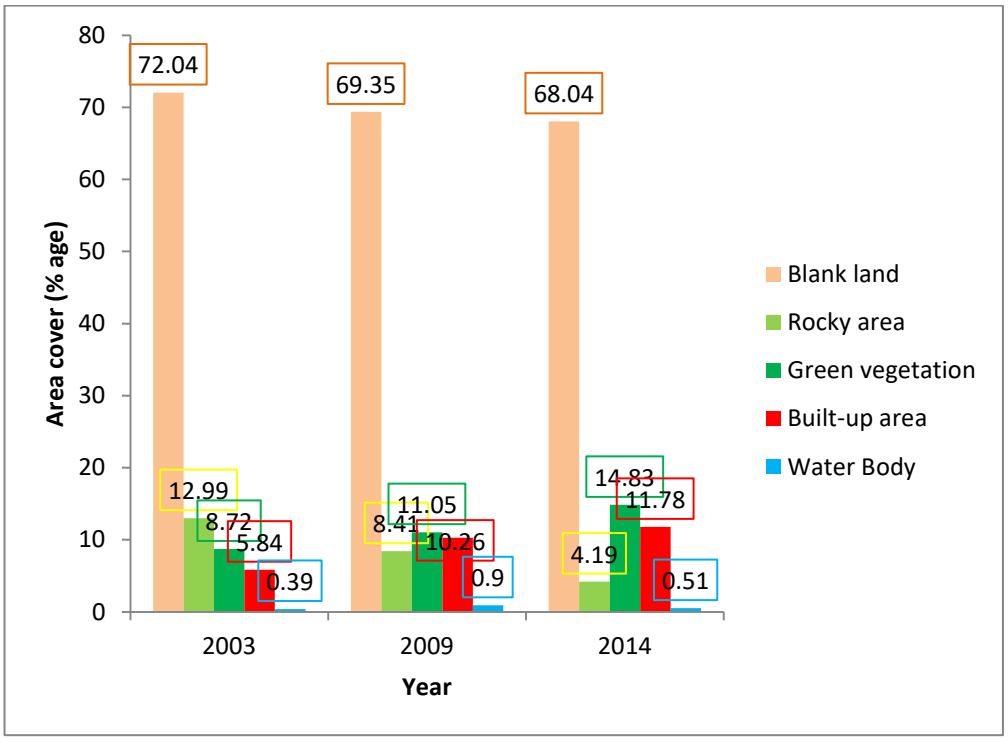

Figure 3.3 LULC area covers in percentage during 2003-2014

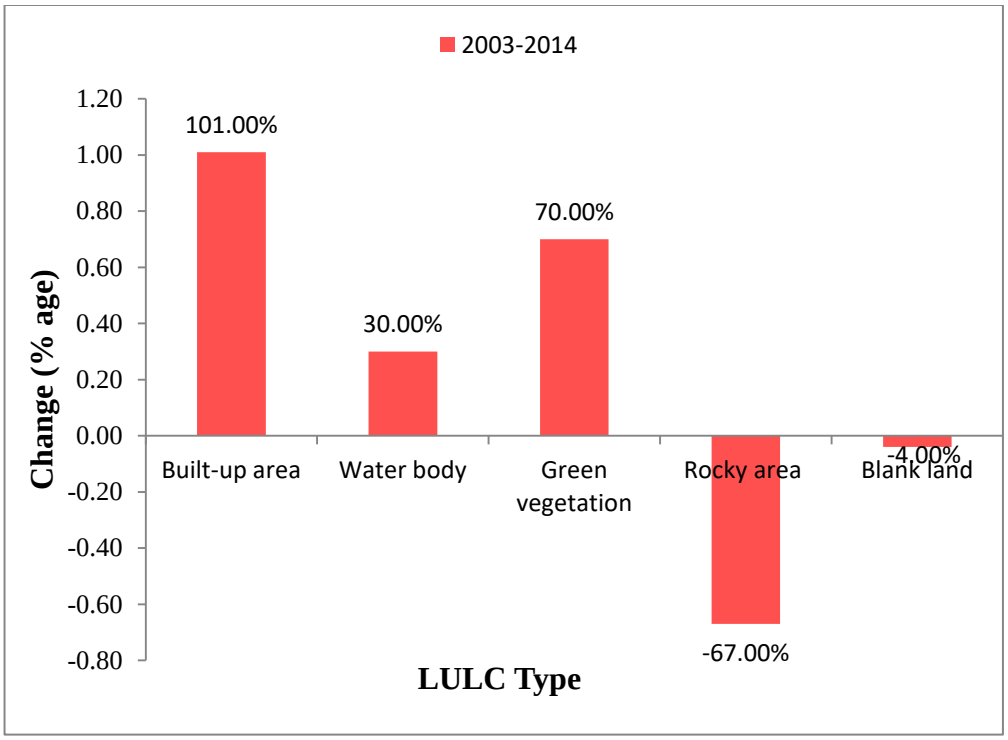

Figure 3.4 Change in different LULC in %age in during 2003-2014

[3.4] Summary

In the present study, it is found that enormous changes have occurred in the spatial pattern of human population in NCR during the period 2000-2015. Percentage of total area covered by different population density classes decreased by 21.8%, 11.95%, 49.50% and 33.67% respectively for Sparse, Lower, moderate and high population density classes. On the other hand, the Highest population density class is found to increase by 118.05% during 2000-2015. Further, significant changes in spatio-temporal patterns of land use and land cover are observed over the study area during the period 2003 to 2014. It is found that there is a noticeable increase in Built-up area by 101% and Green vegetation cover area by 70% at the cost of ridge area (rocky area) and Bare land area which decreased by 67% and 4% respectively. In addition, similar spatial and temporal patterns are seen in the built-up area and highest density population classes as both shows a significant increase over the 10-15 year period.

Chapter-4 *LST and its relation with LULC changes*

[4.1] Introduction

The increasing pace of global urbanization influences the net productivity, biodiversity, weather and climate at local, regional and global arena (Han and Xu 2013; Lasanta et al. 2012; Mohan and Kandya 2015; Vorovencii 2015; Yin et al. 2010). The conversion of one type of LULC to another type affects the process of energy exchange between the terrestrial land and the atmosphere (Wang et al. 2016).

A LULC composition has changed due to rapid expansion of urban area at the cost of natural LULC and has influenced the local meteorological and climatological parameters such as Land Surface Temperature (LST) and air temperature (Ding et al. 2013; Feizhang et al. 2016; Jones et al. 1990; Wang et al. 2016; Weber et al. 2014; Zhang et al. 2013). LST is one of the key tool to study climatic variability and other environmental parameters (Ayanlade 2016; Feng et al. 2014; Nguyen et al. 2015; Pichierri et al. 2014).The changes in LULC influences the LST due to the partitioning of sensible and latent heat flux of different LULC's (Dubreuil et al. 2011).

The enhancement in scientific development of remote sensing techniques by different national and international agencies provides an approach for precise spatio-temporal assessment of land surface phenomenon. Many studies have been done to retrieve LST from remotely sensed images such as Landsat TM/ETM$^+$ (Thematic Mapper and Enhanced Thematic Mapper), MODIS (Moderate Resolution Imaging Spectro-radiometer) spatial resolution 1 km and ASTER (Advanced Space borne Thermal Emission and Reflection) spatial resolution 90 m (Brabyn et al. 2013; Ding et al. 2013; Jimenej-Munoz et al. 2003; Kloog et al. 2012; Liu et al. 2006; Sobrino et al. 2004; Tomlinson et al. 2012). Numerous studies have reported that TM/ETM$^+$ data set is one of the best data available to study the association between LULC composition and LST because its fine spatial resolution and it delivers multiple spectral range band data simultaneously (Ding et al. 2013; Feng et al. 2014; Sobrino et al. 2004).

The present study focusses on influence of LULC composition changes on spatio-temporal pattern of LST during the period of 2003 to 2014 in National Capital Region (NCR) of India. In present chapter, it is an attempt to achieve two prime objectives i.e. 1) Spatio-temporal changes of LST retrieved from Thermal infra-red band of Landsat L_1 images data over NCR region during 2003- 2014 period. 2) To study relationship between spatio-temporal LULC pattern changes due to urbanization (discussed in chapter 3) and LST class over the study region.

[4.2] Data processing and Methodology

[4.2.1] Retrieval of land surface temperature

For retrieving land surface temperature, the thermal Infrared band number 6 (low gain) (10.4-12.4 μm) was used for TM and ETM^+ data and band 10 was used for OLI data. The extraction of LST has been carried out using mono-window algorithm (Qin et al., 2001) and pre-processing of data has described in Handbook of Landsat 7 and 5. For derivation of spectral radiance, Eq. 3.1 (discussed in chapter 3) has been used for TM and ETM^+ band whereas, for OLI b and DN values were converted to spectral radiance by using following equation (Eq. 4.1):

$$L_\lambda = M_L . Q_{cal} + A_L \qquad (4.1)$$

where L_λ is Spectral radiance in $W/m^2.sr.\mu m$, Q_{cal} is level 1 pixel value in DN, M_L and A_L are multiplicative and additive scaling factor for the band 10^{th} of OLI.

Further, the Brightness Temperature (BT) has been retrieved (in Kelvin) at top of the atmosphere from spectral radiance using Eq. 4.2 under assumption of one unit emissivity.

$$BT = \frac{K_2}{\ln(\frac{K_1}{L_\lambda} + 1)} \qquad (4.2)$$

where K_1 and K_2 are thermal conversion constant consisting of metadata file whose values are 660.76 and 1260.56 for TM band, 666.09 and 1282.71 for ETM^+ band, and 774.89 and 1321.08 for OLI band in $Wm^{-2}\ sr^{-1}\ \mu m^{-1}$, respectively. The above derived BT does not reflect the LST value because each LULC has distinct emissivity. Therefore, the BT of black body should be translated into emissivity corrected LST by the following equation 4.3 (Ding et.al. 2013).

$$LST = \frac{(BT)}{1 + \frac{\lambda(BT)}{\rho}.\ln \varepsilon} \quad (4.3)$$

where ε is the Land Surface Emissivity (LSE), λ is wavelength of emitted radiance, $\rho = \frac{hc}{\kappa} = (1.438 \times 10^{-2}\ \text{mK})$, κ is Stefan-Boltzmann constant, h is Planck's constant and c is the velocity of light. LSE with corresponding LULC type were estimated through relationship between emissivity and Normalized Difference Vegetation Index (NDVI). Empirical approaches applied to established relationship between NDVI and LSE reported by Eq. 4.4(Ding et.al. 2013).

$$\varepsilon = 0.004P_V + 0.986 \quad (4.4)$$

where ε is surface emissivity and P_V is the vegetation proportion. P_V was computed from NDVI using following Eq.4.5 (Carlson et al., 1997).

$$P_V = \left[\frac{(NDVI) - (NDVI)_{min}}{(NDVI)_{max} - (NDVI)_{min}}\right]^2 \quad (4.5)$$

where NDVI, $NDVI_{max}$[(ETM^+=0.54) (TM= 0.60) and (OLI= 0.52)] and $NDVI_{min}$[(ETM^+= -0.05) (TM= -0.15) and (OLI= -0.12)] computed from spectral reflectance of band 4 (NIR) and 3 (red) in ETM^+ and TM image. In OLI image, band 5 (NIR) and 4 (red) reflectance have been used for NDVI calculation using following equation:

$$NDVI = \frac{\Gamma(NIR) - \Gamma(R)}{\Gamma(NIR) + \Gamma(R)} \quad (4.6)$$

NDVI maps were generated using this equation for the month of May for the years 2003,2009 and 2014 which are shown in Figure 4.1(a), 4.1(b) and 4.1(c), respectively. It was observed from the maps that NDVI was found very low in the surroundings of Delhi for the month of May in all these three years except in the region lying north-east to the Delhi's surroundings. This is due to the reason that in the month of May, Rabi crop has been cut from the surroundings of Delhi. Further, in the north-east region NDVI was found to be somewhat higher in all the years which isdue to the reason that the sugarcane farming is dominant in this region almost in every season of the year.

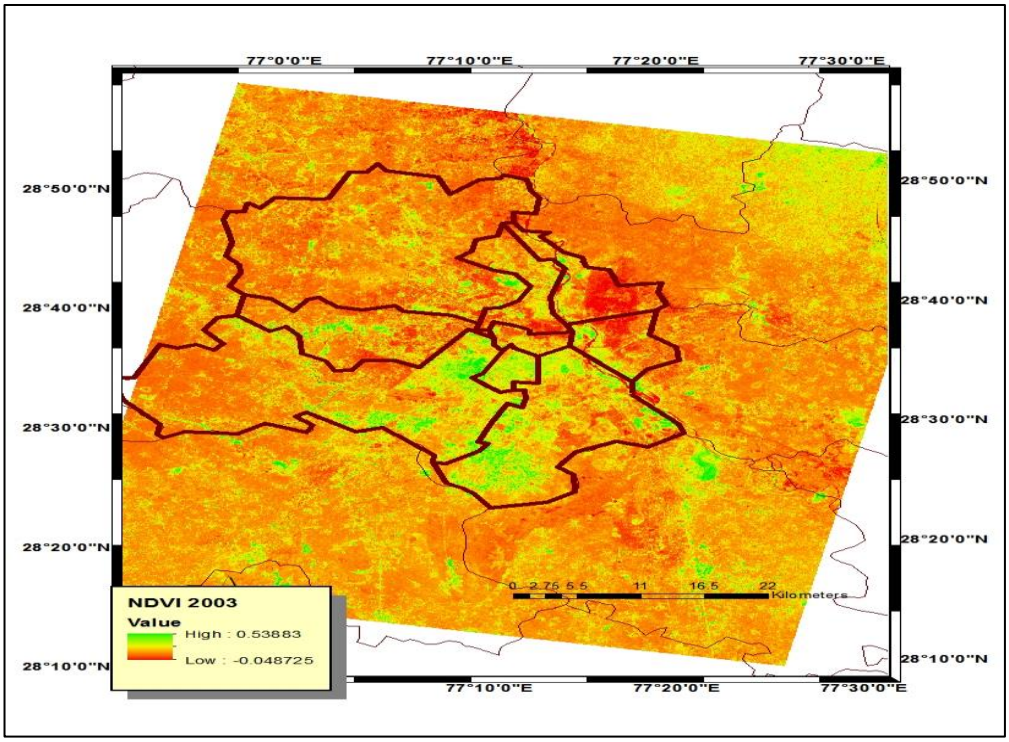

Figure 4.1(a) NDVI during May 2003 in Delhi-NCR

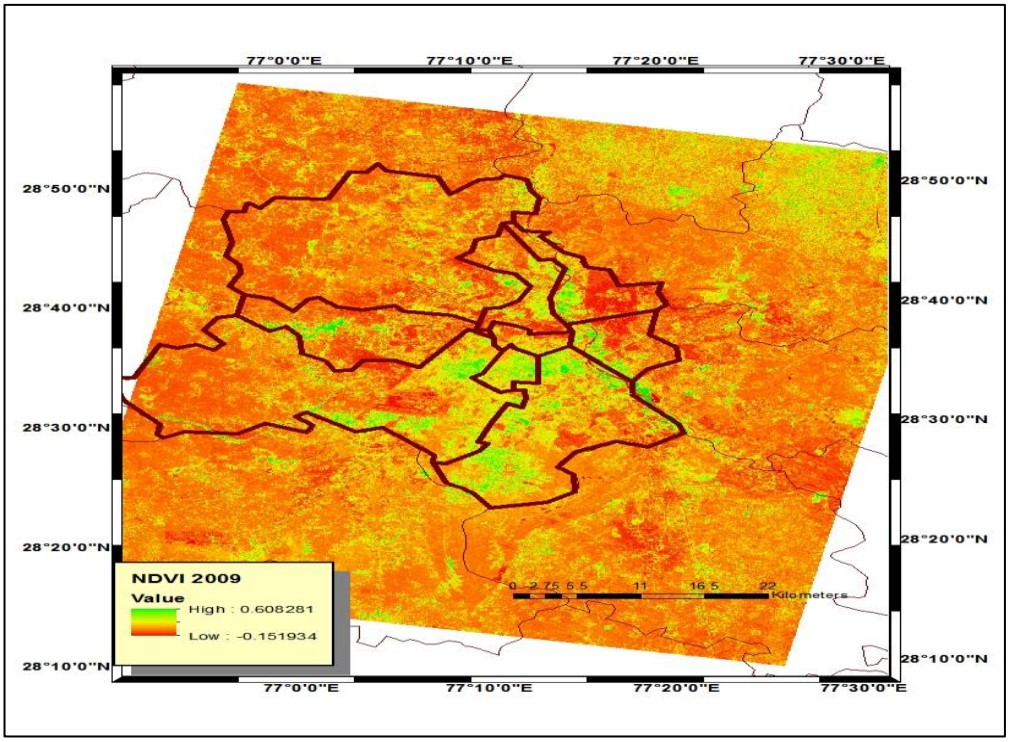

Figure 4.1 (b) NDVI during May 2009 in Delhi-NCR

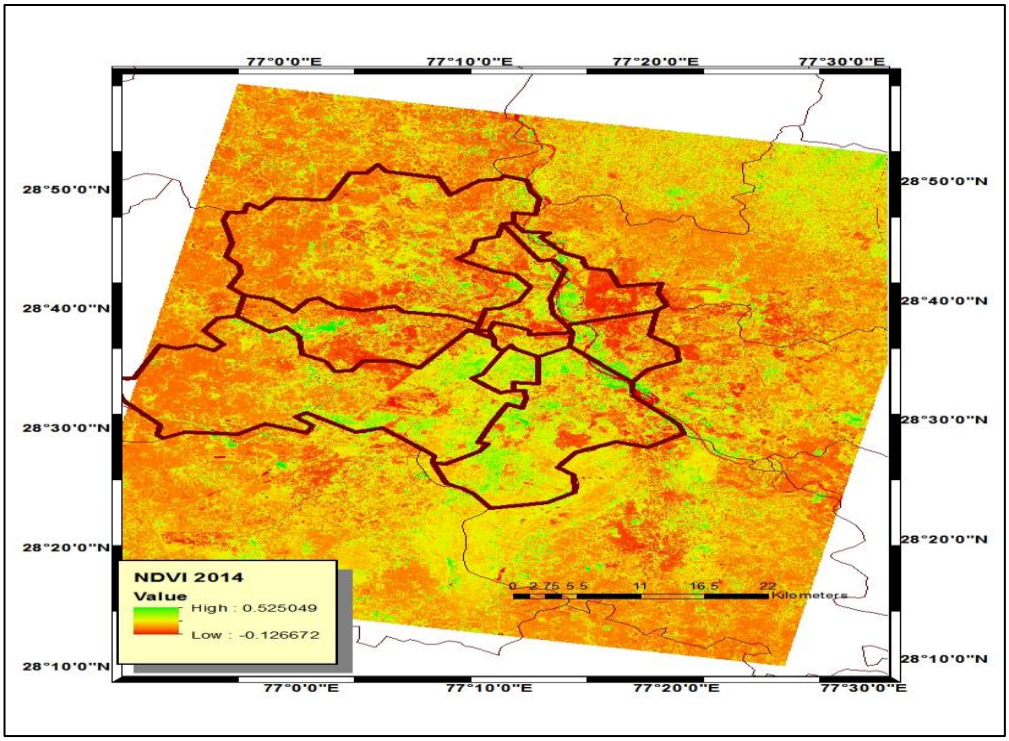

Figure 4.1 (c) NDVI during May 2014 in Delhi-NCR

NDVI maps generated above were then used to estimate emissivity using equations 4.5 and 4.4, which was then used to convert the brightness temperatures into land surface temperatures using equation 4.3.

[4.3] Results and Discussion

[4.3.1] Spatial and temporal pattern of LST

The Spatial and temporal pattern of LST over Delhi-NCR for the months of May 2003, 2009 and 2014 respectively are shown in Figure 4.2 (a-c). It is observed that during May 2003, the LST ranged from 26.36 to 49.36^{o}C with mean value of 39.65^{o}C. While the corresponding LST ranges were observed to be 18.22 to 40.93^{o}C (mean 31.44^{o}C) and 24.30 to 44.58^{o}C (mean 33.66^{o}C) in the months of May 2009 and 2014 respectively. From the statistical parameters, it is observed that the month of May, 2009is found to be cooler with minimum temperature of 18.22^{o}Cas compared to those for the months of May, 2014 and May, 2003 for which the minimum temperatures were found to be 24.30^{o}C and 26.36^{o}C respectively. It is mainly due to the change

in LULC pattern over the Delhi-NCR. The calculation of LST statistics for Delhi-NCR for the months of May 2003, 2009 and 2014 are shown below (Table 4.1):

Table 4.1Statistics of LST classification during 2003-2014

Classification statistics	10 May 2003	18 May 2009	16 May 2014
Max Temp (^{o}C)	49.36	40.93	44.58
Min Temp (^{o}C)	26.36	18.22	24.30
Mean±SD	39.65±3.79	31.44±3.18	33.66±1.87

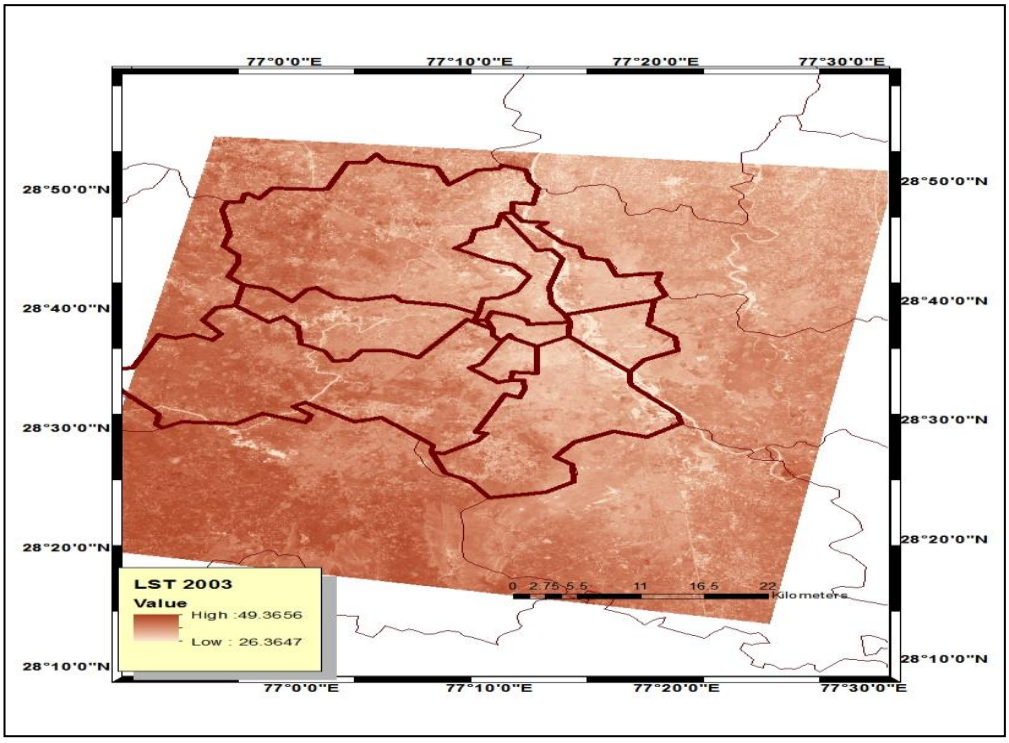

Figure 4.2 (a) LST during May 2003 in Delhi-NCR

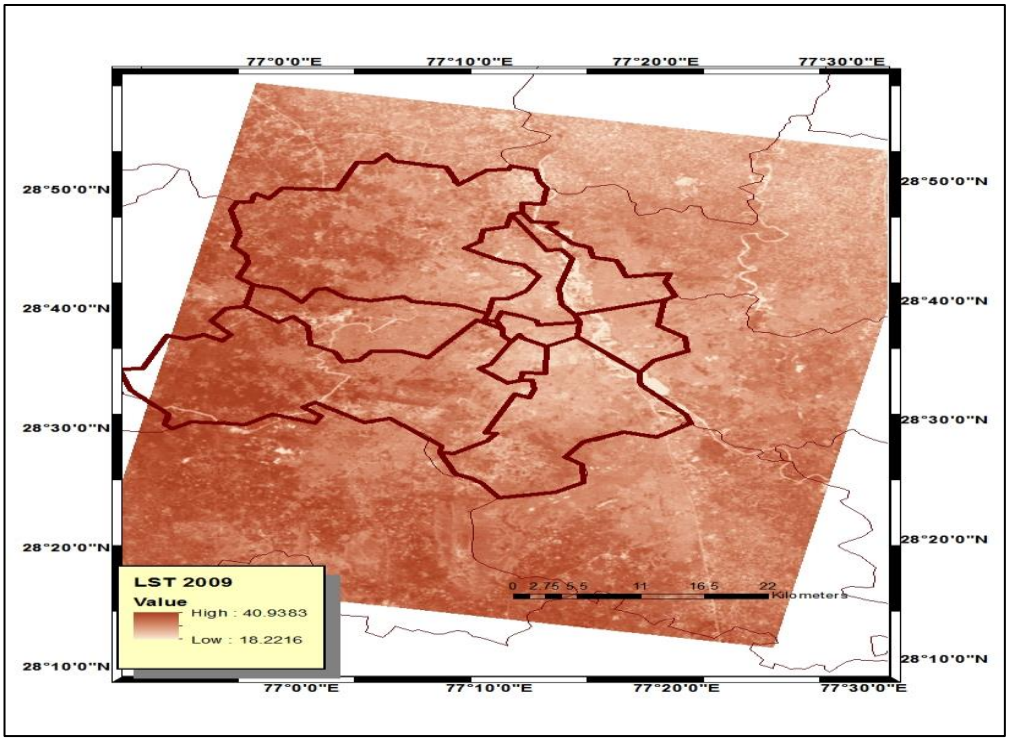

Figure 4.2 (b) LST during May 2009 in Delhi-NCR

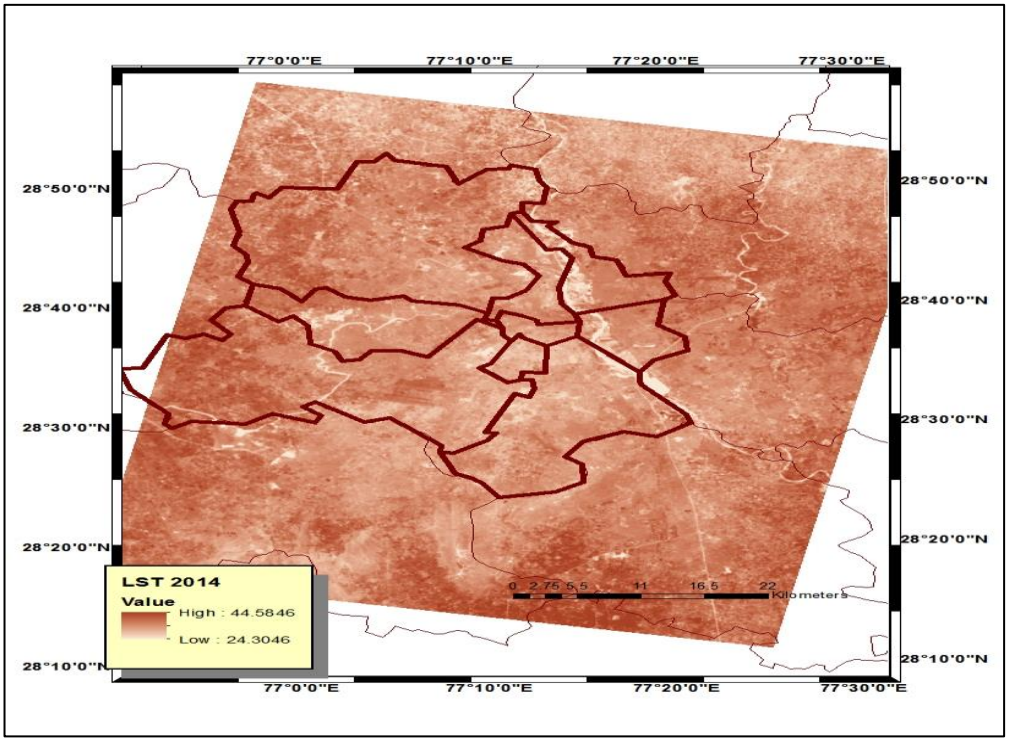

Figure 4.2 (c) LST during May 2014 in Delhi-NCR

Spatial pattern of LST was determined by classifying above derived LST in four classes on the basis of standard deviation (Low, Moderate, High and Extreme) as shown below (Table 4.2). The results of LST have been classified by adding and subtracting the standard deviation from the mean LST value using GIS software.

The LST classification (namely, Lower, Moderate, High and Extreme) of the study area are shown in Table 4.2. In the month of May 2003, it is observed that LST ranged in various classes i.e. Lower (26.00-36.00^{o}C), Moderate (36.00-40.00^{o}C), High (40.00-45.00^{o}C) and Extreme (>> 45.00^{o}C). Further, in the month of May 2009, the corresponding values of LST ranged from 18.00-28.00^{o}C for Lower, 28.00-32.00^{o}C for Moderate, 32.00-37.00^{o}C for High and for Extreme >> 37^{o}C. In addition, in the month of May 2014, the LST values observed in different classes were found to be Lower (24.00-32.00^{o}C), Moderate (32.00-35.00^{o}C), High (35.00-38.00^{o}C) and Extreme (>> 38^{o}C) respectively.

Table 4.2 Different class range of LST in May month in year 2003, 2009 and 2014

Class	10 May 2003 (^{o}C)	18 May 2009 (^{o}C)	16 May 2014 (^{o}C)
Lower	26.00-36.00	18.00-28.00	24.00-32.00
Moderate	36.00-40.00	28.00-32.00	33.00-35.00
High	40.00-45.00	32.00-37.00	35.00-38.00
Extreme	>> 45.00	>> 37.00	>> 38.00

The spatio-temporal maps of LST are shown in Figure 4.3 (a-c) which describes the distribution patterns of different LST classes over the national capital region of India. Distinct temperature ramp was observed among LULC types perceived on the LST maps. It can be seen from the LST maps that the moderate to high scale LST expanded from center to periphery during the years 2009 and 2014 as compared to that of year 2003 because of increased built-up area at that region. Extreme LST range was shrinking gradually in western and southern part of

the study area in stipulated time period because of the conversion of sparse scrub vegetation land (rocky area and desert area) into either green vegetation covers or built-up area. Lower and Moderate LST range cover was expanded from the central part of Delhi and north-eastern region lying to Delhi's surroundings (along the bank of Yamuna River) to the north region in the surroundings of Delhi from May 2003 to May 2009. While in the month of May 2014, Lower and Moderate LST range cover were found to be further expanded towards south-west region in Delhi's surroundings.

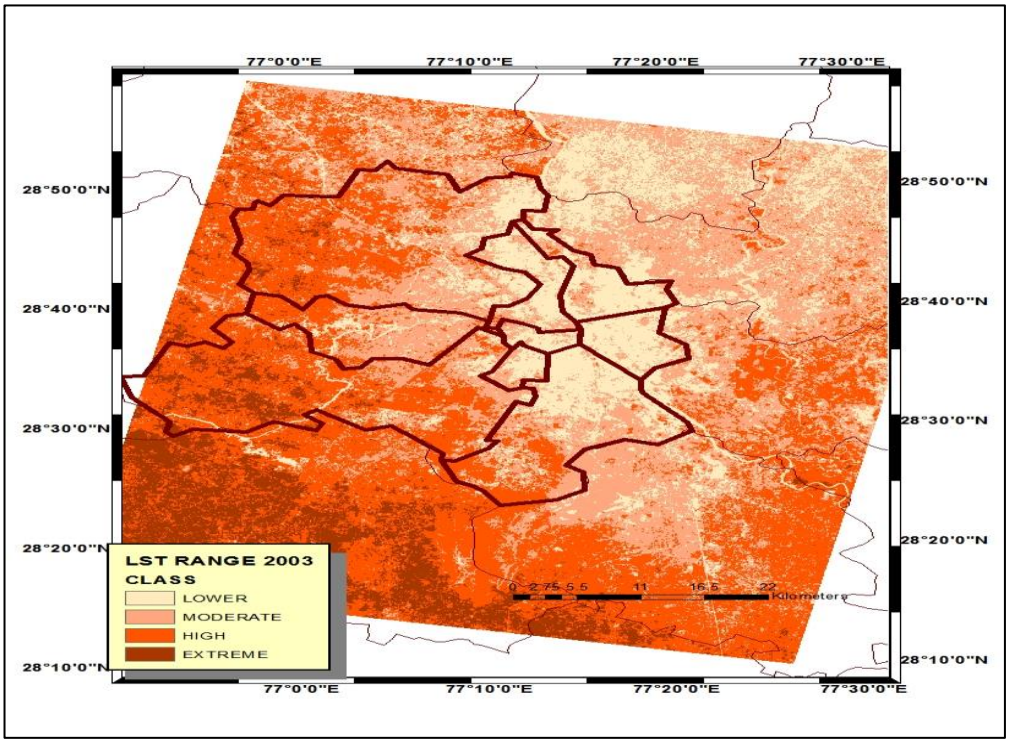

Figure 4.3 (a) LST Class during May 2003 in Delhi-NCR

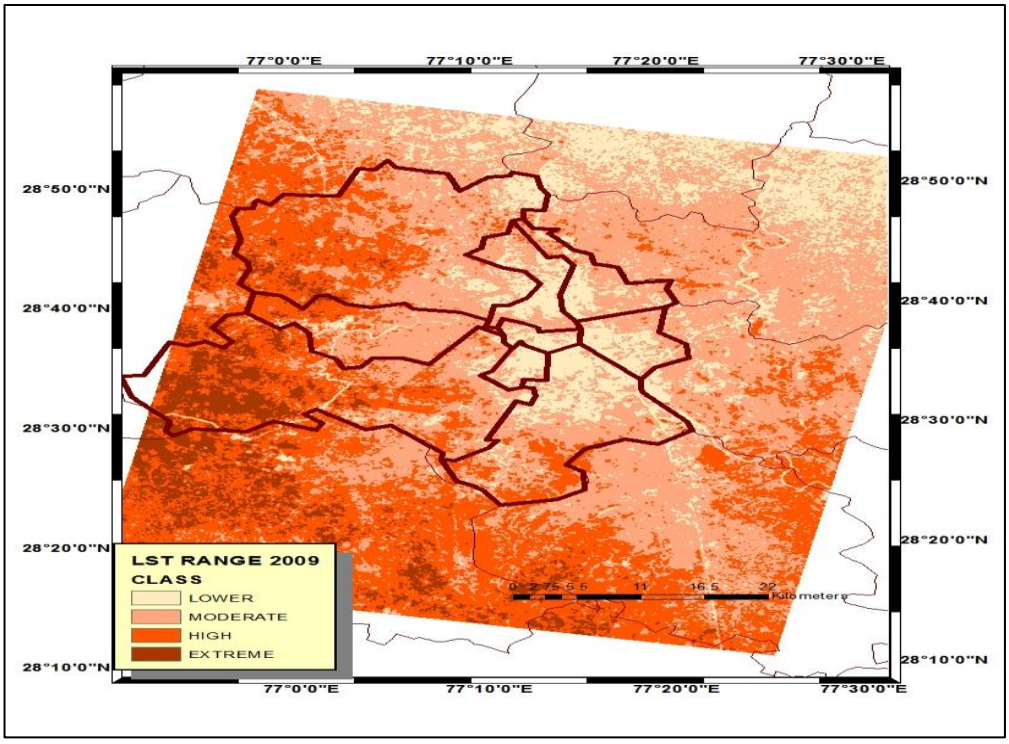

Figure 4.3 (b) LST Class in during May2009 in Delhi-NCR

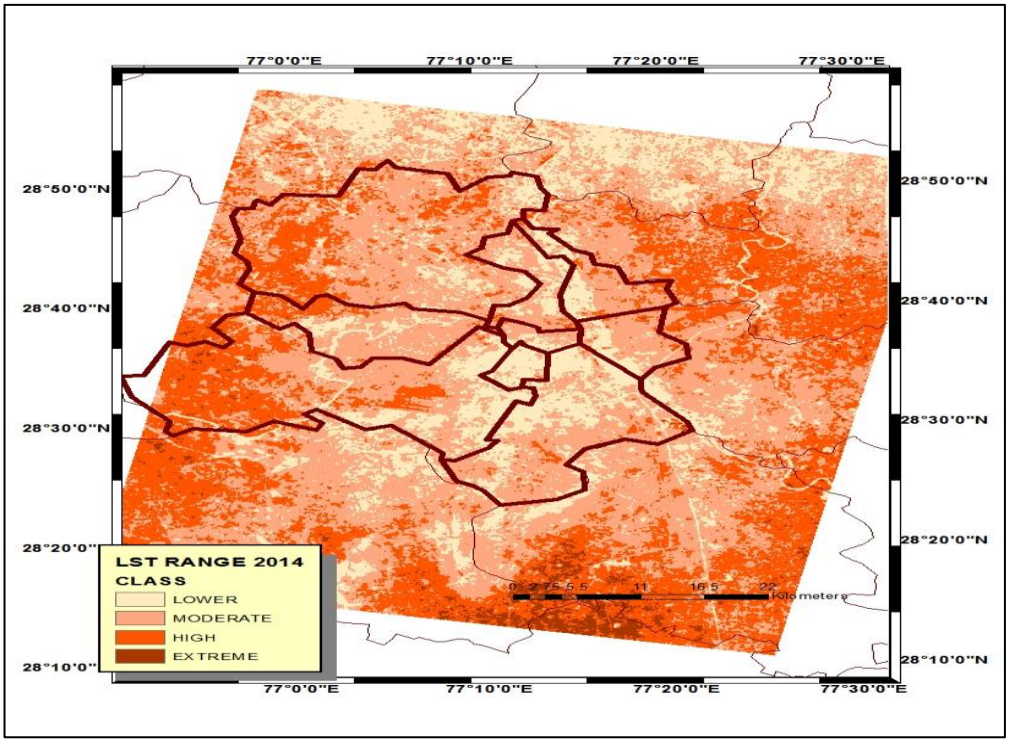

Figure 4.3 (c) LST Class during May 2014 in Delhi-NCR

[4.3.2] Association of LST with LULC

In this section, association of LST with different LULC has been evaluated. Many studies have reported that LST is closely associated with different LULC types such as built-up area, vegetation area, moist soil (agricultural land) and dry land (desert and rocky area) (Jones et al. 1990; Pichierri et al. 2012; Zhang et al. 2013). Therefore, it is important to investigate the relationship between different LULC and LST distribution pattern in the rapidly expanding NCR region of India. The spatial distribution of LST closely associated with LULC in the present study. This association was established through overlay (intersect tool) technique in Arc-GIS software by randomly selected 10000 points in each images (LULC type and LST images). Average LST of different LULCs and corresponding classes of LST are shown in Table 4.3 and Table 4.4, respectively.

Table 4.3 Mean LST of different LULC types in May month in year 2003, 2009 and 2014

Landform types	10 May 2003 (^{o}C)	18 May 2009 (^{o}C)	16 May 2014 (^{o}C)
Built-up area	37.37	29.93	34.85
VWMA area	35.07	27.95	31.69
Rocky area with scrub vegetation	40.10	32.84	35.12
Dry Bare land	45.14	35.56	38.83

Table 4.4 LST class with different LULC types in May month in year 2003, 2009 and 2014.

LST Class	10 May 2003	18 May 2009	16 May 2014
Lower	VWMA area	VWMA area	VWMA area
Moderate	Built-up area	Built-up area	Built-up area
High	Rocky area with scrub vegetation	Rocky area with scrub vegetation	Rocky area with scrub vegetation
Extreme	Dry Bare land	Dry Bare land	Dry Bare land

In the month of May 2003, the mean LST were found to be 37.37^{o}C, 35.07^{o}C, 40.10^{o}C and 45.14^{o}C for built-up area, Green vegetation area including water bodies and Moist Agricultural land (VWMA area), Rocky area and dry Bare land respectively, which suggested that Built-up area, VWMA area, Rocky area and dry Bare land comes under Moderate, Lower, High and Extreme LST Class range respectively.

The results were found to be similar for the month of May 2009 as compared to those of May 2003. The Built-up area belong to moderate LST Class with mean temperature 29.93^{o}C and other LULC types VWMA area belonged to lower (mean LST 27.95^{o}C), rocky area belonged to high (average LST 32.84^{o}C) and desert area belonged to high (average LST 35.56^{o}C) LST Class respectively. Further, it can be observed during 2014, built-up area (mean LST 34.85^{o}C) LST belonged to Moderate class, Rocky area belonged to high class (mean LST 35.12^{o}C), VWMA area belonged to lower class (mean LST 31.69^{o}C) and dry Bare land (mean LST 38.83^{o}C) belonged to extreme LST Class respectively.

The percentage of area cover by different LST class is shown in Figure 4.4 In 2003, the percentage of area cover for different LST class cover comprise Lower (14.08%), Moderate (33.64%), High (40.50%) and Extreme (11.77%) over the study area. In the year 2009, dynamic changes were observed in the area cover of different LST class i.e. Lower (15.16%), Moderate (44.54%), High (33.67%) and Extreme (6.62%) respectively. In the year 2014, total 70.83% area lied under two LST class i.e. Lower (19.33%) and Moderate, (50.80%), as compared to other two class i.e. High (28.01%) and Extreme (1.86%). It is observed (Figure 4.4) that during the study period, area cover by Lower and Moderate class of LST is expanding while area cover by High to Extreme class decreases during this period (2003, 2009 and 2014).

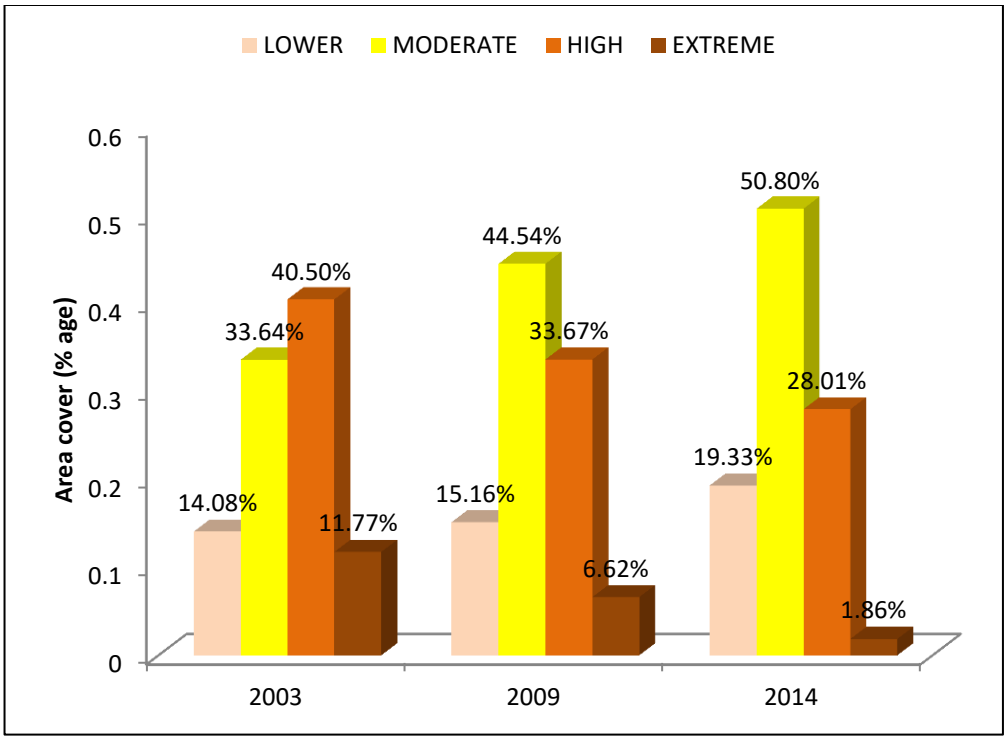

Figure 4.4 LST area covers in percentage during 2003, 2009 and 2014.

As discussed in chapter 3, it is clearly observed (Figure 3.2 a-c) that the built-up area expanding the region lying north of Delhi and in eastern region of Delhi's surroundings which is dominated by agricultural land that leads to rise in average LST. Further, built-up expansion also occurred in south-west part of the city which was primarily covered by ridge and dry Bare land that leads to decrease in average LST over this region. Overall the mean LST for the entire NCR follow decreasing LST trend because of increased level of green vegetation cover during the months of May 2003, 2009 and 2014.

Overlaying (intersection) technique has been adopted to estimate the pattern of LST with LULC type's i.e. Built-up area, Green vegetation and Rocky area changes using ArcGIS software over the study area. From Figure 4.5 (a, b and c), it is clearly observed that the Moderate LST class pattern during 2003, 2009 and 2014 is closely associated with Built-up area pattern. The area by Moderate LST class was changed from 33.64% to 50.80%, which is followed by similar trend as of urban Built-up area that changed from 5.84% to 11.78% in between 2003 to 2014. It can be observed that urban area expansion highly influences the local LST dynamics.

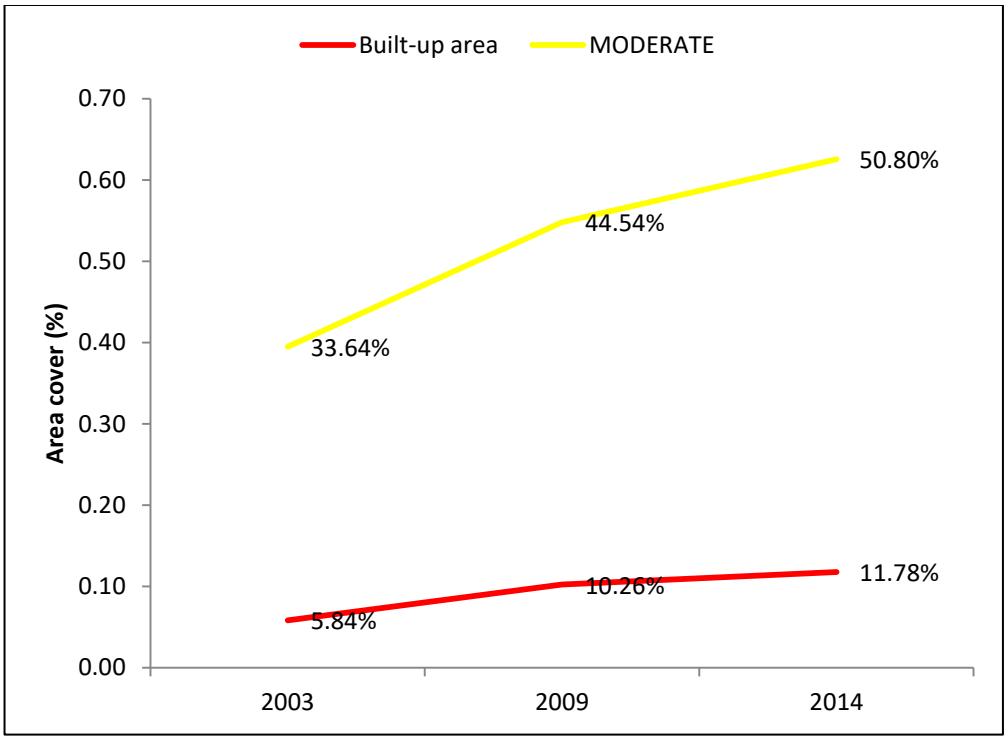

Figure 4.5 (a) Percentage of LST class with built-up area

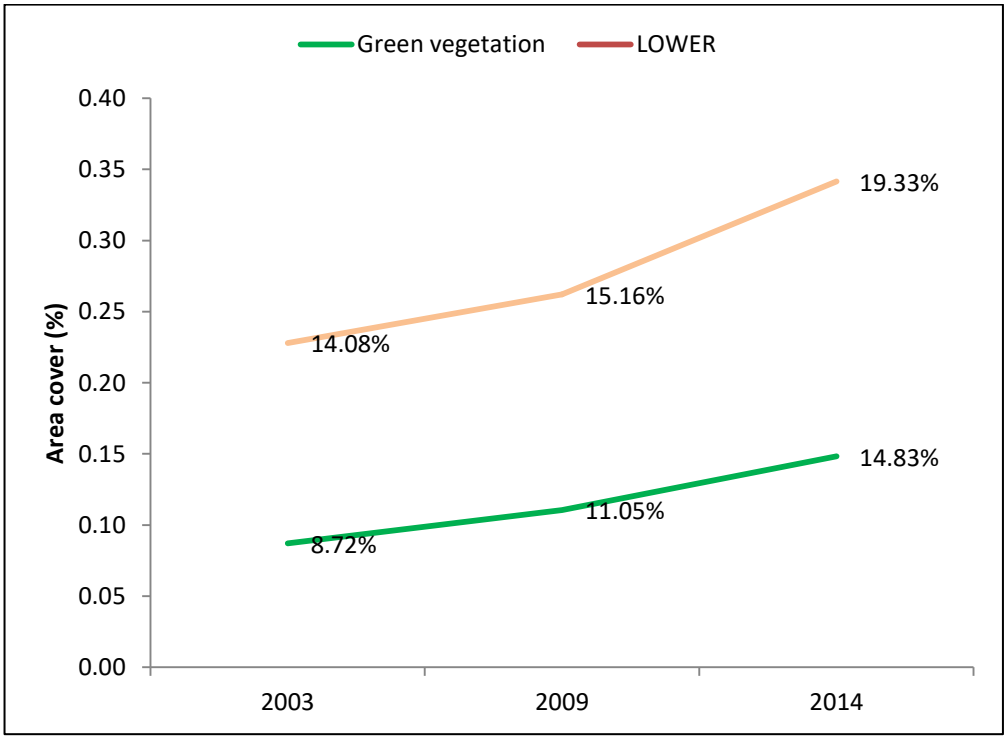

Figure 4.5 (b) Percentage of LST class with Green vegetation area

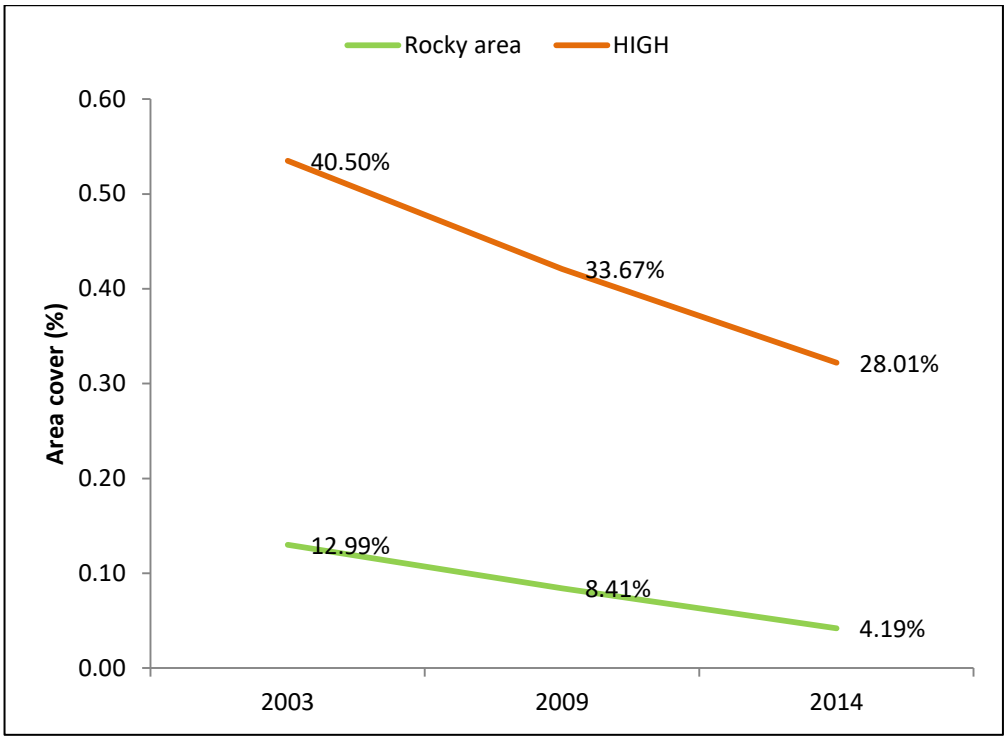

Figure 4.5 (c) Percentage of LST class with Rocky area

Green vegetation area cover expands from 8.72% to 14.83% followed by similar increasing trends with Lower LST class from 14.08% to 19.33% between the years 2003 to 2014. The area cover by High LST class shrinks from 40.50% to 28.01% followed by similar decreasing trend to that of Rocky area which decreased from 12.99% to 4.19% in Delhi-NCR during 2003-2014.

[4.4] Summary

In recent decade, due to fast expansion of Built-up area in peripheral areas of NCR, LULC composition change had influenced the spatio-temporal pattern of local meteorological components. It has also been observed that LULC composition changes are predominant factor in LST anomaly in stipulated time period. Built-up area has expanded more in northern and eastern part of the city which leads to shifting of LST from lower to higher class. The total area cover by

different LST class change occurred during study period in found to be: Lower (37.28%), Moderate (51.01%), High (30.83%) and Extreme (84.19%). Further, it is clearly observed that the Moderate LST class pattern is closely associated with Built-up area pattern. The area by Moderate LST class was changed from 33.64% to 50.80%, which is followed by similar trends for urban Built-up area that changed from 5.84% to 11.78% in between 2003 to 2014. It shows that urban area expansion highly influences the local LST dynamics. In addition, it can be seen that green vegetation area cover expanded from 8.72% to 14.83% followed by similar increasing trends with Lower LST class (~14.08% to 19.33%) between the years 2003 to 2014. Further, the area cover by High LST class decreases from 40.50% to 28.01% followed by similar decreasing trend to that of Rocky area (~12.99% to 4.19%) over Delhi-NCR between the time periods 2003 to 2014. The results of present chapter can provide better understanding of urbanization phenomenon with corresponding change in LULC composition and LST to the policy makers and urban planners. For future studies, there is need for the availability of long term data with higher resolution for LULC composition and LST analysis for better understanding of urbanization process and its impact on environment.

Chapter-5 *Urban air pollution exposure and its relation to LULC*

[5.1] Introduction

In the early stage of urban air pollution, studies were primarily focused on a macro level and the comparison of concentration in air pollutants between the urban and rural area situated at far location (Dockery et al., 1993; Pope et al., 2002). Nowadays, macro level research arena has been shifted to micro-level studies such as intra-urban spatial contrast of air pollution and its exposure to the human population (Hoek et al., 2002; Beelen et al., 2008 & 2013; Saraswat et al., 2013). Long-term exposure to ambient fine particulate matter such as $PM_{2.5}$ (aerodynamic diameter $\leq$ 2.5 μm) has been associated with morbidity and premature mortality in the human population (Dockery et al., 1993; Pope et al., 2009; Brauer et al., 2012). In recent years, $PM_{2.5}$ has been identified as one of the most important factors responsible for premature deaths. Lim et al. (2012) reported 3.2 million deaths per year worldwide due to premature mortality caused by ambient $PM_{2.5}$ exposure. In the last decade, India was recognized as a regional pollution hotspot, (particularly in high-burden aerosol) with more than 1.2 billion population (Dey and Di Girolamo, 2011).

In recent years, the air quality of NCR of India has become one of the most debatable issues in air pollution studies. Therefore, many researchers have focused their efforts towards the study of spatial and temporal distribution of particulate matter and its exposure to the human population in NCR (Goel et al., 2015; Saraswat et al., 2016; Maji et al 2017). Most of the previous studies used particulate matter data from air quality monitoring stations, which were situated in limited areas, mostly in the city centers and a few in rural or semi-urban areas. They used different modeling approaches for pollution exposure assessment based on population data obtained from the census of India. Satellite-derived spatio-temporal concentration of air pollutants (such as $PM_{2.5}$) is more suitable for the studies of long-term exposure assessment because data availability is uniformly distributed over entire study area (Donkelaar et al., 2015; Chowdhury and Dey, 2016). GIS-based modeling approaches provide a fair approximation of

long-term exposure to averaged pollutant concentration range to the human population (Morgenstern et al., 2008).

In the present Chapter, the spatio-temporal trends during 2000-2012 have been estimated using satellite derived $PM_{2.5}$ concentration and its exposure to human population residing in different locations in the NCR of India. We aimed three primary objectives for this study (1). To examine the trend of $PM_{2.5}$ concentration followed in stipulated period at each sampling point (42 points) lied in different LULC using Mann-Kendall trend model. (2). Applying GIS-based modeling approach for evaluating spatial and temporal changes of $PM_{2.5}$ occurred in the study period. (3). Estimation of long-term exposure of $PM_{2.5}$ to the human population living at different locations in the study area via spatial analyst tool of Arc-GIS.

[5.2] Data processing and Methodology

[5.2.1] Data Sources

For the present study, we have used $PM_{2.5}$ concentration data set containing floating point value of three-year running mean grids from 1998 to 2012 obtained from SEDAC. (http://sedac.ciesin.columbia.edu/data/set/sdei-global-annual-avg-pm2-5-modis-misr-seawifs-aod-1998-2012/data-download). The spatial resolution of this product is 10km x 10km (0.1^{o}x0.1^{o}) at the equator which covers 70^{o} north to 55^{o} south of global land surface. It is derived from AOD (Aerosol optical depth) retrieved from the combination of three earth observatories satellite namely as MODIS (Moderate Resolution Imaging Spectroradiometer), MISR Multi-angle Imaging Spectro Radiometer) and SeaWIFS (Sea-Viewing Wide Field-of-View Sensor). For the derivation of $PM_{2.5}$ concentration, GEOS-Chem chemical transport model is used for converting AOD to near-ground level $PM_{2.5}$ in µg/m3 (Donkelaar et al. 2015). Monthly average data of Respirable Suspended Particulate Matter (RSPM), NO_2, SO_2 and CO concentration for May 2009 was obtained from DPCC. (https://www.dpcc.delhigovt.nic.in/Air40.html)

[5.2.2] Methodology

Satellite-derived $PM_{2.5}$ concentration has low biased measurements as compared to the direct measurements (Dey et al., 2012). We have extracted the value of $PM_{2.5}$ concentration to randomly selected 42 points from 10 km x 10km gridded raster dataset for each year from 1998 to 2012 using Arc-GIS software. For statistical significance and trend analysis we have applied Mann-Kendell trend test at 95% confidence level for each 42 points located in different LULC type in the study period. Mann-Kendell trend test is a widely applicable non-parametric test for assessment of environmental time series data (Mann, 1945; Helsel, 2002; yu et a., 2002) Mann-kendell trend statistic (S) is derived by:

$$S = \sum_{i=1}^{n-1} \sum_{j=i+1}^{n} Sign(Tj - Ti) \qquad (1)$$

$$Sing\ Tj - Ti = \begin{Bmatrix} 1\ if\ Tj - Ti > 0 \\ 0\ if\ Tj - Ti = 0 \\ -1 if\ Tj - Ti < 0 \end{Bmatrix} \qquad (2)$$

where, data point Tj and Ti are annual value in year i and j, j>i respectively

Statistics of variance has been calculated by (ties are not considered):

$$Var(S) = \frac{n(n-1)(2n+5)}{18} \qquad (3)$$

The standard test statistic Z is computed as follows (Drapela and Drapelova., 2011)

$$Z = \begin{Bmatrix} \frac{S-1}{\sqrt{Var(S)}}\ if\ S > 0 \\ 0 \qquad\quad if\ S = 0 \\ \frac{S+1}{\sqrt{Var(S)}}\ if\ S < 0 \end{Bmatrix} \qquad (4)$$

Air pollutants RSPM, NO_2, SO_2, CO and $PM_{2.5}$ data were converted to a raster floating point data format in 30 m spatial resolution by an ordinary Kriging model (Interpolation method) technique using spatial analyst tool of Arc-GIS software. Geographic interpolation and extrapolation are the tools which are used in order to complete the maps with incomplete data either absence of value in the dataset or missing data for a location in the region of interest. Kriging model is a geo-statistical method of interpolation, which measure the geo-statistical association amongst the points and predicts the missing value with high accuracy at high confidence level (Zhou et al., 2007). Kriging is the most common and statistically sound method used in interpolation technique for spatial analysis with missing data at a location between known data values. Ordinary Kriging is linear because it estimates weighted linear combination of known data and unbiased since it tries to maintain mean residual (MR) or error tends to zero (Chun and Griffith, 2013).

[5.3] Results and Discussion

[5.3.1] Trend analysis of $PM_{2.5}$ for the studied period (2000-2012) using Mann-Kendall trend model (MKTM)

The annually average $PM_{2.5}$ concentration at all 42 points for the entire NCR region have shown increasing trend during the study period as shown in Figure 5.1. For the classification of LULC pattern for NCR, image data from GLOVIS for the month of May 2014 have been used (already discussed in Methodology section of Chapter 3). The month of May has been selected because of its clean atmosphere (cloud free data) and high air temperature (i.e. no fog formation) which is suitable for study related to surface phenomenon via satellite observation. For the purpose of

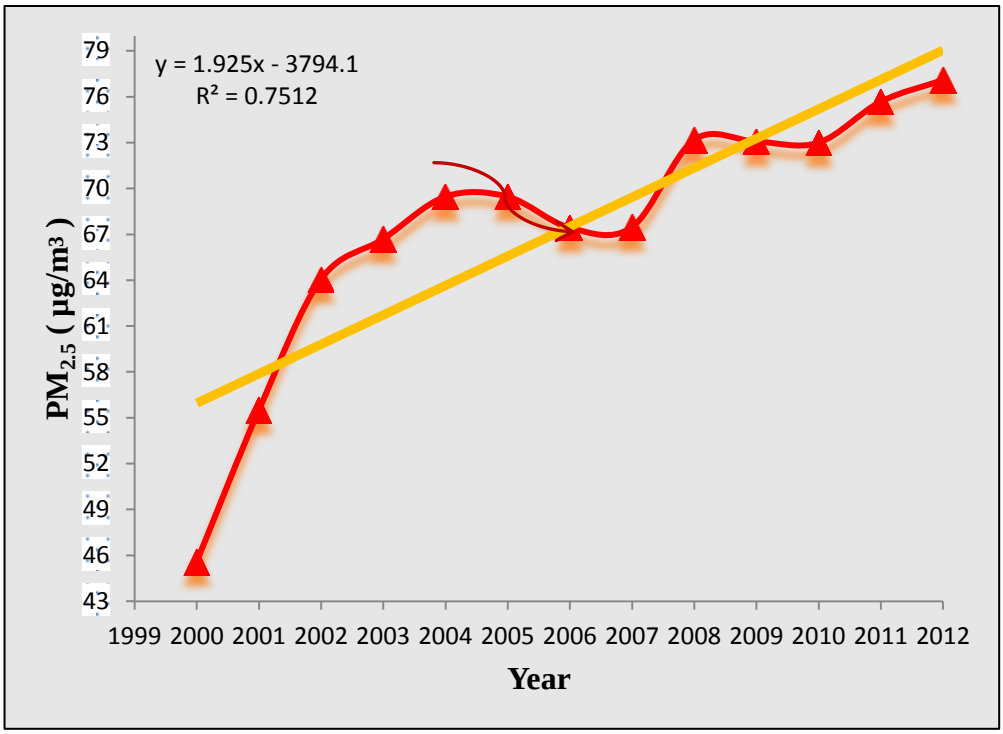

Figure 5.1 Annually averaged $PM_{2.5}$of all 42 locations with trend line during 2000-2012

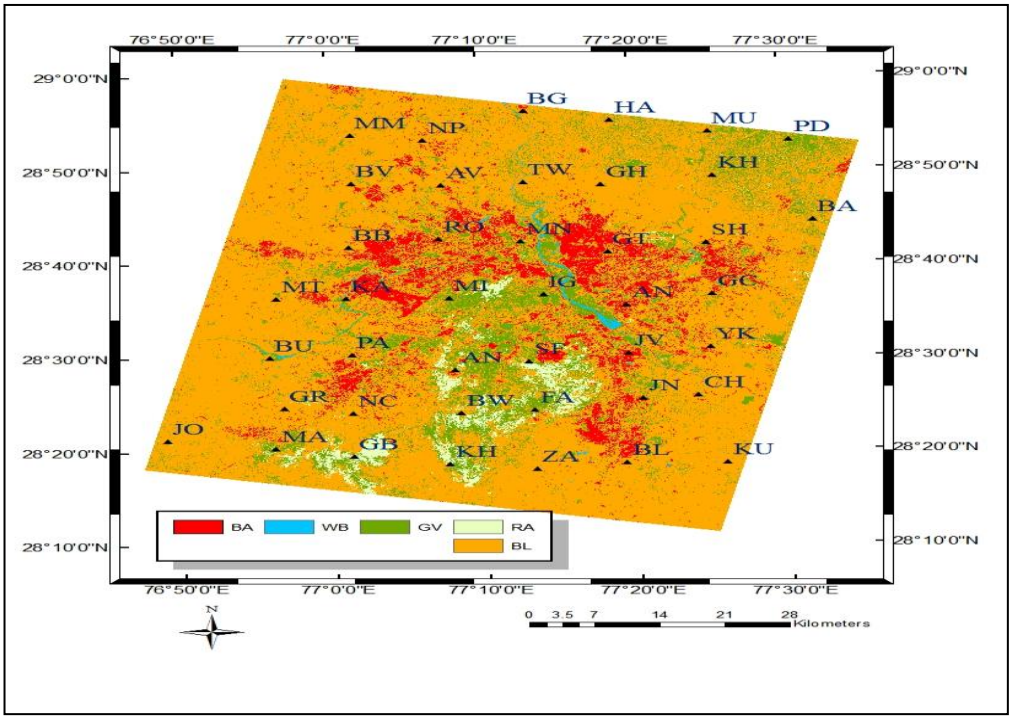

Figure 5.2 LULC types showing selected 42 points of entire study area

analysis, a buffer area of radius 1 km was created around each of the 42 points shown in Figure 5.2 was created. This buffer area was classified as Dense Urban Area (UA), developing Rural and Semi-urban Area (RSA), Ridge Area (RA) and Bare Agricultural Land (BAL) according to the dominant LULC in the buffer area.

Results showed that there is a significant increasing trend at all the points with different positive z-value. It showed that probability p-value was very less than the confidence level of alpha value (α= 0.05), which clearly indicated that there is a increasing trend at all points, irrespective of points under which canopy layer exists during the study period. The significance of trend is measured by the statistic z-value. If z-value is larger than $z_{\alpha/2}$ ($z_{0.025}$=1.96), where α= 0.05, the null hypothesis are rejected, or trend is significant.

The Z-values in table 5.1 indicate the significance of observed results of MKTM test at each point for $PM_{2.5}$ trends. It is seen that z-values for the sites Sehanikhurd (SH), Gaur City (GC), Jeevan Nagar (JN), GTB Staff colony (GT), Jaitpur Village (JV) and Balmiki Basti (BB) are on the higher side among the urban area (UA) sites. This indicates the presence of a strong increasing trend at these sites. On the other hand, the z-values of the sites Mukharjee Nagar (MN), Mayapuri Industrial area (MI), Nirvana country (NC), and Ballabhgarh (BL) are on the lower side among the urban area sites (UA) which suggests a comparatively weaker trend at these sites.

Among the rural and semi- urban points, the sites which are situated in western to northern region of study area i.e. Jori (JO), Mitraon (MT), Bwana Village (BV) and Alipur Village (AV) experienced more significant trend as compared to sites lying in the eastern region i.e. Yakubpur (YK), Ghitora (GH) and Chakmajai(CH).

In ridge area, Zakopur (ZA), Faridabad Ridge Area (FA), Bandhwari (BW), Gratpur Bas (GB), Kheria (KH) and Manesar (MA) lying towards southern region of study area have also shown significant increasing trend due to a rapid expansion of Extended Urban Agglomeration (EUA) in the vicinity of that region.

Points lying under bare land and agricultural land such as Patala Dehat (PD), Mukari (MU), Baraka Arifpur (BA) and Khorajpur (KH) in eastern and north eastern region have shown more significant trend as compared to sites located in western region Budhera (BU), in northern MalhaMajra (MM) and in southern region Kurali (KU).

Table 5.1 MKTM model results for $PM_{2.5}$ concentration trend in different subclass

SN	Site Name	ID	Sub-types	s-value	z-value	p-value	Trend
1	Ballabhgarh	BL	UA	41	2.44	1.47E-02	[+Ve]
2	Mayapuri Industrial area	MI	UA	44	2.62	8.71E-03	[+Ve]
3	Mukharjee Nagar	MN	UA	52	3.11	1.86E-03	[+Ve]
4	Nirvana country	NC	UA	54	3.23	1.22E-03	[+Ve]
5	Aya Nagar	AN	UA	56	3.36	7.92E-04	[+Ve]
6	Rohini	RO	UA	56	3.36	7.92E-04	[+Ve]
7	New Ashok Nagar	AN	UA	58	3.48	5.06E-04	[+Ve]
8	Palam	PA	UA	60	3.60	3.19E-04	[+Ve]
9	Kakrola	KA	UA	62	3.72	1.98E-04	[+Ve]
10	India Gate	IG	UA	62	3.72	1.98E-04	[+Ve]
11	South Sainik Farm	SF	UA	62	3.72	1.98E-04	[+Ve]
12	BalmikiBasti	BB	UA	64	3.84	1.21E-04	[+Ve]
13	Jaitpur Village	JV	UA	64	3.84	1.21E-04	[+Ve]
14	GTB Staff colony	GT	UA	64	3.84	1.21E-04	[+Ve]
15	Jeevan Nagar	JN	UA	66	3.97	7.30E-05	[+Ve]
16	Gaur City	GC	UA	70	4.21	2.60E-05	[+Ve]
17	SehaniKhurd	SH	UA	72	4.33	1.50E-05	[+Ve]
18	Chakmajai	CH	RSA	41	2.44	1.47E-02	[+Ve]
19	Ghitora	GH	RSA	48	2.87	4.14E-03	[+Ve]
20	Yakubpur	YK	RSA	53	3.17	1.51E-03	[+Ve]
21	Greenopolis	GR	RSA	58	3.48	5.06E-04	[+Ve]

22	Nathupur	NP	RSA	60	3.60	3.19E-04	[+Ve]
23	TehariDawlatpur	TW	RSA	62	3.72	1.98E-04	[+Ve]
24	Alipur Village	AV	RSA	64	3.84	1.21E-04	[+Ve]
25	Jori	JO	RSA	66	3.97	7.30E-05	[+Ve]
26	Mitraon	MT	RSA	72	4.33	1.50E-05	[+Ve]
27	Bwana Village	BV	RSA	72	4.33	1.50E-05	[+Ve]
28	Manesar	MA	RA	58	3.48	5.06E-04	[+Ve]
29	Kheria	KH	RA	61	3.66	2.52E-04	[+Ve]
30	Gratpur Bas	GB	RA	62	3.72	1.98E-04	[+Ve]
31	Bandhwari	BW	RA	64	3.84	1.21E-04	[+Ve]
32	Faridabad Ridge Area	FA	RA	66	3.97	7.30E-05	[+Ve]
33	Zakopur	ZA	RA	71	4.27	1.90E-05	[+Ve]
34	Kurali	KU	BAL	37	2.20	2.81E-02	[+Ve]
35	MalhaMajra	MM	BAL	48	2.87	4.14E-03	[+Ve]
36	Budhera	BU	BAL	50	2.99	2.79E-03	[+Ve]
37	Baghpat	BG	BAL	60	3.60	3.19E-04	[+Ve]
38	Harchandipur	HA	BAL	60	3.60	3.19E-04	[+Ve]
39	Khorajpur	KH	BAL	64	3.84	1.21E-04	[+Ve]
40	Baraka Arifpur	BA	BAL	72	4.33	1.50E-05	[+Ve]
41	Mukari	MU	BAL	73	4.39	1.10E-05	[+Ve]
42	PatalaDehat	PD	BAL	75	4.51	6.00E-06	[+Ve]

[5.3.2] Spatial and temporal pattern of $PM_{2.5}$ concentration in NCR the Interpolation of $PM_{2.5}$

Spatial distribution of $PM_{2.5}$ concentration in raster data file at 30 m spatial resolution have been created for four year interval from 2000 to 2012 (Figure 5.3 a-d). Overlaying of the LULC map (five class map) of Landsat 8 data have been created by supervised classification (Figure 5.2) over the study region with the corresponding $PM_{2.5}$ concentration map. It was observed that urban agglomeration mainly consist of built-up area which was found to be dominated in eastern and central region have higher $PM_{2.5}$ concentration in contrast to prevailing ridge area in southern and bare land in western part of studied area.

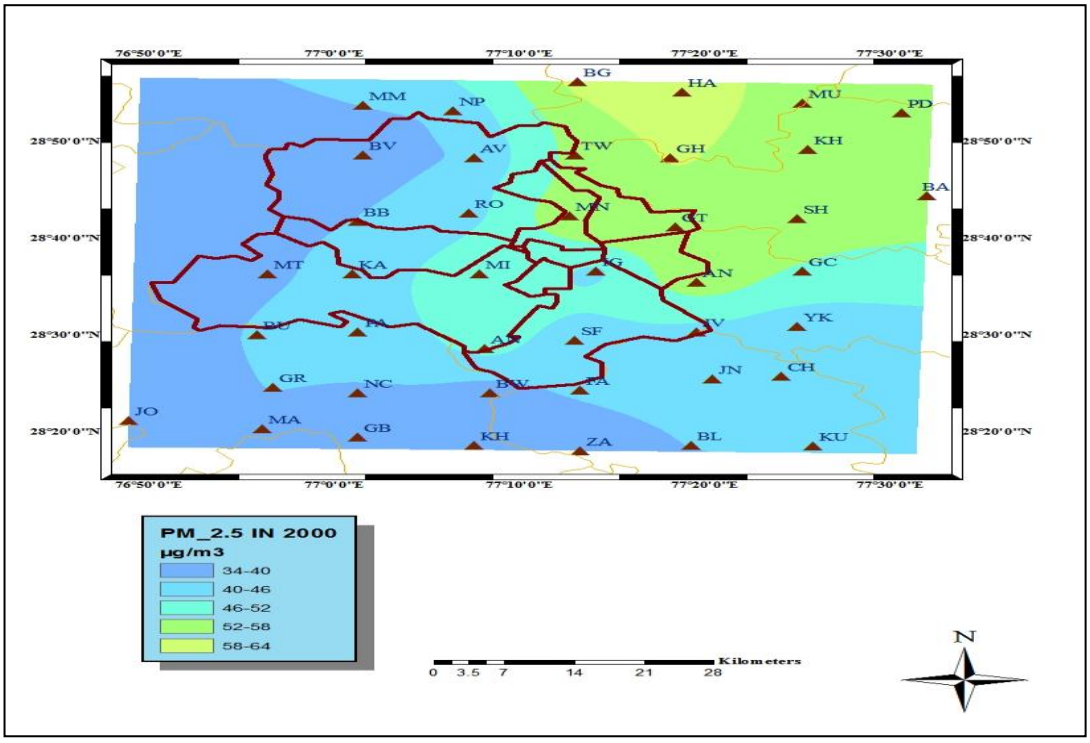

Figure 5.3 (a) Range of $PM_{2.5}$ concentration across Delhi-NCR during 2000

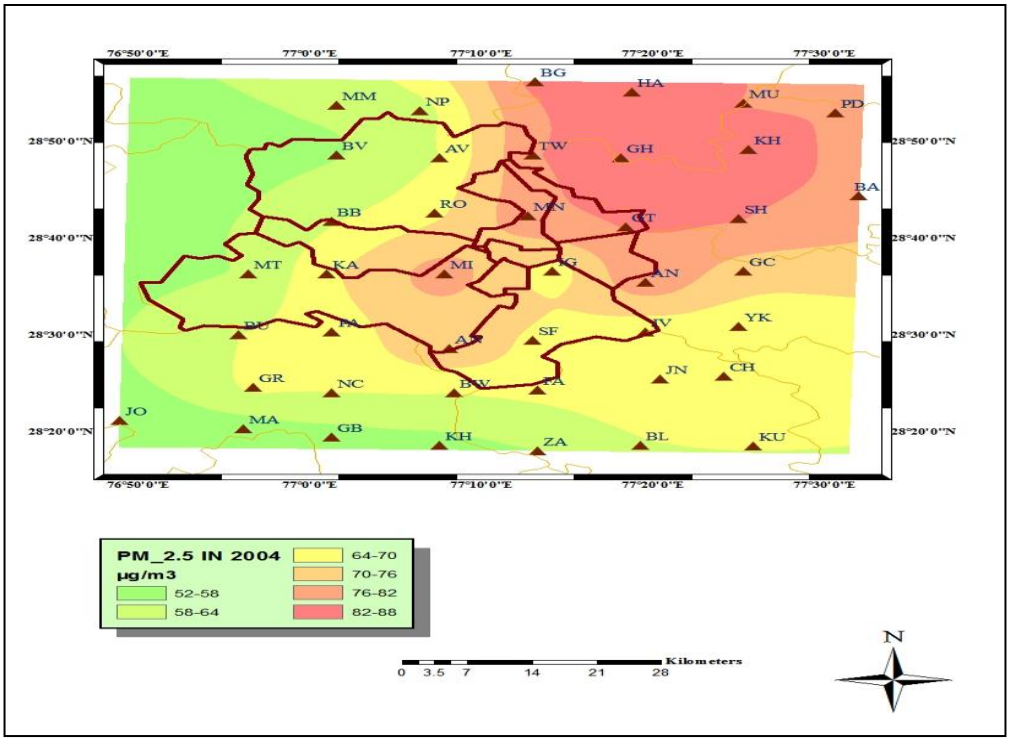

Figure 5.3 (b) Range of $PM_{2.5}$ concentration across Delhi-NCR during 2004

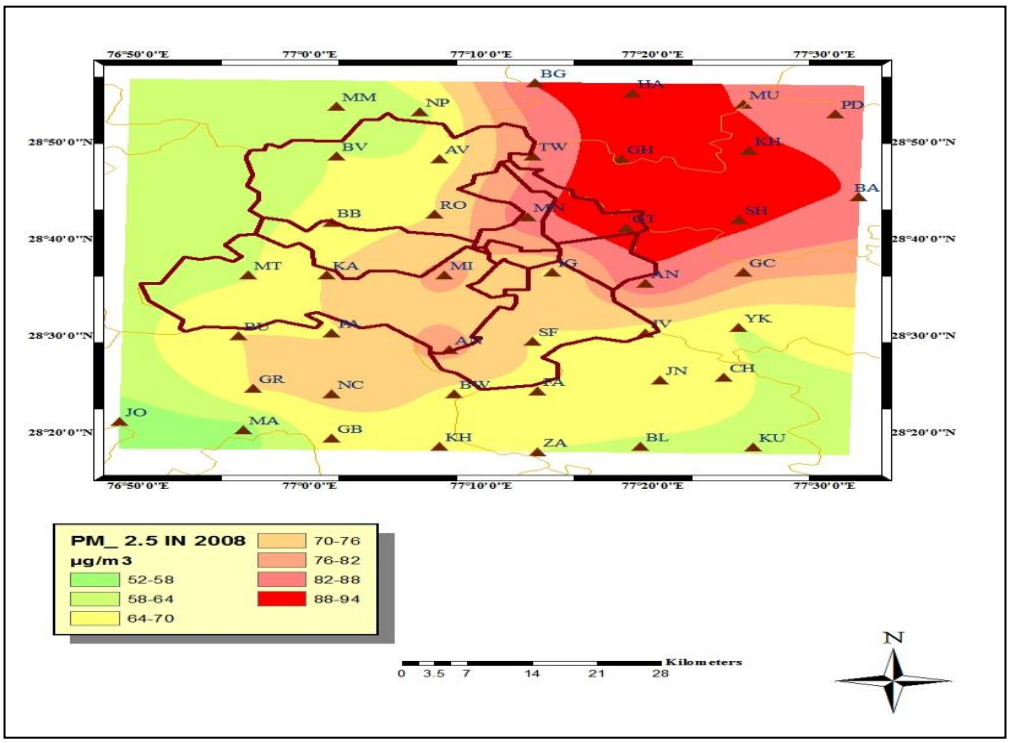

Figure 5.3 (c) Range of $PM_{2.5}$ concentration across Delhi-NCR during 2008

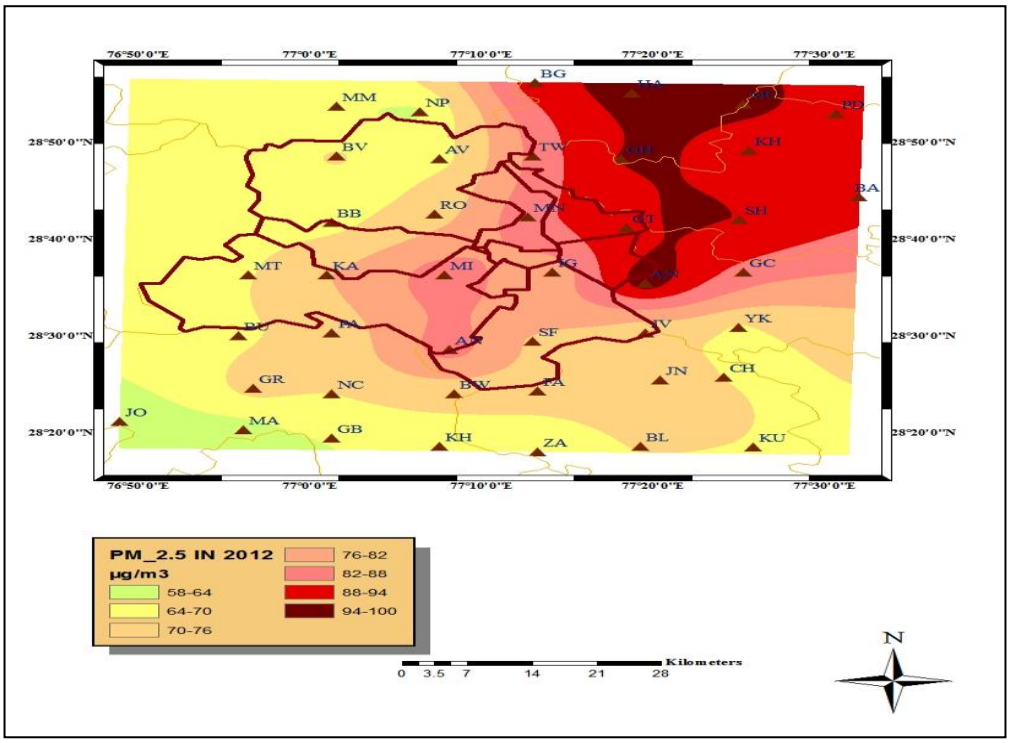

Figure 5.3 (d) Range of $PM_{2.5}$ concentration across Delhi-NCR during 2012

The changes occurred in $PM_{2.5}$ concentration levels during 2000 to 2004, 2008 and 2012 have been displayed in Figure. 5.4 (a-c). A significant change was observed during 2000 and 2004 towards eastern and central-southern part of study area which further gets a wider range of changes in the later year of 2008 and 2012. It can be due to both anthropogenic such as rampant construction carried out in the region and meteorological parameters as prevailing wind were northwesterly. This wind carries a huge amount of particulate matter from bare land in the western and northern region (desert in the western region and agricultural land in northern region) to Delhi-NCR (Statistical Abstract 2014.).

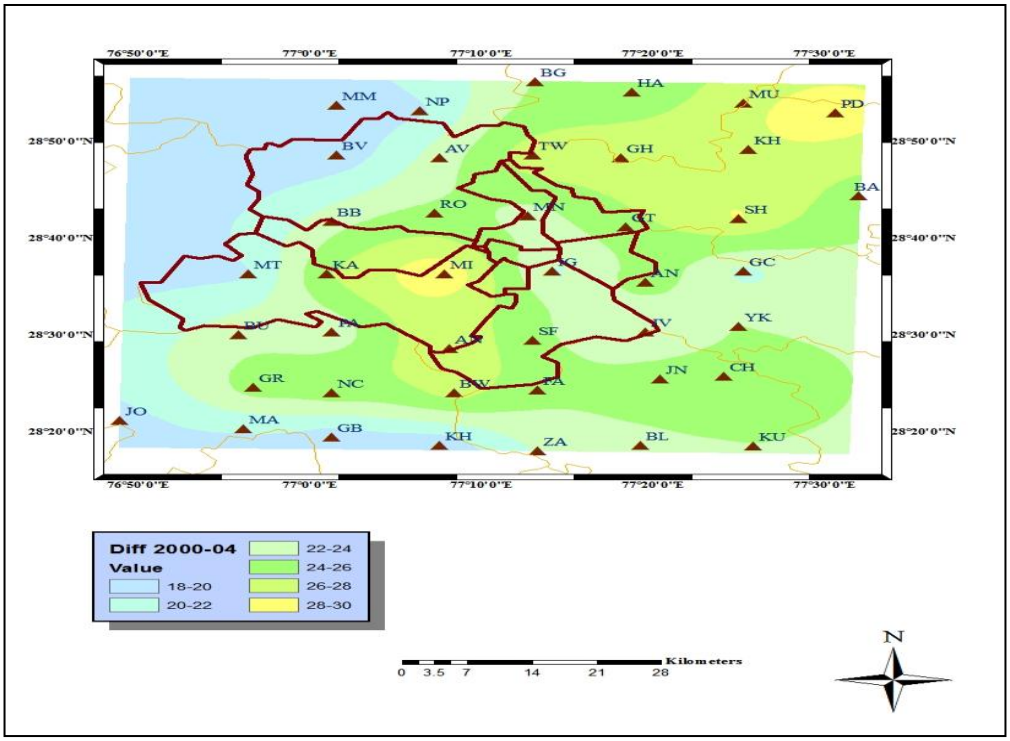

Figure 5.4 (a) $PM_{2.5}$ concentration anomaly across Delhi-NCR for 2004 with reference of 2000

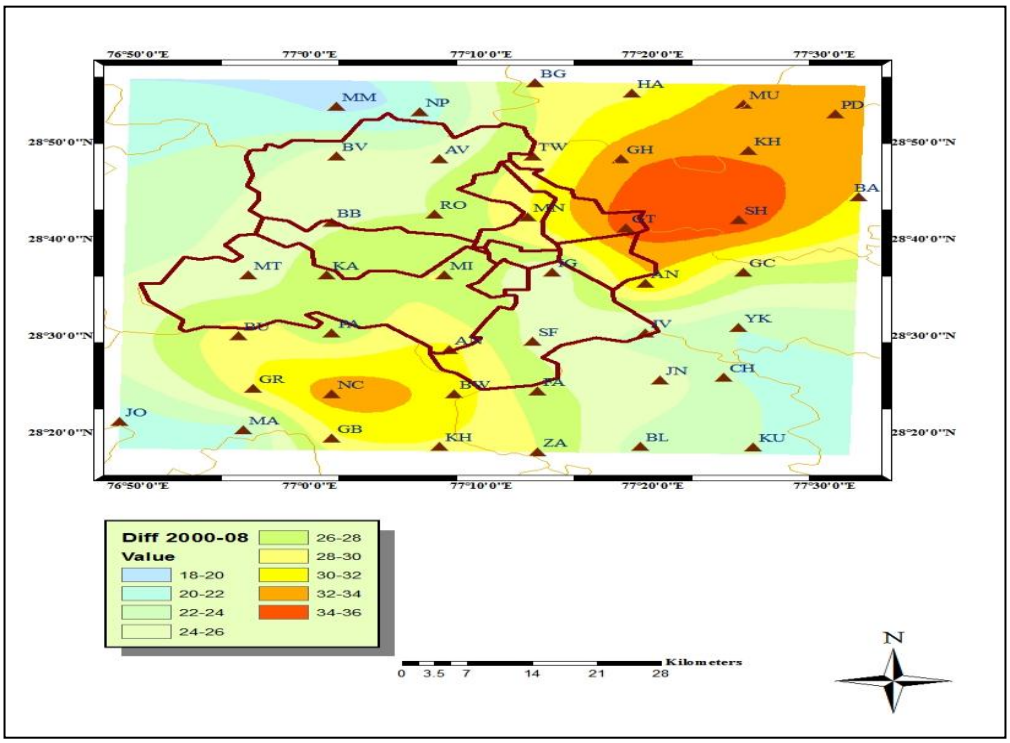

Figure 5.4 (b) $PM_{2.5}$ concentration anomaly across Delhi-NCR for 2008 with reference 2000

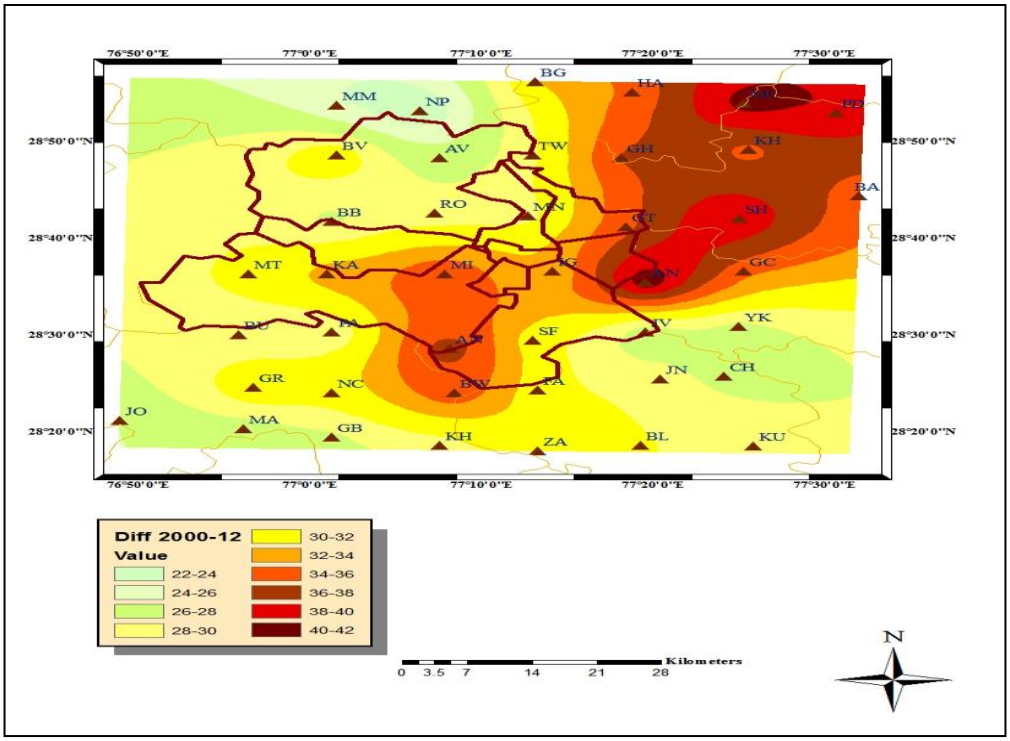

Figure 5.4 (c) $PM_{2.5}$ concentration anomaly across Delhi-NCR for 2012 with reference 2000

$PM_{2.5}$ concentration range was manually classified in 11 vulnerability classes i.e. from Class 1 to Class 11 in increasing concentration order using Arc-GIS. As per Table 5.3 (b), we have observed that there was prominent variation in the different class range of $PM_{2.5}$ (%) of the total study area. In 2000, we can see that most of the area (62.60%) lied in two classes that ranged from Class 1 (31.49%) to Class 2 (31.11%) and rest of the area covered by another three classes as Class 3 (13.7%), Class 4 (20.61%) and Class 5 (3.07%). Further, a shift in $PM_{2.5}$ concentration was observed in 2004, 63.64% of the total area covered by three classes namely Class 4 (15.64%), Class 5 (18.98%), and Class 6 (26.93%) and remaining area covered by Class 7 (14.07%), Class 8 (11.86%) and Class 9 (12.39%). In 2008, major fraction (70.02%) of the study area covered by three classes such as Class 5 (24.45 %), Class 6 (27.73) and Class 7 (17.84) and other minor fraction 30.08% covered by Class 4 (1.82%), Class 6 (6.15%), Class 9 (9.71%), and Class 10 (12.68%). Dynamics further shifted to higher range in 2012, area covered by following classes as class 5 (2.93 %), Class 6 (34.66 %), Class 7 (22.44 %), Class 8 (11.66 %), Class 9 (7.89 %), Class 10 (14.82 %) and Class 11 (5.56 %).

Table 5.2 Area covered by different $PM_{2.5}$ class during 2000-2012

SN	Range (µg/m^3)	Class	Area (% age)			
			2000	2004	2008	2012
1	34-40	Class 1	31.49	-	-	-
2	40-46	Class 2	31.11	-	-	-
3	46-52	Class 3	13.7	-	-	-
4	52-58	Class 4	20.61	15.73	1.82	-
5	58-64	Class 5	3.07	18.98	24.45	2.93
6	64-70	Class 6	-	26.93	27.73	34.66
7	70-76	Class 7	-	14.07	17.84	22.44
8	76-82	Class 8	-	11.86	6.15	11.66
9	82-88	Class 9	-	12.39	9.71	7.89
10	88-92	Class 10	-	-	12.68	14.82
11	92-98	Class 11	-	-	-	5.56

[5.3.3] Spatial and temporal pattern of human population and exposure of $PM_{2.5}$

For assessment of spatial population distribution in the different part of the study area has been exposing divergent range of $PM_{2.5}$ concentration through overlaying $PM_{2.5}$ map (Figure 5.3 a, b, c and d) and population map Figure 3.1 (in Chapter 3). We have seen here that population residing in north-east and eastern part of Delhi-NCR exposing higher $PM_{2.5}$ concentration range as compare to the southern and southwest region in the year 2000. In the later stage of study period (2012) population that is living in the southern and south-western part of an area is getting exposure of a higher range of $PM_{2.5}$.

Exposure of 11 vulnerability categories of the $PM_{2.5}$ concentrations to human population density class has been examined through spatial analyst tool embedded in ArcGIS software. Figure 5.5 (a-b) illustrates the exposure of $PM_{2.5}$ on population density class during the year 2000 and 2012. In the year 2000, Class 1 to Class 5 $PM_{2.5}$ concentration range are predominantly

exposed to Highest and High class population density range, respectively. However, Moderate to Lower population density classes are exposed to Class 4 and Class 5 of $PM_{2.5}$ concentration range and sparse population density class predominantly exposed to Class 1 of $PM_{2.5}$ concentration range. During 2012, Highest to High density population have been exposed from Class 7 to Class 11 range of $PM_{2.5}$. Further, Class 6 to Class 10 $PM_{2.5}$ concentration range is exposed from Moderate to Lower population density. While, sparse population either predominantly exposed from Class 5 or Class 11 concentration range of $PM_{2.5}$.

The various air quality standards for $PM_{2.5}$ exposure threshold to human population are given by United States Environment Protection Agency, (12.5 µg/m^3), WHO interim target (IT) iii (15 µg/m^3), IT ii (25 µg/m^3), IT i (35 µg/m^3), and Indian standard (40 µg/m^3) (Chowdhury et al., 2016; Donkelaar et al., 2015). It was observed that Class 1 to Class 2 $PM_{2.5}$ concentration range near to IT (i) and Indian standard exposed to Sparse and Highest density population in the study area during 2000. Further, in the year 2012, it is observed that almost 100% population living in studied area is exposed to above any standard threshold value.

According to WHO report (2013), life expectancy of human population has been reduced by average of 8.6 months with high exposure of $PM_{2.5}$ in countries of European Union. When daily exposure of $PM_{2.5}$ increased by10 µg/m^3 accordingly hospitalization rate raised by 8 % and prevalence rate of respiratory diseases increased by 2.07 % (Dominici et al 2006; Zanobetti et al., 2009). A study conducted in United States for 7 years (during 2000-2007) showed that average life expectancy was extended by 0.35 years for every 10 µg/m^3 decreases of $PM_{2.5}$ exposure to population (Correia et al., 2013). After comparing our results with the previous studies, it is estimated that the levels of $PM_{2.5}$ is largely increased by approximately 77 % in the present study area during 2000 to 2012 (Figure 5.3a). It is also concluded that the range between 34-64 µg/m^3 of $PM_{2.5}$ were dominant during year 2000 while this range significantly increased up to the range of 64-98 µg/m^3 during 2012 (Table 5.3b). This clearly indicates that the exposure due to $PM_{2.5}$ is largely increased in total covering area of NCR and to high population density group.

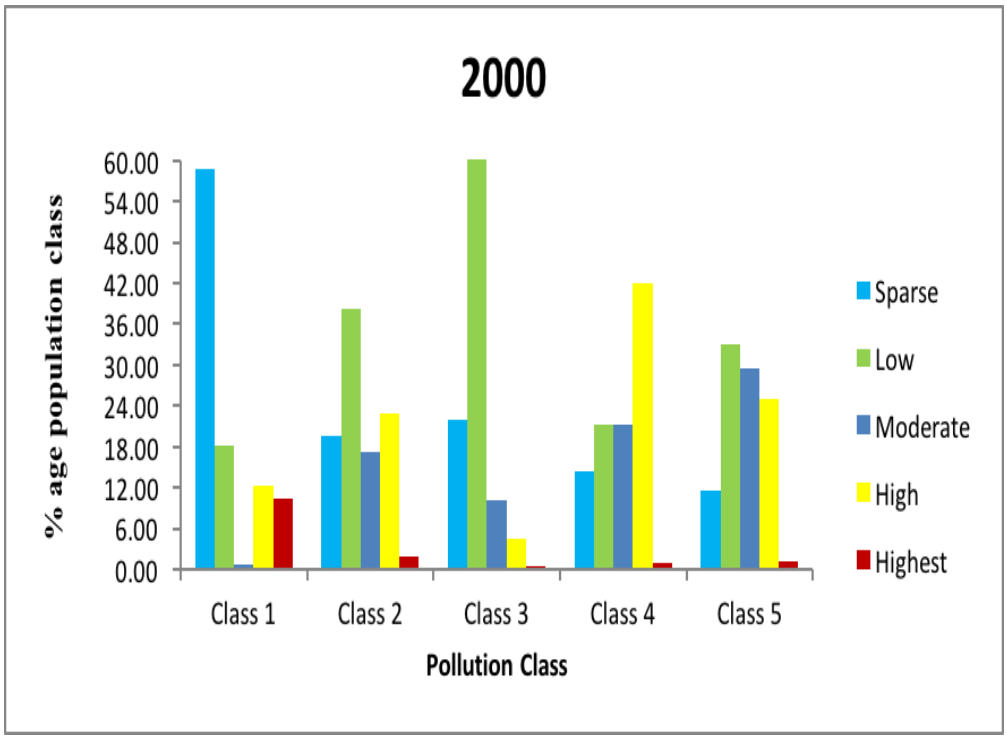

Figure 5.5 (a) $PM_{2.5}$ exposure to population density class during 2000

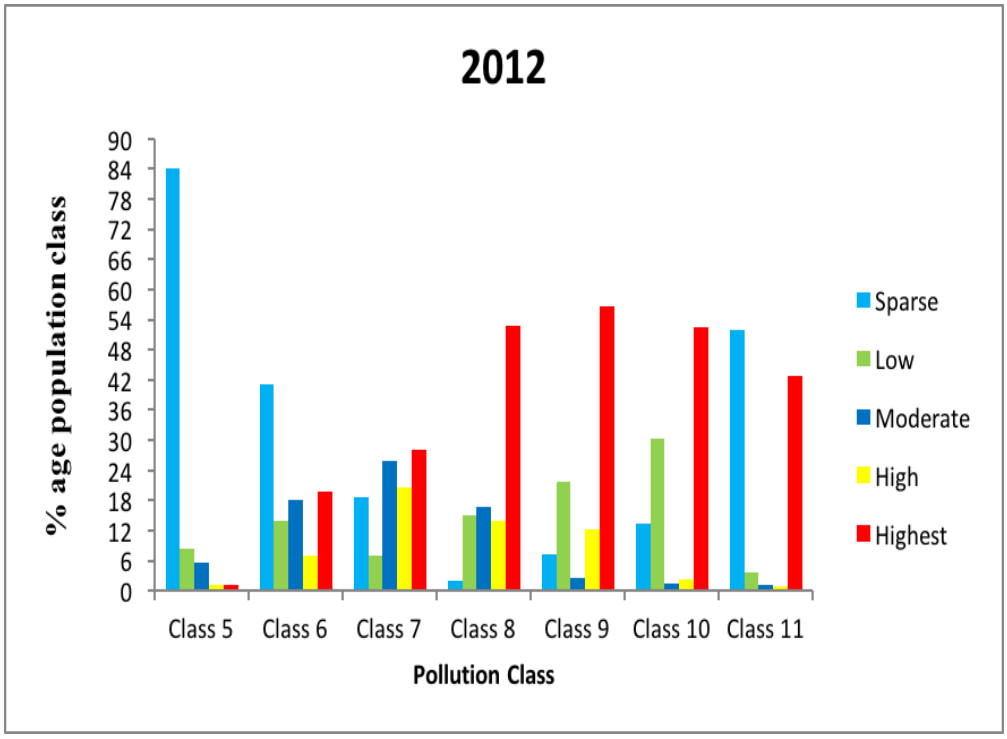

Figure 5.5 (b) $PM_{2.5}$ exposure to population density class during 2012

[5.4] Spatial pattern of Air pollutants and it's relation to LST and LULC in Delhi region

In this section, the influence of LULC changes on spatial air pollutants concentration distribution pattern in Delhi region is examined. Further, different pollutant concentration relation with LST is also estimated. Figure 5.6 (a) explained the LULC spatial distribution in region of interest area .Green Vegetation and Built-up area dominated as 38% and 25% respectively. Bare land, Water bodies and Rocky land have composition of 30%, 4% and 3% respectively of the total Delhi area {Figure 5.6 (b)}. Built-up area has dominated in eastern to north-western region and Green vegetation has primarily situated in south to central region of Delhi. LST spatial distribution has seen in Figure 5.7. LST pattern clearly indicated as western region have higher LST range in compare with center to eastern region.

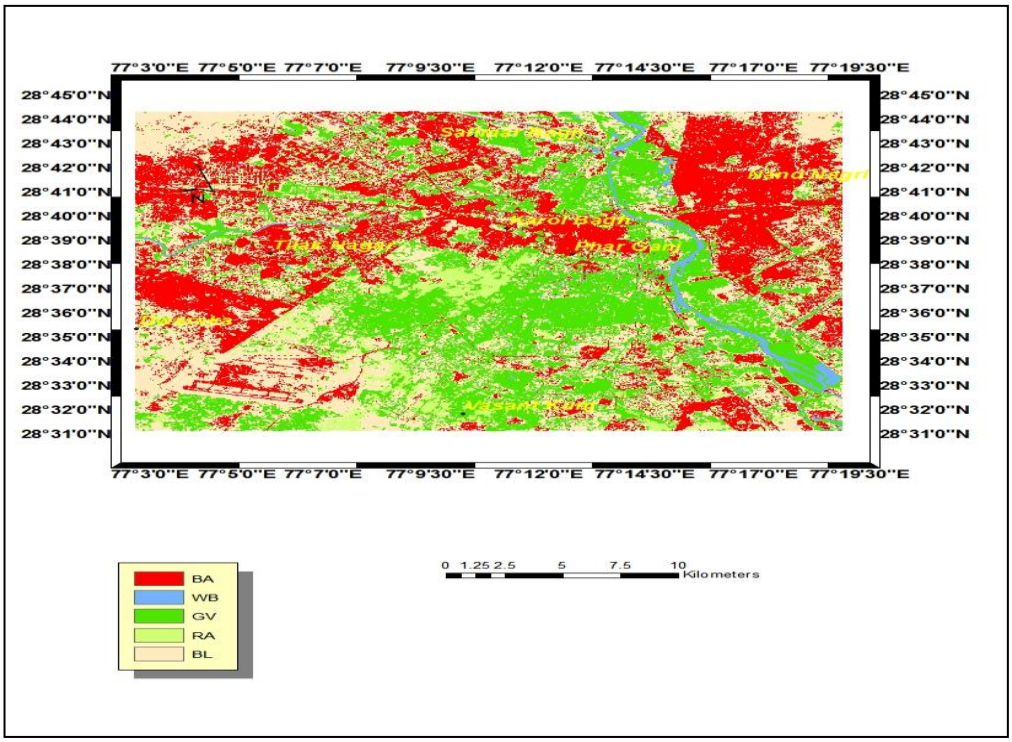

Figure 5.6 (a) Spatial distribution LULC types in May 2009 in Delhi region

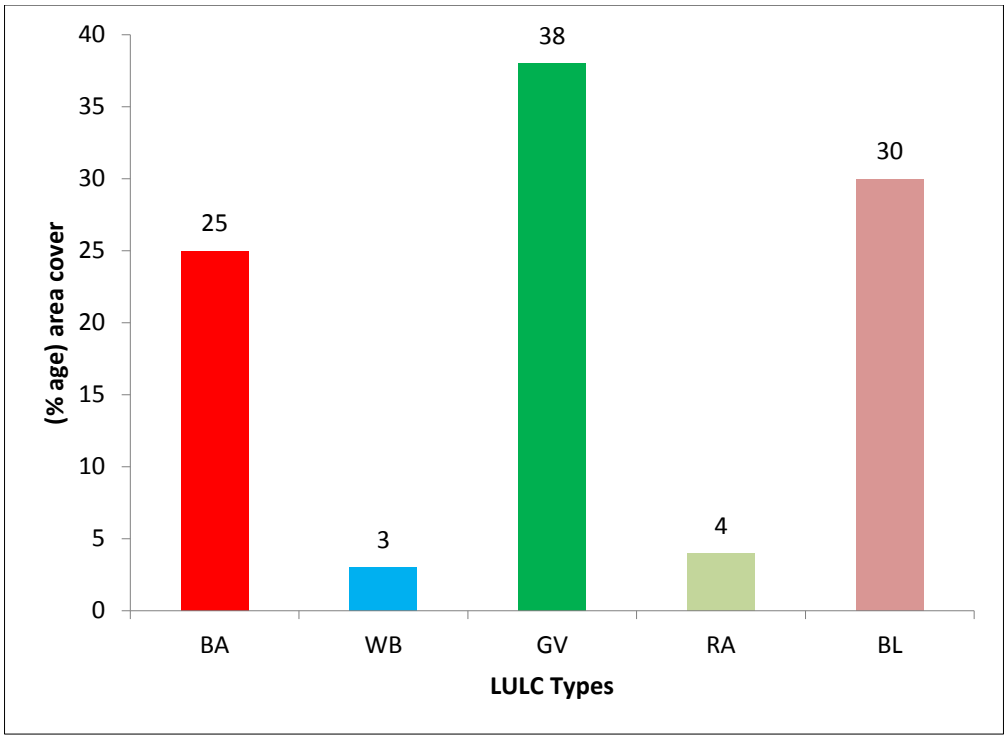

Figure 5.6 (b) Composition of LULC types in May 2009

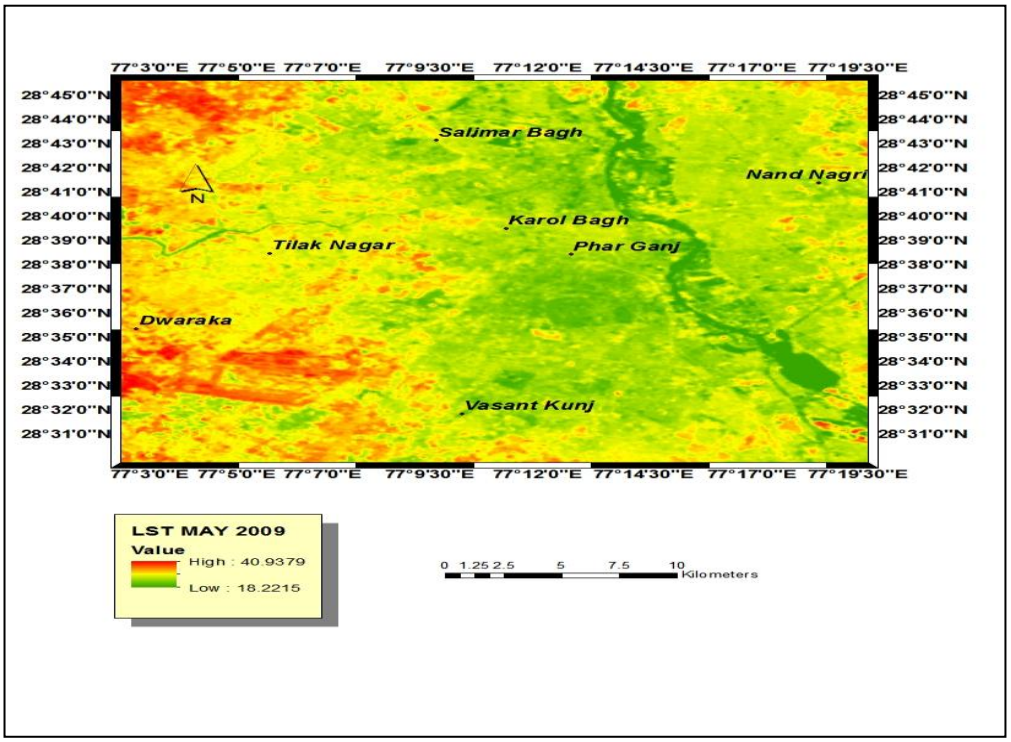

Figure 5.7 Spatial distribution LST in May 2009 in Delhi region

Air pollutants concentration has manually been classified into five classes from low to high i.e. Lower, Moderate, High, Very High and Extreme concentration range using Arc-GIS software. Figure 5.8 to 5.11 shows the spatial pattern of air pollutants concentration in Delhi region in the month of May 2009. Very High to Extreme class of RSPM concentration has distributed over east to south-east region. Moderate to High class of RSPM has covered west to central region and Lower class is primarily located at central region of Delhi Figure 5.8. Spatial distribution of NO_2 has seen in Figure 5.9. Very High to Extreme concentration of NO_2 has lied over eastern region and Lower to Moderate class has distributed central to western region of Delhi. Wide distribution of SO_2 has seen over Delhi region in the month of May 2009 (Figure 5.10). Very-High and Extreme class are sparsely distributed in south-east to central region and High class has distributed in patchy form in all the regions. Lower and Moderate class has primarily cover in central to western region of studied area. Spatial distribution in CO concentration has shown in Figure 5.11. There was no distinct class cover found while most widely Moderate class is evenly distributed in the entire area. High and Extreme class is lying in patchy form in east to central region of Delhi.

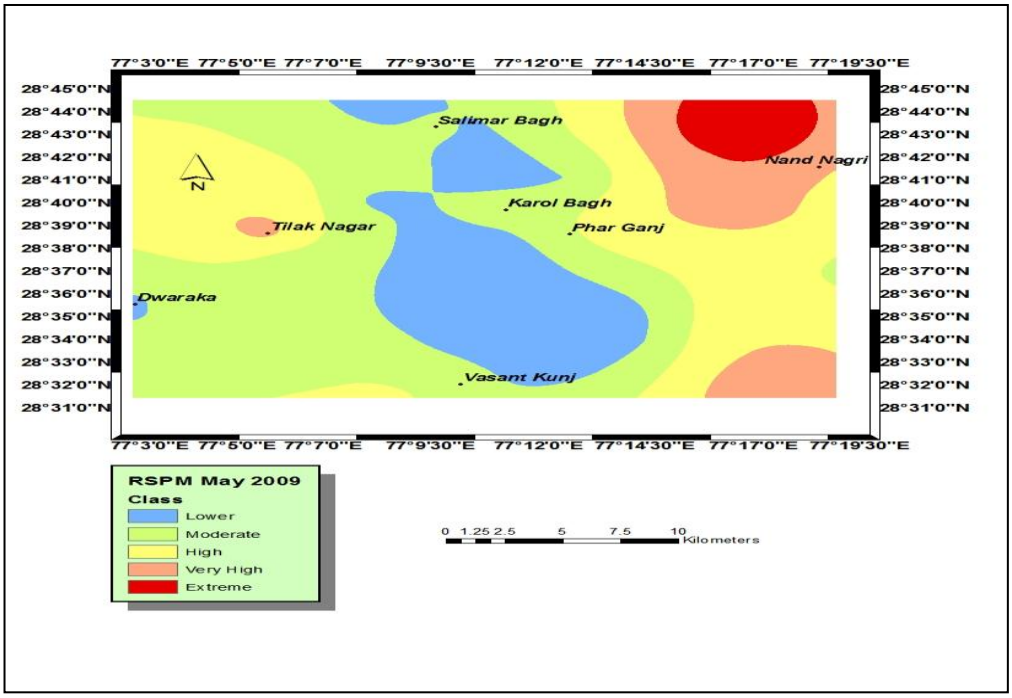

Figure 5.8 Spatial pattern of RSPM concentration class in May 2009 over Delhi region

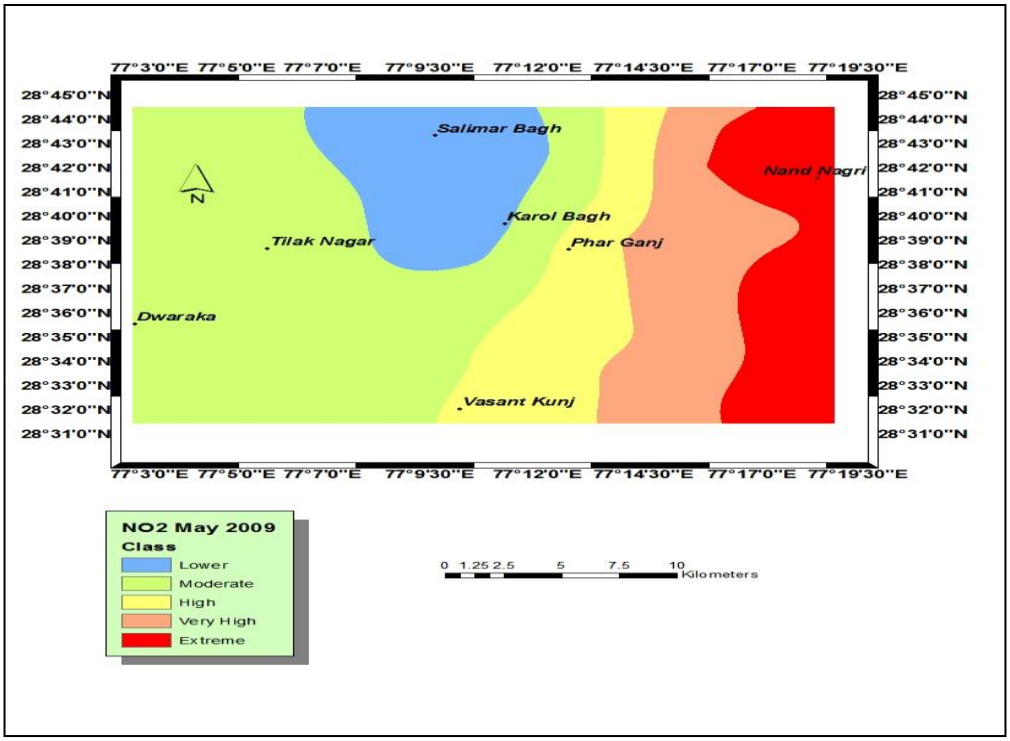

Figure 5.9 Spatial pattern of NO_2 concentration class in May 2009 over Delhi region

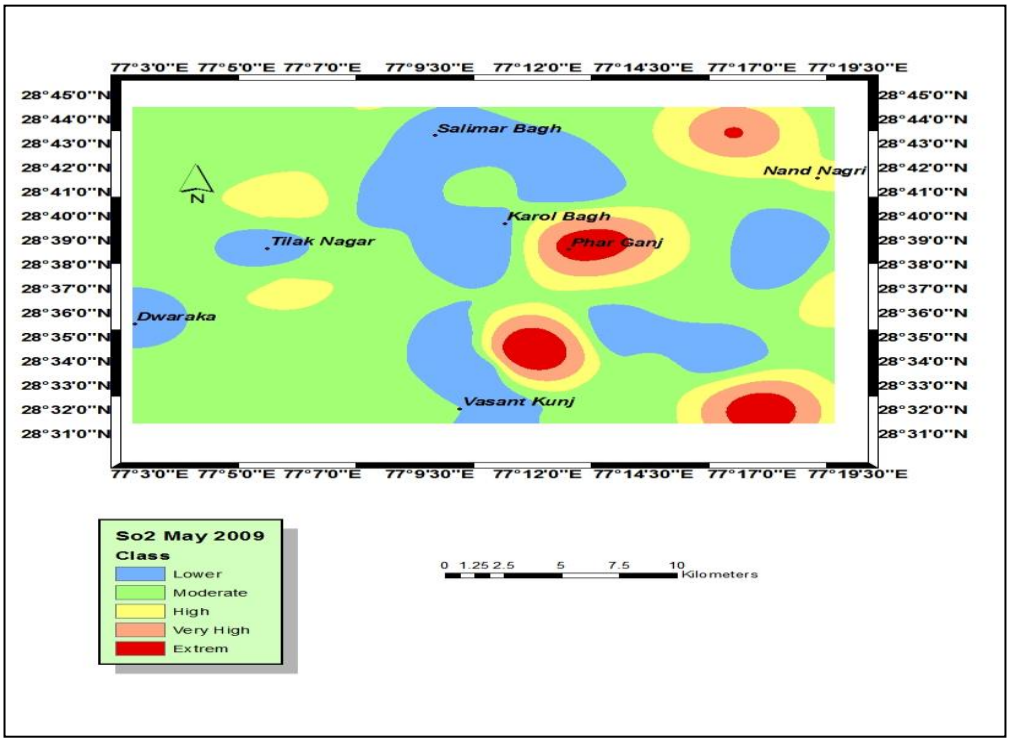

Figure 5.10 Spatial pattern of SO_2 concentration class in May 2009 over Delhi region

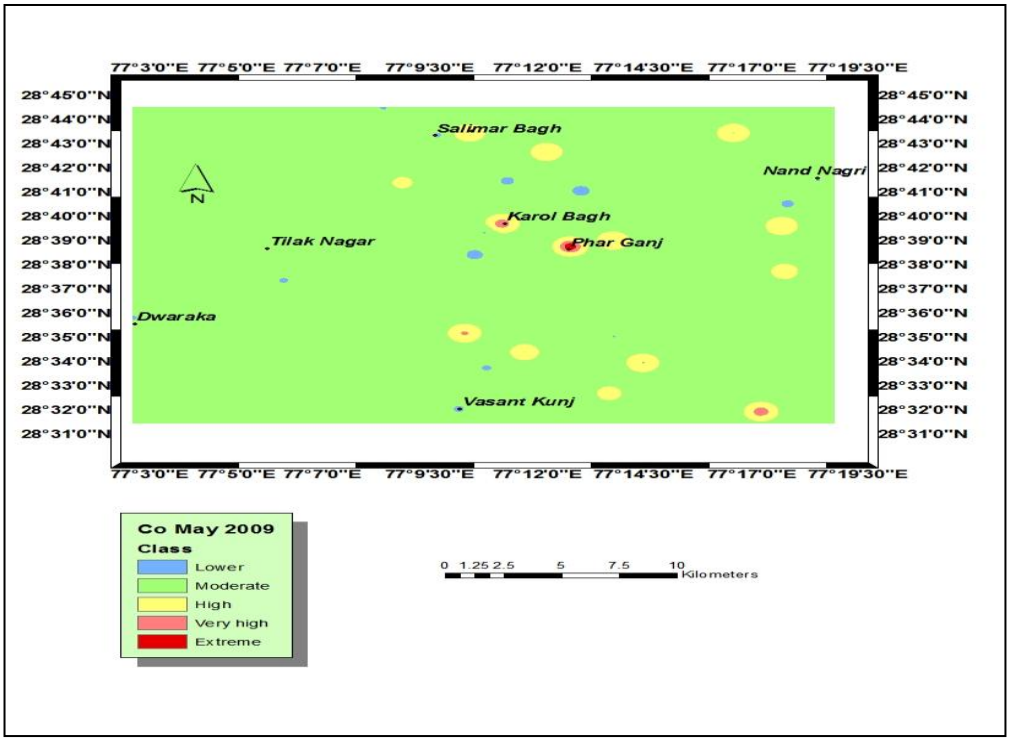

Figure 5.11 Spatial pattern of SO_2 concentration class in May 2009 over Delhi region

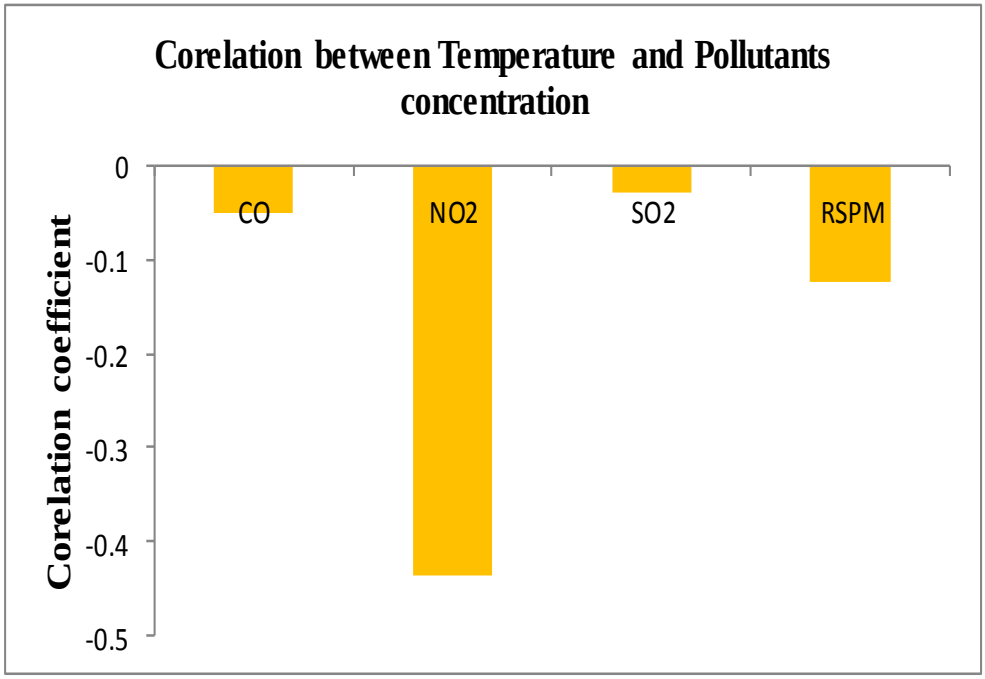

Figure 5.12 Correlation coefficient between pollutants concentration and LST in May 2009

All discussed air pollutants (RSPM, NO_2, SO_2, CO) are negatively co-related with LST. The relation between NO_2 and RSPM concentrations with LST is significant in comparison to SO_2 and CO. The co-relation coefficient of NO_2, RSPM, SO_2 and CO are found to be -0.43, -0.12, -0.02, and -0.04 respectively Figure 5.12.

Most of the studied area has lied under Moderate to High pollutants concentration class in the month of May 2009. Moderate and High class of RSPM cover 62% of total area and rest lies under Extreme, Very High and Lower classes which covered 10%, 10% and 18% of the total area respectively. Different classes of NO_2 namely; Lower, Moderate, High, Very-High and Extreme has covered 8%, 43%, 17%, 16% and 16% of the total area of Delhi respectively. Extreme, Very-High, High, Moderate and Lower class of SO_2 has covered 4%, 9%, 13%, 55% and 19% of total area respectively in Delhi region Figure 5.13.

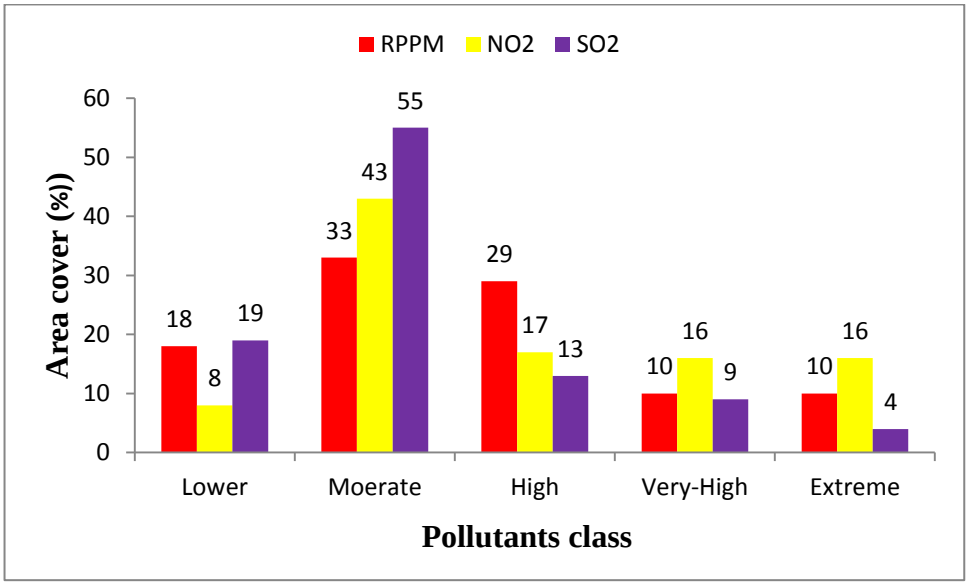

Figure 5.13 Percentage area covers by different air pollutants concentration class in May 2009

The relation between different classes of air pollutants concentration and LULC types are shown in Figure 5.14 (a-e). Lower class of all air pollutants (RSPM, NO_2 and SO_2) were found over green vegetation area in Delhi region during May 2009. Bare Land cover in Delhi region has been found to be dominated by Moderate pollutants concentration class in May 2009. Most part of the Very-High to Extreme pollutants concentration class existed over the Built-up Area of

Delhi region in May 2009. In other words, Built-up area has lied under Extreme and Very-High pollutants class in May 2009 at Delhi region Figure 5.15. Extreme and Very-High pollutants class has primarily lied over Built-up area situated in east region in Delhi. Population residing in east zone of Delhi region has been exposed to higher pollution class as compared to population residing in central and south zone in May 2009.

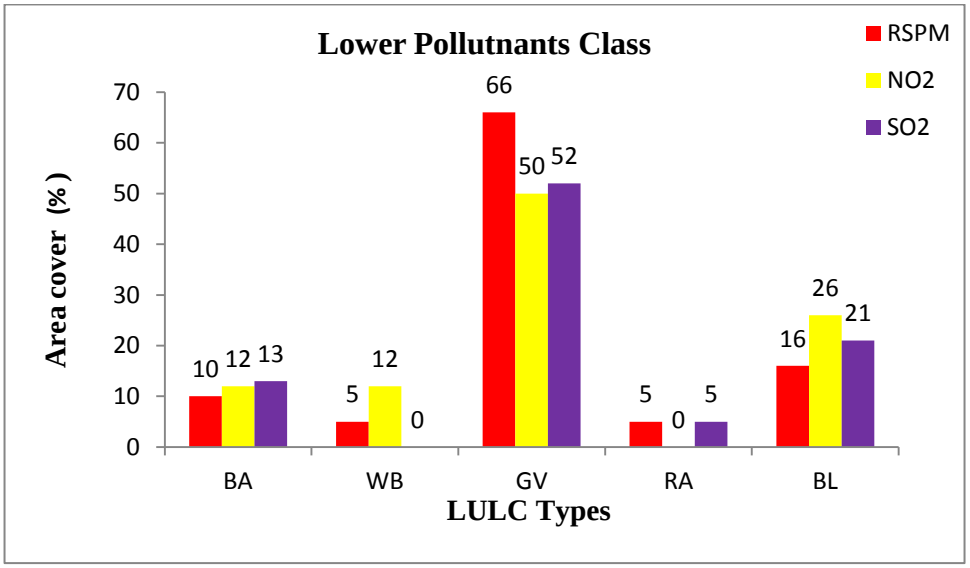

Figure 5.14 (a) Percentage area covers by Lower pollutants class in different LULC in May 2009

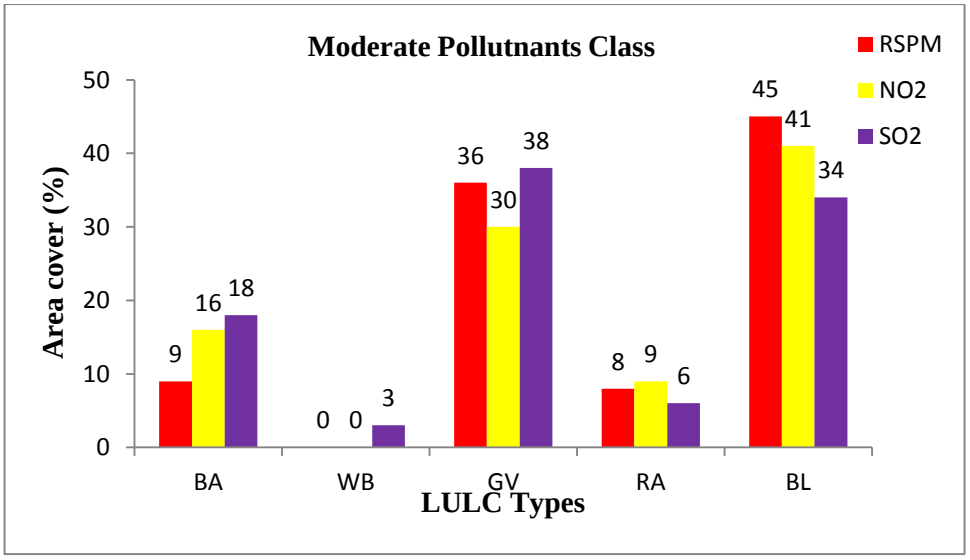

Figure 5.14 (b) Percentage area covers by Moderate pollutants class in different LULC in May 2009

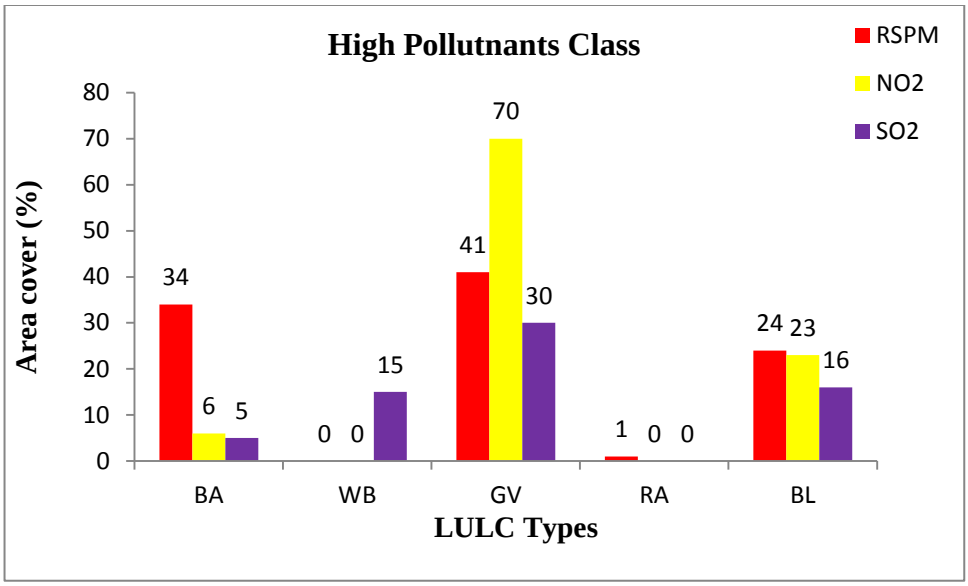

Figure 5.14 (c) Percentage area covers by Moderate pollutants class in different LULC in May 2009

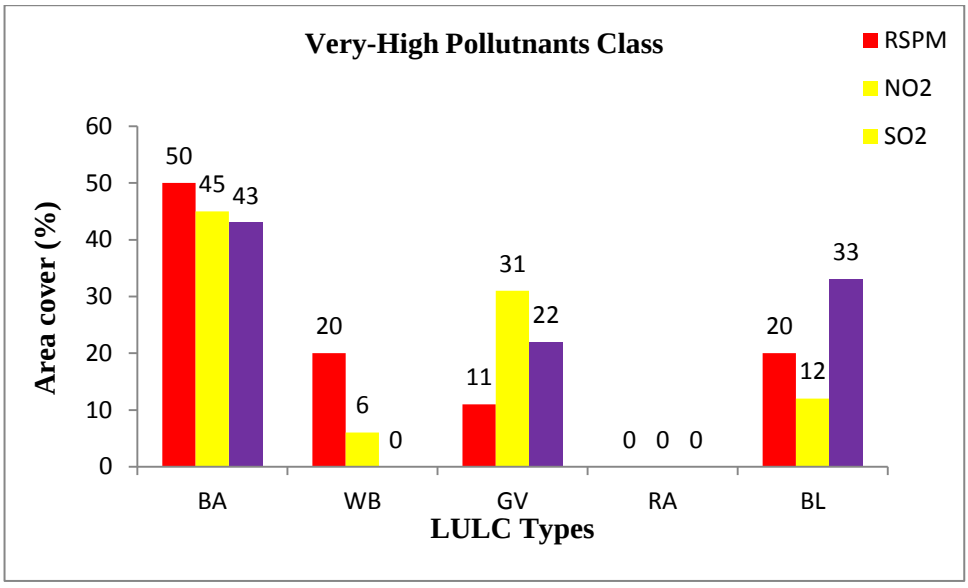

Figure 5.14 (d) Percentage area covers by Very-High pollutants class in different LULC in May 2009

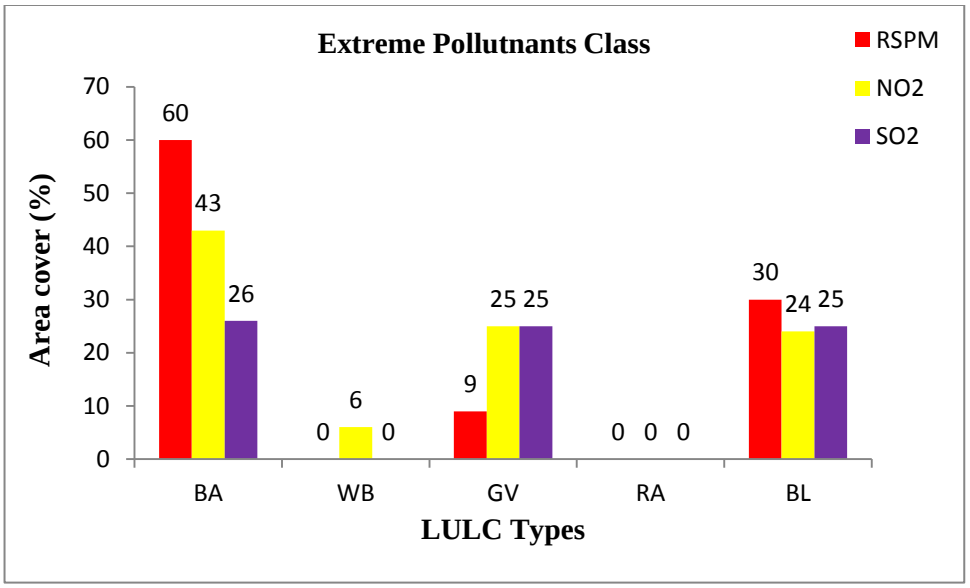

Figure 5.14 (e) Percentage area covers by Extreme pollutants class in different LULC in May 2009

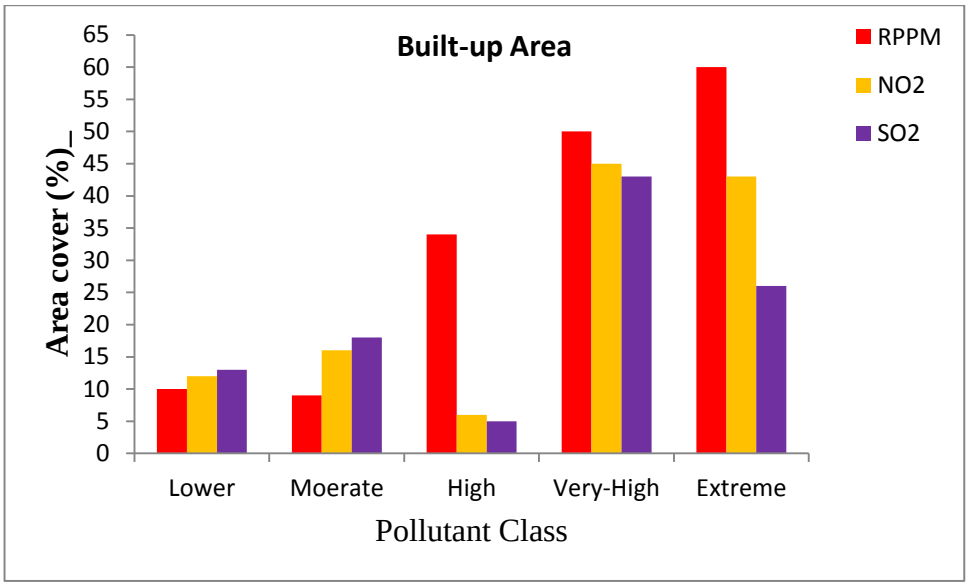

Figure 5.15 Percentage of pollutants concentration class covered over Built-up area in May 2009

[5.4] Summary

In the present study, we analyzed the location wise statistics of a satellite-derived annual average of $PM_{2.5}$ concentration and its long-term exposure assessment of regional concentration to the

human population in National Capital Region, India. Our results showed the micro level spatial and temporal continuous heterogeneity of $PM_{2.5}$ concentration over the study area. Major conclusions of our study are as follows:

1. MKTM revealed that overall increasing trend of $PM_{2.5}$ concentration is noticed in last decade at all 42 points of the study area. Significant increasing trend was found in extended urban agglomeration and developing area (RSA, BAL, and RA) as compared to already developed urban area. Therefore, it is concluded that LULC change influences the location specific concentration of $PM_{2.5}$.
2. The dynamics of the spatio-temporal distribution of $PM_{2.5}$ concentration range significantly changed during the study period (2000-2012). In the year 2000, most of the area covers 62.60 % by Class 1 to Class 2 range of $PM_{2.5}$ and it changes to 62.37% cover by Class 7 to Class 11 concentration range in the year 2012. A dense urban area in the eastern and central region have higher $PM_{2.5}$ concentration range as compared to prevailing ridge area in the southern and blank land in western zone of studied area.
3. In 2000, Class 1 to Class 2 $PM_{2.5}$ concentration range is predominantly exposed to Highest to High population density area. However, in 2012 Highest to High population density area are exposed Class 7 to Class 11 concentration range of $PM_{2.5}$.
4. After examining the exposure assessment, it is indicated that Highest density population area exposed to the annual average of $PM_{2.5}$ concentration ≤ 40 $\mu g/m^3$ (Indian standard thresholds) during 2000. Further, it changes to Higher and Highest population density during 2012 which exposed to ≥ 70 $\mu g/m^3$ annual concentration of $PM_{2.5}$.
5. RSPM, NO_2, SO_2, and CO concentration are negatively co-related with LST
6. Most part of the Very-High to Extreme pollutants concentration class existed over the Built-up Area of Delhi region in May 2009.
7. Population residing in east zone of Delhi region has been exposed to higher pollution class as compared to population residing in central and south zone in May 2009.

Chapter 6 *Conclusions*

In the present study, it is found that enormous changes have been occurred in spatial pattern of human population changes in NCR during the period 2000-2015. Percentage of total area cover by different population density class is decreased by 21.8%, 11.95%, 49.50% and 33.67% for Sparse, Lower, moderate and high density class respectively. Highest density class is found to increase by 118.05% during 2000-2015. Further, extreme changes in spatio-temporal pattern of land use and land cover is observed over the study area during period 2003 to 2014. It is found that there is coherent increase in Built-up area by 101% and Green vegetation cover area by 70% at the cost of ridge area (rocky area) and Blank land area decreases by 67% and 4% of total area cover.

It has also been observed that LULC composition changes are predominant factor in LST anomaly in stipulated time period. Built-up area has expanded more in northern and eastern part of the city which leads to shifting of LST from lower to higher class. The total area cover by different LST class change occurred during study period in found to be: Lower and Moderate increased by 37.28% and 51.01% respectively. High and Extreme class decreases by 30.83% and 84.19%. It is clearly observed that the Moderate LST class pattern is closely associated with Built-up area pattern. The area by Moderate LST class was changed from 33.64% to 50.80%, is follow similar trend as urban Built-up area changed 5.84% to 11.78% in between 2003 to 2014. It shows that urban area expansion highly influences the local LST dynamics. Lower LST class corresponding to Green vegetation is concentrated in the central to northeast area of NCR during the year 2003 which gradually expanded to southern direction in later years due to conversion of scrub vegetation cover to ridge area into Green vegetation.

Our results showed that micro level spatial and temporal continuous heterogeneity of air pollutants as RSPM, NO_2, SO_2 CO and $PM_{2.5}$ concentration in the studied area. MKTM revealed that overall increasing trend of $PM_{2.5}$ concentration is noticed in last decade at all 42 points of the studied area. Significant increasing trend was found in extended urban agglomeration and

developing area (RSA, BAL, and RA) as compared to already developed urban area. Therefore, it is concluded that LULC change influences the location specific concentration of $PM_{2.5}$. The dynamics of the spatio-temporal distribution of $PM_{2.5}$ concentration range significantly changed during the study period (2000-2012). In the year 2000, most of the area covers 62.60 % by Class 1 to Class 2 range of $PM_{2.5}$ and it changes to 62.37% cover by Class 7 to Class 11 concentration range in the year 2012. A dense urban area in the eastern and central region have higher $PM_{2.5}$ concentration range as compared to prevailing ridge area in the southern and blank land in western zone of studied area. In 2000, Class 1 to Class 2 $PM_{2.5}$ concentration range is pre dominantly exposed to Highest to High population density area. However, in 2012 Highest to High population density area are exposed Class 7 to Class 11 concentration range of $PM_{2.5}$. RSPM, NO_2, SO_2, and CO concentration is negatively co-related with LST in May 2009 in Delhi region. Most part of the Very-High to Extreme pollutants concentration class existed over the Built-up Area of Delhi region in May 2009. Population residing in east zone of Delhi region has been exposed to higher pollution class as compared to population residing in central and south zone in May 2009.

References

Anderson, J. R., Hardy E. E., Roach, J. T. and Witmer, R. E. (1971). A Land Use And Land. Cover Classification System For Use With Remote Sensor Data, United States Government Printing Office, Washington.

Aslam, M. Y., Krishna, K. Rama, Beig, G., Tinmaker, M. I. R. and Chate, D. M. (2017). Seasonal Variation of Urban Heat Island and Its Impact on Air-Quality Using SAFAR Observations at Delhi, India. American Journal of Climate Change. 6, 294-305.

Atta-ur-Rahman and Dawood, M. (2016). Spatio-statistical analysis of temperature fluctuation using Mann Kendall and Sen's slope approach. Climate Dynamics. https://doi.org/10.1007/s00382-016-3110-y: 1–15.

Ayanlade, A. (2016). Seasonality in the daytime and night-time intensity of land surface temperature in a tropical city area. Science of the Total Environmental, 557-558, 415–424.

Balçik, F. B. (2014). Determining the impact of urban components on land surface temperature of Istanbul by using remote sensing indices. Environmental Monitoring and Assessment,186,859–872.

Barsi, J. A., Barker, J. L. and Schott, J. R. (2003). An atmospheric correction parameter calculator for a single thermal band earthsensing instrument. In: Processdings of the 2003 IEEE International Geoscience and Remote Sensing Symposium IGARSS '03. Melbourne, Australia, 21–25 July 2003; Volume 5, p. 3014–3016.

Barsi, J. A., Schott, J. R., Palluconi, F. D. and Hook, S. J. (2005). Validation of a web-based atmospheric correction tool for single thermal band instruments, pp. 58820E–58820E-58827.

Barsi, J. A., Schott, J.R., Palluconi, F.D. and Hook, S. J. (2005). Validation of a web-based atmospheric correction tool for single thermal band instruments. In: JJ Butler, editor. Proceedings of SPIE, Earth Observing Systems X. Volume 5882, Paper 58820E, Bellingham, WA: SPIE Aug 22, 2005.

Becker, F. and Li Z. L. (1995). Surface temperature and emissivity at various scales: definition, measurement and related problems. Remote Sensing Reviews, 12: 225-53.

Beelen, R., Hoek, G. and Vienneau, D. (2013). Development of NO2and NOx land use regression modelsfor estimating air pollution exposure in 36 study areas in Europe The ESCAPE project, Atmospheric Environment 72 (2013) 10-22.

Bellander, T., Berglind, N., Gustavsson, P., Jonson, T., Nyberg, F. and Pershagen, G. et al.(2001). Using geographic information systems to assess individual historical exposure to air pollution from traffic and house heating in Stockholm. Environ Health Perspect, 109(6): 633–639.

Bereitschaft, B. and Debbage, K. (2013). Urban Form, Air Pollution, and CO_2 Emissions in Large U.S.Metropolitan Areas, The Professional Geographer, 65(4), pages 612–635.

Binder, S., Levitt, A. M., Sacks, J. J., and Hughes, J. M. (1999). "Emerging infectious diseases: Public Health Issues for the 21st Century," Science, 284(5418):1311- 1313.

Blodget, H., Taylor, P. and Roark, J. (1991). Shoreline changes along the Rosetta-Nile Promontory: monitoring with satellite observations. Marine Geology, 99 67–77.

Bowler, D. E., Buyung-Ali, L., Knight, T. M. and Pullin, A. S. (2010). Urban greening to cool towns and cities: A systematic review of the empirical evidence. Landscape and Urban Planning, 97(3), 147–155.

Brabyn, L., Zawar-Reza, Peyman, Stichbury, G., Cary, C., Storey, B., Laughlin, D. C. and Marwan, K. (2014).Accuracy assessment of land surface temperature retrievals from Landsat 7 ETM + in the Dry Valleys of Antarctica using iButton temperature loggers and weather station data. Environmental Monitoring and Assessment, 186, 2619–2628.

Brauer, M., Amann, M., Burnett, R. T., Cohen, A., Dentener, F., Ezzati, M. and Thurston, G. D. (2012). Exposure assessment for estimation of the global burden of disease attributable to outdoor air pollution. Environmental Science and Technology. 46(2): 652–660.

Briggs, D. Exposure assessment. In: Elliott, P., Wakefield, J., Best, N. and Briggs, D. (Eds.). (2000). Spatial Epidemiology: Methods and Applications. Oxford University Press, Oxford. pp 335–359.

Buchholz, S., Krein, A., Junk, J., Heinemann, G. and Hoffmann, L. (2013). Simulation of Urban-Scale Air Pollution Patterns in Luxembourg: Contributing Sources and Emission Scenarios, Environ Model Assess, 18:271–283 DOI 10.1007/s10666-012-9351-1.

Carlson, T. N. and Ripley, D. A. (1997). On the relation between NDVI, fractional vegetation cover, and leaf area index. Remote Sens Environ. 62:241–252.

Carlson, T. N. and Riziley, D. A. (1997).On the Relation between NDVI, Fractional Vegetation Cover, and Leaf Area Index.Remote Sensing of Environment, 62, 241-252.

Caspersen, J. P., Pacala, S. W., Jenkins, J. C., Hurtt, G. C., Moorcroft, P. R., and Birdsey, R. A. (2000). "Contributions of Land-Use History to Carbon Accumulation in U.S. Forests," Science, 290(5494):1148-1151.

Cavan, G., Lindley, S., Jalayer, F., Yeshitela, K., Pauleit, S. and Renner, F. et al. (2014). Urban morphological determinants of temperature regulating ecosystem services in two African Cities. Ecological Indicators 42, 43-57

Chakraborty, S. D., Kant,Y. and Mitra, D. (2013). Assessment of land surface temperature and heatfluxes over Delhi using remote sensing data, Journal of Environmental Management, 1-10.

Chander, G. and Markham, B. (2003). Revised Landsat-5 TM Radiometric Calibration Procedures and Postcalibration Dynamic Ranges, IEEE Trans. Geosciences and Remote Sensing.41(11), 2674–2677.

Chowdhury, S. and Dey, S. (2016). Cause-specific premature death from ambient $PM_{2.5}$ exposure in India: Estimate adjusted for baseline mortality. Environment International, 91: 283-290.

CIESIN [Center for International Earth Science Information Network - Columbia University]. (2016). Documentation for the Gridded Population of the World, Version 4 (GPWv4).

Palisades NY: NASA Socioeconomic Data and Applications Center (SEDAC) http://dx.doi.org/10.7927/H4D50JX4 [Accessed 03 June 2016].

Cilliers, S., Cilliers, J., Lubbe, R. and Siebert, S. (2012). Ecosystem services of urban green spaces in African countries—Perspectives and challenges. Urban Ecosystems, 16, 681–702.

Cohen, J. E. (1995a). "Population Growth and Earth's Human Carrying Capacity," Science, 269(5222):341-346.

Couzin, J. (1999). "Landscape Changes Make Regional Climate Run Hot and Cold," Science, 283(5400):317-319.

Cresswell, M. P. (1999). Estimating surface air temperatures, from Meteosat land surface temperatures, using an empirical solar zenith angle. International Journal of Remote Sensing, 20(6), 1125–1132.

Chun. Y and Griffith D. A (2011). Spatial statistics & geostatistics

Daily, G. C. (Ed.) (1997). Nature's Services: Societal Dependence on Natural Ecosystems, Washington, DC: Island Press, 392 p.

Dasgupta, S., Laplante, B., Meisner, C., Wheeler, D. and Yan, J. (2007)s. The impact of sea level rise on developing countries: A comparative analysis. World Bank Policy Research Working Paper 4136, World Bank, Washington, DC.

Dewan, A. M. and Yamaguchi, Y. (2009). Land use and land cover change in Greater Dhaka, Bangladesh: Using remote sensing to promote sustainable urbanization. Applied Geography, 29(3), 390–401.

Dey, S. and Di Girolamo, L. (2011). A decade of change in aerosol properties over the Indian subcontinent.Geophysical Research Letters. 38:L14811.

Dey, S., Di Girolamo, L., van Donkelaar, A., Tripathi, S., Gupta, N. T. and Mohan M. (2012). Variability of outdoor fine particulate (PM 2.5) concentration in the Indian Subcontinent: A remote sensing approach. Remote Sensing of Environment. 127: 153-161.

Diner, D.D., Braswell, B.H., Davies, R., Gobron, N., Hu, J. and Jin, Y. et al. (2005). The value of multiangle measurements for retrieving structurally and radiatively consistent properties of clouds, aerosols, and surfaces. Remote Sens Environ 97:495–518.

Ding, H. and Shi, W. (2013). Land-use/land-cover change and its influence on surface temperature: a case study in Beijing City. Intl J Remote Sensing, 34(15), 5503–5517.

Dockery, D. W., Pope, C. A. III, Xu. X., Spengler, J. D., Ware, J. H. and Fay, M. E. et al. (1993). An association between air pollution and mortality in six U.S cities. N Engl J Med. 329:1753–1759.

Dockery, D., and Pope, C. A. (1994). Acute respiratory effects of particulate air pollution. Annu Rev Public Health, 15: 107–132.

Drápela, K., Drápelová, I. and Drápelová, R. I. (2011). Application of Mann-Kendall test and the Sen's slope estimates for trend detection in deposition data from BílýKříž (Beskydy Mts., the Czech Republic) 1997–2010.Beskydy.4(2): 133–146.

Duan, N. (1982). Models for human exposure to air pollution, Environ. Int. 8:305–309.

Dubreuil, V., Debortoli, N., Funatsu, B., Nédélec, V. and Durieux, L. (2012). Impact of land-cover change in the Southern Amazonia climate: a case study for the region of Alta Floresta, MatoGrosso, Brazil. Environmental Monitoring and Assessment, 184, 877–891.

Eeftensa, M., Beekhuizen, J., Beelen, R., Wang, M., Vermeulen, R., Brunekreef, B., Huss, A. and Hoek, G. (2013). Quantifying urban street configuration for improvements in air pollution models, Atmospheric Environment, 72 (2013) 1-9.

Eplee Jr, R. E., Meister, G., Patt, F. S., Franz, B. A. and McClain, C. R. (2011). Uncertainty assessment of the SeaWiFS on-orbit calibration. In: Earth Observing Systems XVI, Vol. 8153 (Butler JJ, Xiong X, Gu X, eds). Proc SPIE 8153; doi:10.1117/12.892340.

Feizizadeh, B. and Blaschke, T. (2013). Examining Urban Heat Island Relations to Land Use and Air Pollution: Multiple Endmember Spectral Mixture Analysis for Thermal Remote Sensing, IEEE journal of selected topics in applied earth observations and remote sensing, VOL. 6.

Feng, H., Liu, H. and Wu, L. (2014). Monitoring the relationship between the land surface temperature and urban growth in Beijing, China. IEEE J Applied Earth Observation and Remote Sensing, 7, 4410-4019.

Goel, R., Gani, S., Guttikunda, S. K., Wilson, D. and Tiwari, G. (2015). On-road PM2.5 pollution exposure in multiple transport microenvironments in Delhi. Atmospheric Environment. 123:129-138.

Grimm, N. B., Faeth, S. H., Golubiewski, N. E., Redman, C. L., Wu, J., Bai, X. and Briggs, J. M. (2008). Global change and the ecology of cities. Science 319:756–60.

Han, G. and Xu, J. (2013). Land surface phenology and land surface temperature changes along an urban–rural gradient in Yangtze River Delta, China. Environmental Management, 52, 234–249.

Han, G. and Xu, J. (2013). Land surface phenology and land surface temperature changes along an urban-rural gradient in Yangtze river delta, China Environ. Manage., 52. pp. 234-249.

Helsel, D.R. and Hirsch R.M. (1992). Statistical Methods in Water Resources. Elsevier Science Publishers B.V. ISBN 0-444-81463-9: chapter 12.

Herold, M., Goldstein, N. C. and Clarke, K. C. (2003). The spatiotemporal form of urban growth: measurement, analysis and modeling. Remote Sensing of Environment, 86, 286– 302.

Hewitt, C. N. (1991). Spatial variations in nitrogen dioxide concentration in an urban area. Atmospheric Environment, **25B**, 429± 34.

Hoek, G., Brunekreef, B., Goldbohm, S., Fischer, P. and Van Den Brandt, P. A. (2002). Association between mortality and indicators of traffic-related air pollution in the Netherlands A cohort study. Lancet. 11280:3.

Hoek, G., Fischer, P., Van Den, B. P., Goldbohm, S. and Brunekreef, B. (2001). Estimation of long-term average exposure to outdoor air pollution for a cohort study on mortality. J Expos Anal Environ Epidemiol, 11: 459–469.

Houghton, R. A., Hackler, J. L. and Lawrence, K. T. (1999). "The U.S. Carbon Budget: Contributions from Land-Use Change," Science, 285(5427):574-578.

Hurtt, G. C., Pacala, S. W., Moorcroft, P. R., Caspersen, J., Shevliakova, E., Houghton, R. A., and Moore, B. (2002). "Projecting the Future of the US Carbon Sink," Proceedings of the National Academy of Sciences USA, 99(3):1389-1394

Jacobson, M. Z. (2008). On the causal link between carbon dioxide and air pollution mortality. Geophysical Research Letters, 35:L03809.

Jerrett, M., Arain, A., Kanaroglou, P., Beckerman, B., Potoglou, D., Sahsuvaroglu, T., Morrison, J. and Giovis, C. (2005). A review and evaluation of intraurban air pollution exposure models. Journal of Exposure Analysis and Environmental Epidemiology, 15: 185–204.

Jerrett, M., Burnett, R. T., Kanaroglou, P. S., Eyles, J., Brook, J.R. and Giovis, C. et al. (2001a). A GIS F environmental justice analysis of particulate air pollution in Hamilton, Canada. Environ Plann A. 33: 955–973.

Jime´nez-Munoz, J. C. and Sobrino, J. A. (2003). A generalized single-channel method for retrieving land surface temperature from remote sensing data.Journal of Geophysical Research, 108 (22), 4688.

Jimenez-Munoz, J.C., Cristobal, J., Sobrino, J. A., Soria, G., Ninyerola, M., Pons, X. and Pons, X. (2009). Revision of the single-Channel algorithm for land surface temperature retrieval from landsat thermal-infrared data. Geosci. Remote Sens. IEEE Trans. 47, 339–349.

Jones, P. D., Groisman, P. Y., Coughlan, M., Plummer, N., Wang, W.C. and Karl, T. R. (1990). "Assessment of Urbanization Effects in Time Series of Surface Air Temperature Over Land."Nature, 347: 169–172.

Jusuf, S. K., Wong, N.H., Hagen, E., Anggoro, R. and Hong, Y. (2007). The influence of landuse on the urban heat island in Singapore, Habitat International, 31, 232–242.

Kalnay, E. and Cai, M. (2003). "Impact of Urbanization and Land-Use Change on Climate," Nature, 423(6939):528-531.

Kandlikar, M. (2007). Air pollution at a hotspot location in Delhi: Detecting trends, seasonal cycles and oscillations. Atmospheric Environment 41, 5934–5947.

Kennedy, R. E., Andrefou, et, S., Cohen, W. B., G€omez, C., Grif-fiths, P. and Hais, M., et al. (2014). Bringing an ecological view of change to Landsat-based remote sensing. Frontiers in Ecology and the Environment, 12, 339e346.

Kloog, I., Chudnovsky, A. A., Just, A. C., Nordio, F., Koutrakis, P. and Coull, B.A. et al. (2014a). A new hybrid spatio-temporal model for estimating daily multiyear PM2.5 concentrations across northeastern USA using high resolution aerosol optical depth data. Atmos Environ, 95:581–590.

Kloog, I., Chudnovsky, A., Koutrakis, P. and Schwartz, J. (2012). Temporal and spatial assessments of minimum air temperature using satellite surface temperature measurements in Massachusetts, USA. Science of the Total Environmental, 432, 85–92.

Lambin, E. F., Geist, H. J. and Lepers, E. (2003). Dynamics of land-use and land-cover change in tropical regions. Annual Review of Environment and Resources, 28, 205–241. doi: 10.1146/annurev.energy.28.050302.105459.

Landsat 7, Handbook (1972). Science Data Users Handbook Landsat, 7.

Landsat 8, Handbook (2015). ScienceData Users HandbookVer 1.0 June, 2015.

Lasanta, T. and Vicente-serrano, S. M. (2012). Remote Sensing of Environment Complex land cover change processes in semiarid Mediterranean regions: An approach using Landsat images in northeast Spain. Remote Sensing of Environment, 124, 1–14.

Law, P., Lioy, P., Zelenka, M., Huber, A. and McCurdy, T. (1997). Evaluation of a probabilistic exposure model applied to carbon monoxide (pNEM/ CO) using Denver personal exposure monitoring data. JAWMA, 47: 491–500.

Levy, R. C., Mattoo, S., Munchak, L. A., Remer, L. A., Sayer, A. M. and Patadia, F. et al. (2013). The Collection 6 MODIS aerosol products over land and ocean. Atmos Meas Tech, 6:2989–3034.

Li, Z. L., Wu, H., Wang, N., Qiu, S., Sobrino, J. A., Wan, Z., Tang, B. H. and Yan, G. (2013b). Land surface emissivity retrieval from satellite data. Int J Remote Sens. 34:3084–3127.

Lillesand, T., Kiefer, R. and Chipman, J. (2004). Remote sensing and image interpretation. Chichester: John Wiley.

Lim, S., Vos, S. T., Flaxman, A. D., Danaei, G., Shibuya, K., Adair-Rohani, H. and Ezzati, M. A. (2012). comparative risk assessment of burden of disease and injury attributable to 67 risk factors and risk factor clusters in 21 regions, 1990-2010: A systematic analysis for the Global Burden of Disease Study 2010. The Lancet, 380(9859): 2224–2260.

Lin, B. S. and Lin, Y. J. (2010). Cooling effect of shade trees with different characteristics in a subtropical urban park. Hort Science, 45(1), 83–86.

Liu, Y., Hiyama, T. and Yamaguchi, Y. (2006). Scaling of land surface temperature using satellite data: A case examination on ASTER and MODIS products over a heterogeneous terrain area.Remote Sensing of Environment,127(105), 115–128.

Liu, Z., He, C., Zhou, Y. and Wu, J. (2014). How much of the world's land has been urbanized, really? A hierarchical framework for avoiding confusion.Landscape Ecology, http://doi.org/10.1007/s10980-014-0034-y

Liuhua Shi, Antonella Zanobetti, Itai Kloog, Brent, A. Coull, Petros Koutrakis, Steven, J. Melly, and Joel, Schwartz D. (2016). Low-Concentration PM2.5 and Mortality: EstimatingAcute and Chronic Effects in a Population-Based Study. Environmental Health Perspectives, 124 ;1.

Lu, D., Mausel, P., Brondiozio, E. and Moran, E. (2004). Change detection techniques. International Journal of Remote Sensing, 25(12), 2365–2407.

MacIntosh, D., Xue, J., Ozkaynak, H., Spengler, J. and Ryan P.B. (1995). A population-based exposure model for benzene. J Expos Anal Environ Epidemiol, 5 (3): 375–403.

Maimaitiyiming, M., Ghulam , A., Tiyip , T., Pla , F., LatorreCarmona , P., Halik , Ü. and Sawut , M. (2014). CaetanoEffects of green space spatial pattern on land surface temperature: implications for sustainable urban planning and climate change adaptation ISPRS J. Photogramm. Remote Sens., 89, pp. 59-66.

Maji, S., Ahmed, S., Siddiqui, W. A. and Ghosh, S. (2017). Short term effects of criteria air pollutants on daily mortality in Delhi. Atmospheric Environment, 150: 210-219

Mallick, J., Kant, Y. and Bharath, B. D. (2008). Estimation of land surface temperature over Delhi using Landsat-7 ETM +. J IndGeophys Union, 12(3), 131-140.

Mallick, J., Rahman, A. and Singh C. K. (2013). Modeling urban heat islands in heterogeneous land surface and its correlation with impervious surface area by using night-time ASTER satellite data in highly urbanizing city, Delhi-India, Advances in Space Research 52, 639–655.

Mallick, J., Singh, C. K., Shashtri, S., Rahman, A. and Mukherjee, S. (2012). Land surface emissivity retrieval based on moisture index from LANDSAT TM satellite data over heterogeneous surfaces of Delhi city. International Journal of Applied Earth Observation and Geoinformation, 19, 348–358.

Mann, H. B. (1945). Nonparametric Tests Against Trend1.Econometrica, 13(3): 245-259.

Martonchik, J. V., Kahn, R. A. and Diner, D. J. (2009). Retrieval of aerosol properties over land using MISR observations. In: Satellite Aerosol Remote Sensing Over Land (Kokhanovsky AA, de Leeuw G, eds). Berlin, Germany:Springer Praxis Books, 267–293.

McCurdy, T. (1995). Estimating human exposure to selected motor vehicle pollutants using the NEM series of models: Lessons to be learned. J. Expos Anal Environ Epidemiol, 5 (4): 533–550.

Miller, K. A., Siscovick, D. S., Sheppard, L., Shepherd, K., Sullivan, J. H. and Anderson, G.L. et al. (2007). Longterm exposure to air pollution and incidence of cardiovascular events in women. New Engl J Med, 356:447–458.

Mohamed, A.A., Odindi, J. and Mutanga, O. (2017). Land surface temperature and emissivity estimation for Urban Heat Island assessment using medium- and low resolution space-borne sensors: A review, Geocarto International, 32:4, 455-470, DOI: 10.1080/10106049.2016.1155657.

Mohan, M. and Kandya, A. (2015). Impact of urbanization and land-use / land-cover change on diurnal temperature range : A case study of tropical urban airshed of India using remote sensing data. Science of the Total Environmental, 506-507, 453–465.

Mohan, M., Kikegawa, Y., Gurjar, B. R., Bhat, S. and Kolli, N. R. (2013). Assessment of urban heat island effect for different land use–land cover from micrometeorological measurements and remote sensing data for megacity Delhi, Theor Appl Climatol, 112:647–658 DOI 10.1007/s00704-012-0758-z.

Momeni, M. and Saradjian, M. (2007). Evaluating NDVI-based emissivities of MODIS bands 31 and 32 using emissivities derived by Day/Night LST algorithm. Remote Sens Environ. 106:190–198.

Morgenstern, V., Zutavern, A., Cyrys, J., Brockow, I., Koletzko, S., Krämer, U. and Schäfer, T. A. (2008). Diseases, allergic sensitization, and exposure to traffic-related air pollution in children. American Journal of Respiratory and Critical Care Medicine. 177: 1331-1337.

Neteler, M. (2010). Estimating daily land surface temperatures in mountainous environments by reconstructed MODIS LST Data. Remote Sensing, 2, 333–351.

National Oceanic Atmospheric Administration (2003). Air Resources Laboratory (ARL), Atmospheric Modeling Division (AMD) and U.S. Environmental Protection Agency (EPA). http://www.epa.- gov/asmdnerl/.

Nguyen, O.V., Kawamura, K., Trong, D. P., Gong, Z. and Suwandana, E. (2015). Temporal change and its spatial variety on land surface temperature and land use changes in the Red River Delta, Vietnam, using MODIS time-series imagery. Environmental Monitoring and Assessment, 187,464.

Nichol, J., Hang, T. P. and Ng, E. (2013). Temperature projection in a tropical city using remote sensing and dynamic modelling, Clim Dyn , DOI 10.1007/s00382-013-1748-2.

Nobre, C. A., Sellers, P. J. and Shukla, J. (1991). "Amazonian Deforestation and Regional Climate Change," Journal of Climate, 4(10):957-988.

O'Meara, M. (1999). Reinventing cities for people and the planet. Worldwatch Papers, 149.

Ott, W. R. (1985). Total human exposure, Environ. Sci. Technol. 19:880–885.

Ott, W., Mage, D. and Wallace, L. (1988). Validation of the simulation of human activity and pollutant exposure (SHAPE) model using paired days from the Denver, Colorado, carbon monoxide field study. Atmos Environ. 22: 2101–2113.

Parenteau, M. P. and Sawada, M. C. (2012). The role of spatial representation in the development of a LUR model for Ottawa, Canada. Air Quality, Atmosphere and Health, 5, 311–323.

Parham, A. and Mirzaei, F. H. (2010). Approaches to study Urban Heat IslandeAbilities and limitations, Building and Environment 45, 2192-2201.

Parham, A. and Mirzaei, F. H. (2012). A procedure to quantify the impact of mitigation techniques on the urban ventilation Building and Environment, 47, 410-420.

Peskin, H. M. (1990). Accounting for Natural Resource Depletion and Degradation in Developing Countries, Washington, DC: World Bank, Environment Department Working Paper, 13, 39 p.

Petrenko, M. and Ichoku, C. (2013). Coherent uncertainty analysis of aerosol measurements from multiple satellite sensors. Atmos Chem Phys, 13:6777–6805.

Pichierri, M., Bonafoni, S. and Biondi, R. (2012). Remote Sensing of Environment Satellite air temperature estimation for monitoring the canopy layer heat island of Milan. Remote Sensing of Environment, 127,130–138.

Pichierria, M., Bonafoni, S. and Biondi, R. (2012). Satellite air temperature estimation for monitoring the canopy layer heat island of Milan, Remote Sensing of Environment, 127, 130–138.

Pope iii, C. A., Burnett, R. T., Thun, M. J., Calle, E. E., Krewski, D., Ito, K. and Thurston, G. D. (n.d.) (2002). Lung Cancer, Cardiopulmonary Mortality, and Long-term Exposure to Fine Particulate Air Pollution.JAMA. 287(9): 1132–1141.

Pope, A. C., Burnett, R. T., Krewski, D., Jerrett, M., Shi, Y., Calle, E. E. and Thun, M. J. (2009). Cardiovascular mortality and exposure to airborne fine particulate matter and cigarette smoke shape of the exposure-response relationship Circulation, 120: 941-948.

Pope, C. A., Bates, D. and Raizenne, M. (1995). Health effects of particulate air pollution: Time for reassessment. Environ Health Perspect, 103: 472–480.

Prata, A. J., Caselles, V., Coll, C., Sobrino, J. A. and Ottlé, C. (1995). Thermal remote sensing of land surface temperature from satellites: Current status and future prospects. Remote Sensing Reviews, 12, 175–224.

Puett, R. C., Hart, J. E., Yanosky, J. D., Paciorek, C., Schwartz, J. and Suh, H. et al. (2009). Chronic fine and coarse particulate exposure, mortality, and coronary heart disease in the Nurses Health Study. Environ Health Perspect, 117:1697–1701; doi:10.1289/ehp.0900572

Qin, Z., and Karnieli, A. (2001). A mono-window algorithm for retrieving land surface temperature from Landsat TM data and its application to the Israel-Egypt border.Int J Remote Sensing, 22(18), 3719–3746.

Raaschou-Nielsen, O., Andersen, Z. J., Beelen R., Samoli, E., Stafoggia, M., Weinmayr, G. and Hoek, G. (2013). Air pollution and lung cancer incidence in 17 European cohorts: Prospective analyses from the European Study of Cohorts for Air Pollution Effects (ESCAPE). The Lancet Oncology, 14: 813-822.

Ripley, E. A., Archibold, O. W. and Bretell, D. L. (1996). Temporal and spatial temperature patterns in Saskatoon. Weather,1:398e405. [60] Rosenzweig C, Solecki WD, Parshall L, Chopping.

Richards. J. A and Jia. X (1998). Remote sensing digital image analysis 4th Edition.

Rozenstein, O., Agam, N., Serio, C., Masiello, G., Venafra, S., Achal, S. and Karnieli, A. (2015).Diurnal emissivity dynamics in bare versus biocrusted sand dunes.Science of the Total Environment, 506-507, 422–429.

S.A. Delhi, Statistical Abstract of Delhi, (2012). Directorate of Economics and Statistics, Govt. of NCT of Delhi.

S.A. Delhi, Statistical Abstract of Delhi, (2014). Directorate of Economics and Statistics, Govt. of NCT of Delhi.

Salmond, J. A., Williams, D. E., Laing, G., Kingham, S., Dirks, L. and Henshaw, G. S. (2013). The influence of vegetation on the horizontal and vertical distribution of pollutants in a street canyon, Science of the Total Environment 443, 287–298.

Samet, J., Zeger, S. and Berhane, K. (1995). Particulate Air Pollution and Daily Mortality: Replication and Validation of Selected Studies. Health Effects Institute, Cambridge, MA.

Santiago, J. L., Martín, F. and Martilli, A. (2013). A computationalfluid dynamic modelling approach to assess the representativeness of urban monitoring stations, Science of the Total Environment, 454–455, 61–72.

Saraswat, A., Apte, J. S., Kandlikar, M., Brauer, M., Henderson, S. B. and Marshall, J. D. (2013). Spatiotemporal land use regression models of fine, ultrafine, and black carbon

particulate matter in New Delhi, India. Environmental Science and Technology, 47: 12903−12911.

Saraswat, A., Apte, J. S., Kandlikar, M., Brauer, M., Henderson, S. B. and Marshall, J. D. (2013). Spatiotemporal Land Use Regression Models of Fine, Ultrafine, and Black Carbon Particulate Matter in New Delhi, India. Environ. Sci. Technol. 47, 12903−12911.

Saraswat, A., Milind, K., Brauer, M. and Srivastava, A. (2016). PM2.5 Population Exposure in. New Delhi Using a Probabilistic Simulation Framework. Environ. Sci. Technol. 50, 3174−3183

Scha ¨ffler, A. and Swilling, M. (2013). Valuing green infrastructure in an urban environment under pressure: The Johannesburg case. Ecological Economics, 86, 246–257.

Schimel, D., Melillo, J., Tian, H., McGuire, A. D., Kicklighter, D., Kittel, T., Rosenbloom, N., Running, S., Thornton, P., Ojima, D., Parton, W., Kelly, R., Sykes, M., Neilson, R. and Rizzo, B. (2000). "Contribution of Increasing CO2 and Climate to Carbon Storage by Ecosystems in the United States," Science, 287(5460):2004-2006.

Schwartz, J. (1994). Air pollution and daily mortality: A review and meta-analysis. Environ Res. 64: 36–52.

Serra, P., Pons, X. and Saurı´, D. (2008). Land-cover and land-use change in a Mediterranean landscape: a spatial analysis of driving forces integrating biophysical and human factors. Applied Geography, 28, 189–209.

Singh, A. (1989). Digital change detection techniques using remotely sensed data. International Journal of Remote Sensing, 10(6), 989–1003.

Smits, P. C., Dellepiane, S. G. and Schowengerdt, R. A. (1997). Quality assessment of image. classification algorithms for land-cover mapping: a review and a proposal for a cost-based approach, International Journal of Remote Sensing. vol. 20, no. 8, 1461-1486

Snyder, W. C., Wan, Z., Zhang, Y. and Feng, Y. Z. (1998). Classification-based emissivity for land surface temperature measurement from space. Int J Remote Sens. 19:2753–2774.

Sobrino, J. A., Jiménez-Muñoz, J. C., Sòria, G., Romaguera, M., Guanter, L., Moreno, J., Plaza, A. and Martínez, P., (2008). Land surface emissivity retrieval from different VNIR and TIR sensors. IEEE Trans Geosci Remote Sens. 46:316–327.

Sobrino, J. A., Oltra-Carrió, R., Sòria, G., Bianchi, R. and Paganini, M. (2012). Impact of spatial resolution and satellite overpass time on evaluation of the surface urban heat island effects. Remote Sensing of Environment, 117,50–56.

Sobrinoa, J. A., Munoz, J. C. J. and Paolini, L. (2004). Land surface temperature retrieval from LANDSAT TM 5. Remote Sensing of Environment, 90, 434–440.

Squires, G. D. (2002). Urban Sprawl and the Uneven Development of Metropolitan America. In Gregory D. Squires (Ed.), Urban sprawl: Causes, consequences, and policy responses (pp. 1– 22). Washington, D.C.' Urban Institute Press.

Steinecke, K. (1999). Urban climatological studies in the Reykjavik subarctic environment, Iceland. Atmospheric Environment,33:4157e62.

Sun, Y. J., Wang, J. F., Zhang, R. H., Gillies, R. R., Xue, Y. and Bo, Y. C. (2005). Air temperature retrieval from remote sensing data based on thermodynamics. Theoretical and Applied Climatology, 80(1), 37–48.

Tomlinson, C. J., Chapman, L., Thornes, J. E. and Baker, C. J. (2012). Derivation of Birmingham's summer surface urban heat island from MODIS satellite images.International Journal of Climatology, 32, 214–224.

Tropek, R.,Sedla cek, O., Beck, J., Keil, P., Musilova, Z. and Símova, I. et al. (2014). Comment on "High-resolution global maps of 21st-century forest coverchange". Science, 344. http://dx.doi.org/10.1126/science.1248753, 981e981.

Turner, B. L., Lambin, E. F. and Reenberg, A. (2007). The emergence of land change science for global environmental change and sustainability. Proceedings of the National Academy of Sciences, 104 (52), 20666–20671.

United Nations (2011). World urbanization prospects: The 2009 revision population database, http://esa.un.org/unpd/wup/index.htm.

Valor, E. and Caselles, V. (1996). Mapping land surface emissivity from NDVI: application to European, African, and South American areas. Remote Sens Environ. 57:167–184.

Van de Griend A. A. and owe, M. (1993). On the relationship between thermal emissivity and the normalized difference vegetation index for natural surfaces. Int J Remote Sens. 14:1119–1131.

Van den, P. A. and Alexandra, R. (2008). Long-Term Effects of Traffic-Related Air Pollution on Mortality in a Dutch Cohort (NLCS-AIR Stud. Environmental Health Perspective, 116, 2: Research Library pg. 196.

Van Donkelaar, A., Martin, R. V., Brauer, M. and Boys, B. L. (2015). Use of Satellite Observations for Long-term Exposure Assessment of Global Concentrations of Fine Particulate Matter. Environmental Health Perspectives, 123 (2): 135-143.

Van Donkelaar, A., Martin, R. V., Brauer, M. and Boys,B. L. (2015). Global Annual PM2.5 Grids from MODIS, MISR and SeaWiFS Aerosol Optical Depth (AOD), 1998-2012. Palisades, NY: NASA Socioeconomic Data and Applications Center (SEDAC), http://dx.doi.org/10.7927/H4028PFS[Accessed 4 March 2016].

Venn, A., Lewis, S., Cooper, M., Hubbard, R., Hill, I. and Boddy, R. et al. (2000). Local road traffic activity and the prevalence, severity, and persistence of wheeze in school children: combined cross sectional and longitudinal study. Occup Environ Med. 57: 152–158.

Voogt. J. A. and Oke, T. R. (2003). Thermal remote sensing of urban climates. Remote Sens Environ. 86:370–384.

Vorovencii, I. (2015). Assessing and monitoring the risk of desertification in Dobrogea, Romania, using Landsat data and decision tree classifier. Environmental Monitoring and Assessment, 187, 204.

Wang, S., Ma, Q., Ding, H. and Liang, H. (2016). Detection of urban expansion and land surface temperature change using multi-temporal landsat images.Resources Conservation andRecycling, doi:10.1016/j.resconrec.2016.05.011.

Ward, K., Lauf, S., Kleinschmit, B. and Endlicher, W. (2016). Heat waves and urban heat islands in Europe : A review of relevant drivers. Science of the Total Environment, 569-570, 527–539.

Weber, N., Haase, D. and Franck, U. (2014). Zooming into temperature conditions in the city of Leipzig : How do urban built and green structures in fluence earth surface temperatures in the city ?, Science of the Total Environment, 496, 289–298.

Weng, Q. (2009). Thermal infrared remote sensing for urban climate and environmental studies: methods, applications, and trends ISPRS J. Photogramm. Remote Sens., 64, pp. 335-344.

Weng, Q., Lu, D. and Schubring, J. (2004). Estimation of land surface temperature–vegetation abundance relationship for urban heat island studies. Remote Sensing of Environment, 89, 467–483.

Wilcove, D. S., Rothstein, D., Dubow, J., Phillips, A. and Losos, E. (1998). "Quantifying Threats to Imperiled Species in the United States," BioScience, 48(8):607-615.

Wilson, E. O. (2002). The Future of Life, New York, NY: Alfred A. Knopf, 229 p.

Windahl, E. and Beurs, Kirsten de (2016). An intercomparison of Landsat land surface temperature retrieval methods under variable atmospheric conditions using in situ skintemperature, International Journal of Applied Earth Observation and Geoinformation 51 11–27.

World Energy Outlook (2008). International Energy Agency, Paris.

World Urbanization Prospects (2014). The Revision United Nations Department of Economic and Social Affairs/Population Division World Urbanization Prospects, pp xxi.

Wulder, M. A., White, J. C., Loveland, T. R., Woodcock, C. E., Belward, A. S. and Cohen, W. B. et al. (2015). The global Landsat archive: Status, consolidation, and direction. Remote Sensing of Environment. http://dx.doi.org/10.1016/ j.rse.2015.11.032.

Yang, X. (2002). Satellite monitoring of urban spatial growth in the Atlanta metropolitan area. Photogrammetric Engineering and Remote Sensing, 68(7), 725–734.

Yin, J., Yin, Z., Haidong, Z., Xu, S., Hu, X., Wang, J. and Wu, J. (2011). Monitoring urban expansion and land use/land cover changes of Shanghai metropolitan area duringthe transitional economy (1979–2009) in China. Environmental Monitoring and Assessment, 177, 609–621.

Yu, P. S., Yang, T. C. and Wu, C. K. (2002). Impact of climate change on water resources in southern Taiwan.Journal of Hydrology, 260:161-175.

Zartarian, V. O., zkaynak, H., Burke, J., Zufall, M., Rigas, M. and Furtaw, E. (2000). A modeling framework for estimating children's residential exposure and dose to chlorpyrifosvia dermal residue contact and nondietary ingestion. Environ Health Perspect, 108: 505–514.

Zhan, W., Zhang, Y., Ma, W., Yu, Q. and Chen, L. (2013). Estimating influences of urbanizations on meteorology and air quality of a Central Business District in Shanghai, China, Stoch Environ Res Risk Assess. 27:353–365 DOI 10.1007/s00477-012-0603-z.

Zhang, B. P., Yao, Y. H., Cheng, W. M., Zhou, C. H., Lu, Z. and Chen, X. D. (2002). Human-Coppin, P., Jonckheere, I., Nackaerts, K., Muys, B. and Lambin, E. (2004). Digital change detection methods in ecosystem monitoring: a review. International Journal of Remote Sensing, 25(9), 1565–1596

Zhang, F., Tiyip, T., Kung, H. and Johnson, V. C. (2016). Dynamics of land surface temperature (LST) in response to land use and land cover (LULC) changes in the Weigan and Kuqariver Arabian Journal of Geosciences, http://doi.org/10.1007/s12517-016-2521-8.

Zhang, H., Qi, Z., Xin-yue, Y., Cai,Y., Ma, W. and Chena, M. (2013). Analysis of land use/land cover change, population shift, and their effects on spatiotemporal patterns of urban heat islands in metropolitan Shanghai, China Applied Geography 44, 121-133.

Zhang, H., Qi, Z., Ye, X., Cai, Y., Ma, W. and Chen, M. (2013). Analysis of land use/land cover change, population shift, and their effects on spatiotemporal patterns of urban heat islands in metropolitan Shanghai, China. Applied Geography, 44, 121–133.

Zhou, F., GuoH,C., Ho, Y. S. and Wu, C. Z. (2007). Scientometric analysis of geostatistics using multivariate methods.BudapestScientometrics Dordrecht.Scientometrics, 73(73): 265–279.

Zmirou, D., Gauvin, S., Pin I., Momas, I., Just, J. and Sahraoui F. et al. Five epidemiological studies on transport and asthma: objectives, design and descriptive results. J Expos Anal Environ Epidemiol 2002: 12(3): 186–196.